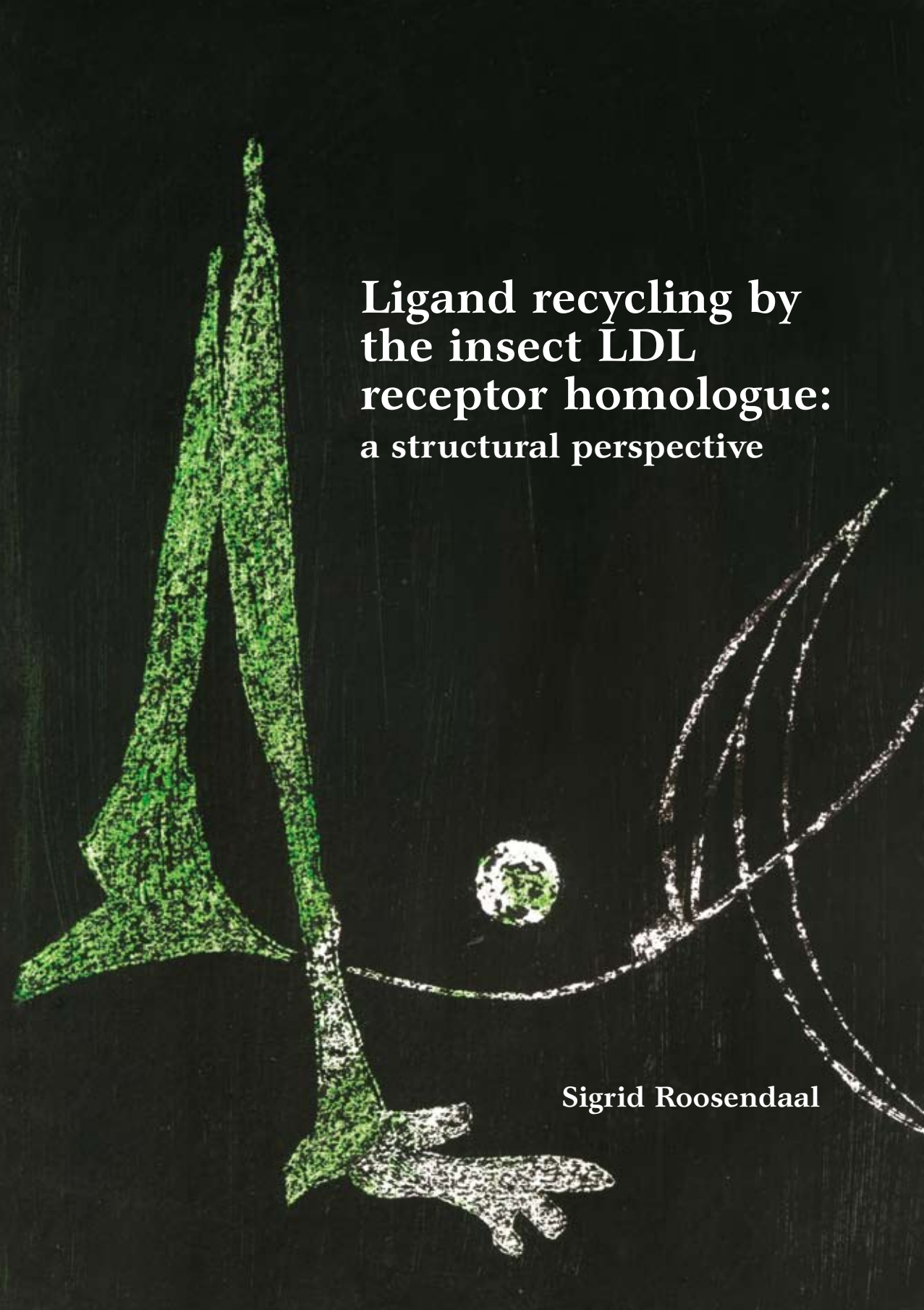

Ligand recycling by the insect LDL receptor homologue:
a structural perspective

Sigrid Roosendaal

Ligand recycling by the insect LDL receptor homologue:
a structural perspective

Sigrid Roosendaal

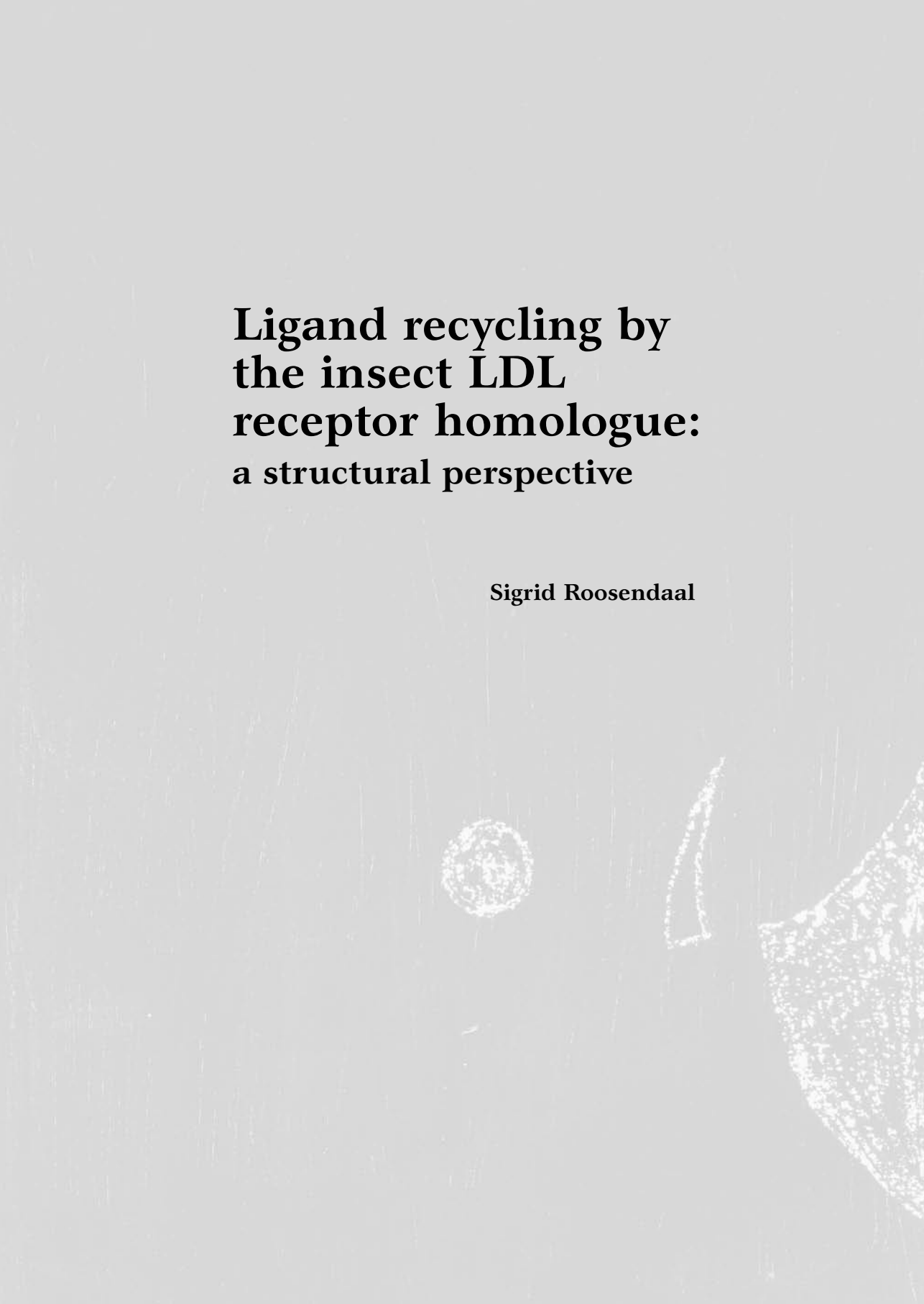

The research described in this thesis was performed at the Division of Endocrinology and Metabolism within the Department of Biology and Institute of Biomembranes, Utrecht University, The Netherlands.

ISBN 978-90-393-4806-2
Cover design Kirsten Roosendaal
Cover & layout Noenus Design, Soest
Print Print Partners Ipskamp, Enschede

Ligand recycling by the insect LDL receptor homologue: a structural perspective

Ligand recycling door de insecten LDL receptor homoloog: een structurele invalshoek

(met een samenvatting in het Nederlands)

Proefschrift

ter verkrijging van de graad van doctor aan de Universiteit Utrecht
op gezag van de rector magnificus, prof.dr. J.C. Stoof,
ingevolge het besluit van het college voor promoties
in het openbaar te verdedigen
op maandag 9 juni 2008 des ochtends te 10.30 uur.

door

Sigrid Dagmar Roosendaal

geboren op 29 juni 1980 te Dissen am Teutoburger Wald (Duitsland)

Promotor: Prof.dr. D. J. van der Horst

Co-promotor: Dr. K. W. Rodenburg

Contents

1

Introduction

based on:
Circulatory lipid transport:
lipoprotein assembly and function in an evolutionary perspective

Dick J. Van der Horst, Sigrid D. Roosendaal and Kees W. Rodenburg

Division of Endocrinology and Metabolism, Department of Biology
and Institute of Biomembranes, Utrecht University, Utrecht, the Netherlands

Mol Cell Biochem, in press

Abstract

Circulatory transport of neutral lipids (fat) in animals relies on members of the large lipid transfer protein (LLTP) superfamily, including mammalian apolipoprotein B (apoB) and insect apolipophorin II/I (apoLp-II/I). Latter proteins, which constitute the structural basis for the assembly of various lipoproteins, acquire lipids through microsomal triglyceride transfer protein (MTP) -another LLTP family member- and bind them by means of amphipathic structures. Comparative research reveals that LLTPs have evolved from the earliest animals and additionally highlights the structural and functional adaptations in these lipid carriers. For instance, in contrast to mammalian apoB, the insect apoB homologue, apoLp-II/I, is post-translationally cleaved by a furin, resulting in the appearance of two non-exchangeable apolipoproteins in the insect low-density lipoprotein (LDL) homologue, high-density lipophorin (HDLp).

An important difference between mammalian and insect lipoproteins relates to the mechanism of lipid delivery. Whereas in mammals, endocytic uptake of lipoprotein particles, mediated via members of the LDL receptor (LDLR) family, results in their degradation in lysosomes, the insect HDLp was shown to act as a reusable lipid shuttle which is capable of reloading lipid. Although the recent identification of a lipophorin receptor (LpR) -a homologue of LDLR- reveals that endocytic uptake of HDLp may constitute an additional mechanism of lipid delivery, the endocytosed lipoprotein appears to be recycled in a transferrin-like manner. The above structural similarities and functional adaptations of the lipid transport systems operative in mammals and insects are discussed from an evolutionary perspective.

Introduction

Lipid transport processes in the circulatory system of animals utilize highly specialized lipoprotein complexes, the apolipoproteins of which stabilize the lipid components and mediate particle metabolism. In mammals, lipoprotein metabolism is a complicated process involving several broad classes of lipoproteins. Transport of bulk lipids (triacylglycerol, TAG) in the circulation is mediated by intestine-derived chylomicrons and very-low-density lipoproteins (VLDL) that are produced in the liver. Once in the blood, TAG content of these particles is progressively reduced by the action of lipoprotein lipase, eventually resulting in receptor-mediated endocytic uptake of the remnant particles (chylomicron remnants and low-density lipoproteins (LDL)/ intermediate-density lipoproteins (IDL), respectively) and degradation of their single copy of the non-exchangeable apolipoprotein, apolipoprotein B (apoB) in lysosomes (for reviews, see [1-12]). By contrast, the multifunctional single lipoprotein in insects, high-density lipophorin (HDLp), has revealed another concept for lipid transport. The HDLp particle, which transports diacylglycerol (DAG) rather than TAG, circulates between tissues and alternately delivers and takes up lipids without being internalized or degraded, and thus functions as a reusable lipid shuttle without additional synthesis or increased degradation of its apolipoprotein matrix. The lipoprotein is produced in the fat body (a tissue combining many of the properties and functions of mammalian liver and adipose tissue) and contains single copies of its two non-exchangeable apolipoprotein components, apolipophorin I and II (apoLp-I and -II), which result from cleavage of their precursor apolipophorin II/I (apoLp-II/I) during lipoprotein biosynthesis (for recent reviews, see [2,13-16]).

Also during extensive lipid mobilization, such as during prolonged muscular exercise, circulatory lipid transport in mammals and insects use remarkably different concepts. In the circulation of mammals, the abundant serum protein, albumin, transports the free fatty acids (FFA) resulting from hydrolysis of TAG stores in adipose tissue to the working muscles. By contrast, in insect species that engage in long-term flights, the dramatic increase in lipid transport elicited by flight activity relies on circulatory lipoproteins. Indeed, the pre-existing HDLp particle functions once more as a lipid shuttle. Flight activity triggers the release of peptidergic adipokinetic hormones (AKHs) that act upon the fat body cells to stimulate the conversion of TAG stores to sn-1,2-DAG and its transfer to circulating HDLp (for recent reviews see [15,17,18]). By the loading of DAG, catalyzed by a lipid transfer particle (LTP), HDLp is converted into a low-density lipophorin (LDLp) particle that has almost doubled its diameter. At the same time, the increase in lipid content induces several copies of a low molecular weight amphipathic exchangeable apolipoprotein, apolipophorin III (apoLp-III), to associate with the particle and to unfold to cover its increased surface area. However, when the DAG cargo is hydrolyzed by a lipophorin lipase residing on the flight muscle cell surface and provides the FFA used for oxidative energy generation,

apoLp-III dissociates, regenerating the original HDLp particle which cycles back to the fat body for another round of lipid uptake and transport (Figure 1) (for recent reviews, see [16,17,19]). While apoLp-III, which is also available for an additional cycle of DAG transport, plays a crucial role in this unique insect lipoprotein shuttle mechanism, the apolipoprotein equally bears striking similarities with its human counterparts, particularly the 22 kDa N-terminal domain of human apolipoprotein E (apoE). The insect apolipoprotein has developed to a valuable model that has provided important insight into structure-function relationships of the class of exchangeable apolipoproteins, consisting of a relatively small bundle of amphipathic α-helices that reversibly associate with lipoprotein surfaces (for recent reviews, see [20-22]).

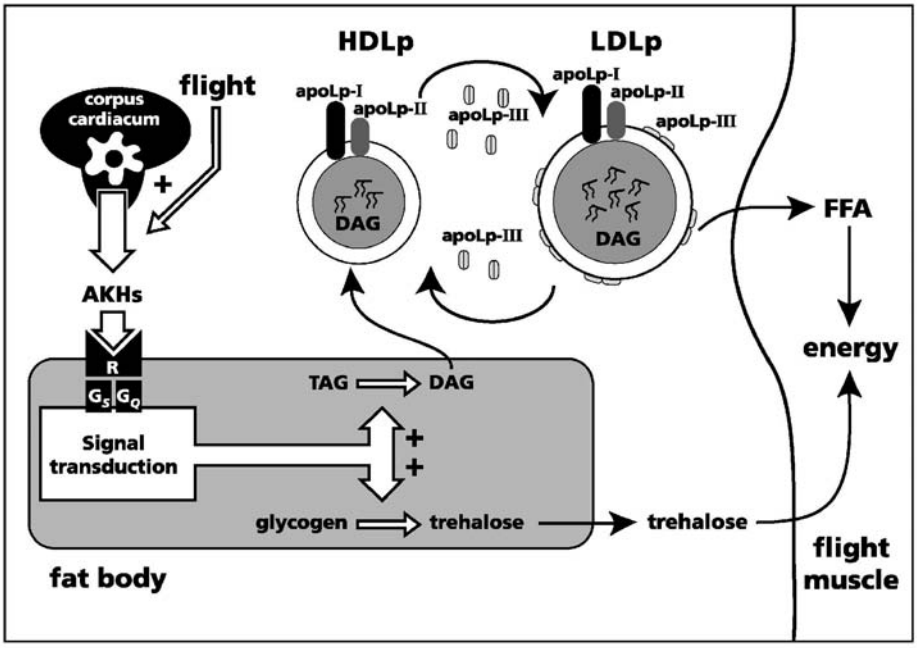

Figure 1. Molecular basis of the lipophorin lipid shuttle. AKH-controlled DAG mobilization from insect fat body during flight activity results in the reversible alternation of lipophorin from a relatively lipid-poor (HDLp) in a lipid-rich (LDLp) state, and apoLp-III from a lipid-free in a lipid-bound state. The reversible conformational change in apoLp-III induced by DAG loading of lipophorin is schematically visualized. AKHs: adipokinetic hormones; R: AKH receptor; G: G protein; HDLp: high-density lipophorin; LDLp: low-density lipophorin; apoLp-I, -II, and -III: apolipophorin I, II and III; TAG: triacylglycerol; DAG: diacylglycerol; FFA: free fatty acids. From[17], based on data from several insect species, particularly *L. migratoria*, reviewed in[15,17,19].

Notwithstanding this important last dimension, with respect to structure and functioning, there are significant differences between lipoprotein systems of mammals and insects. However, from an evolutionary point of view, there are also remarkable similarities, since mammalian apoB and insect apoLp-II/I, which constitute the structural basis for the assembly of their respective lipoproteins, were shown to be homologues[23]. Additionally, microsomal triglyceride transfer protein (MTP), a dedicated cofactor through which both apolipoproteins acquire lipids, is another member of the same family as apoB and apoLp-II/I[23-25]. Based on the sequence homology between apoLp-II/I and apoB, insect HDLp resembles mammalian LDL; the size and the spherical shape of the HDLp particle [26,27] are also similar to those of LDL[28] and both lipoproteins are practically devoid of exchangeable apolipoproteins.
The resemblance of HDLp to LDL was recently extended by the identification of an insect LDL receptor (LDLR) family member that is capable of endocytic uptake of HDLp into fat body cells, indicating that receptor-mediated endocytosis constitutes an additional mechanism for lipid delivery[29,30]. At the same time this suggests that the difference in functioning of the insect lipoprotein system compared to that of mammals may be less pronounced than indicated above. However, in spite of the high structural similarity of the insect lipophorin receptor (LpR) to mammalian LDLR, endocytosed HDLp appears not to be degraded in lysosomes, as is the case for mammalian LDL, but is resecreted in a manner similar to transferrin[30]. Once more, this data highlights structural and functional adaptations that emerge also with respect to the cognate receptors for the lipoprotein lipid carriers in mammals and insects.
The first part of this chapter will be centered on recent developments in the molecular and cellular aspects of lipoprotein-mediated circulatory lipid transport. These are discussed from an evolutionary perspective showing that several aspects of the overall structure and assembly of insect lipoproteins are similar to those of mammalian lipoproteins, even though detailed functioning of both systems have developed differently. Also the receptors for mammalian LDL and its insect homologue, HDLp, are very similar in overall structure, even though the function of the process of lipoprotein uptake and delivery in both systems appears to have evolved differently. Therefore, in the second part, we will focus on the novel mechanism of ligand recycling by an LDLR family member that was uncovered in insects and discuss the current knowledge of this mechanism in comparison with LDLR functioning in mammals, leading to the scope of this thesis.
From the view that insects constitute the largest -and very successful- animal group on earth, understanding of their solutions for circulatory lipid transport has a clear intrinsic value of profound biological significance that additionally may apply insight into corresponding processes in mammalian circulatory lipid transport or, in a more general context, processes that hitherto were not considered to occur in mammals.

Biosynthesis and secretion of insect lipoprotein

Insect apoLp-I and -II result from post-translational cleavage of their common precursor apolipoprotein, apolipophorin II/I (apoLp-II/I)[31], which is arranged with apoLp-II at the N-terminal end and apoLp-I at the C-terminal end[32]. The apoLp-II/I cDNA of several insect species has been isolated and characterized[32-36] or identified in genome analysis projects[37,38]. Based on sequence similarity and ancestral exon boundaries, these insect apolipoprotein precursors belong to the large lipid transfer (LLT) protein (LLTP) superfamily that emerged from an ancestral molecule and includes mammalian apoB, microsomal triglyceride transfer protein (MTP) and vitellogenin (Vtg)[23]. The LLT domain shared by these proteins comprises a large N-terminal domain of about 1000 amino acids containing a large lipid pocket, that is proposed to act as a lipid store and to transfer lipids to the apolipoprotein in a coordinated manner[23,24,39-43] (for reviews see [44,45]). A model of locust apoLp-II/I, constructed on homology with the lamprey lipovitellin crystal structure[46] and a structural model for a nascent human apoB lipoprotein particle[42], reveals a similar putative lipid pocket in the LLT domain[43] (Figure 2). The cleavage of insect apoLp-II/I into apoLp-II and apoLp-I occurs between two residues (720 and 721) of the LLT module, in an 80-residue long loop connecting two β-strands at the base of this putative lipid pocket.

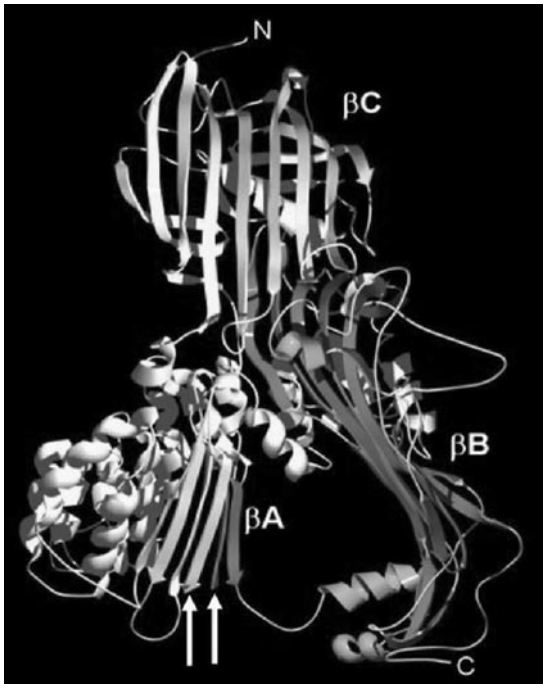

Figure 2. Model of locust apoLp-II/I. Model of *L. migratoria* apoLp-II/I (amino acid residues 22 to 1030)[43], constructed based on sequence homology with silver lamprey lipovitellin[46] and human apoB[42]. The structures that are part of apoLp-I and apoLp-II following apoLp-II/I cleavage are marked in shades of dark and light gray, respectively. The three β-sheets are indicated by βA, βB, and βC. The characters N and C mark the amino- and carboxy-terminal sides of the modeled region, respectively. The arrows indicate the β-strands at the base of the putative lipid pocket that are connected by a loop formed by the amino acid residues 669 to 748 (loop not indicated). ApoLp-II/I is cleaved within this region, between residues 720 and 721.

The co-translational lipidation of apoB-100 in the rough endoplasmic reticulum is completed post-translationally in the smooth endoplasmic reticulum and/or cis-Golgi network by acquiring the bulk of its neutral lipids (TAG), presumably by fusion with an intralumenal neutral lipid droplet[47,48]. The deposition of lipids in the lipid pocket of the apoB LLT module, which constitutes the first step in the lipidation process, requires interaction with MTP[47-49]. Based on the homology between apoB-100 and apoLp-II/I, as well as the discovery of an MTP homologue in the fruit fly, *Drosophila melanogaster*, that was able to promote the assembly and secretion of human apoB[50], insect lipoprotein assembly may also be expected to occur early in the secretory pathway.

Recent evidence showed the cleavage of apoLp-II/I to be mediated by an insect furin[43]. Since protein cleavage by furin homologues is performed late in the secretory pathway, mainly in the trans-Golgi network[51], insect lipoprotein biosynthesis by the fat body was proposed to proceed by the lipidation of apoLp-II/I to a lipoprotein, whereas cleavage of apoLp-II/I into apoLp-I and -II occurs at a later stage[43]. The uncleaved LLT domain in apoLp-II/I, involving intimately linked regions of apoLp-I and apoLp-II, is likely to be essential to enable the first steps in lipidation, as in apoB. Moreover, the occurrence of cleavage prior to lipidation might result in the parting of apoLp-I and apoLp-II, and hence impairment of lipoprotein biosynthesis. In conformity with the above, if cleavage was impaired by a furin inhibitor or mutagenesis of the consensus substrate sequence for furin, uncleaved apoLp-II/I was lipidated and functioned as a single apolipoprotein in the formation a lipoprotein particle, similar to its mammalian homologue, apoB-100. Since a lipoprotein particle with a buoyant density and molecular mass identical to wild-type HDLp was produced, we concluded that cleavage of apoLp-II/I by insect furin is neither required for biosynthesis nor for secretion of the insect lipoprotein[43].

The apparent conservation of apoLp-II/I cleavage in all insects characterized to date reveals the importance of this processing step. Vtg, another LLTP homologous to apoB-100 and apoLp-II/I, is also cleaved at a furin consensus substrate sequence in the LLT domain during biosynthesis in most insect species, however not in vertebrates[52]. The rationale for apoLp-II/I cleavage still awaits disclosure, but has been suggested to constitute a molecular adaptation that relates to the specific functioning of the insect lipoprotein. In this respect, the remarkable functioning of HDLp as a reusable lipid shuttle has been proposed, while the increased flexibility of apoLp-I and –II resulting from cleavage of apoLp-II/I may additionally allow for the loading of the particle with an increased lipid cargo and conversion of HDLp to LDLp during conditions that require enhanced lipid transport, such as insect flight activity. Alternatively, cleavage of apoLp-II/I may be necessary for other post-translational processes such as enabling receptor binding or hemolymph coagulation[43].

In addition to the LLT module, the structural resemblance between apoLp-II/I and apoB extends also to the rest of the polypeptide chains. Prediction of amphipathic

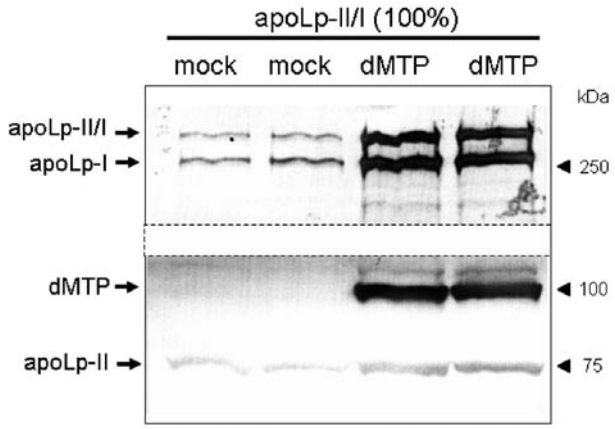

Figure 3. Insect MTP stimulates secretion of recombinant apoLp-II/I proteins. Co-expression of *Drosophila* MTP (dMTP) and recombinant full-length locust apoLp-II/I (100%) cDNA in an insect Sf9 cell system results in a significant increase in secretion of apoLp-I and –II, and also of uncleaved apoLp-II/I, compared to control cells lacking the MTP gene (mock), as analyzed by immunodetection of the different proteins in duplicate. Based on data from[55].

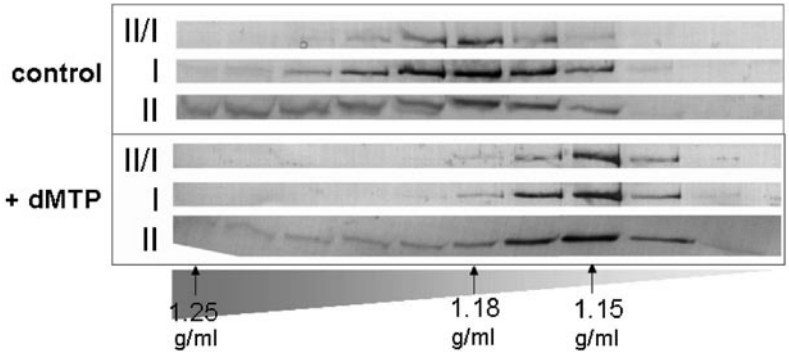

Figure 4. Insect MTP increases lipidation of recombinant apoLp-II/I proteins. Density-gradient ultracentrifugation and subsequent analysis of the buoyant density (g/ml) of the secreted proteins resulting from expression of recombinant full-length apoLp-II/I cDNA in Sf9 cells by immuno-detection shows that co-expression of dMTP results in the recovery of apoLp-I and -II (I and II, respectively), and also uncleaved apoLp-II/I (II/I), at a lower density (g/ml), indicating increased lipidation. Based on data from[55].

clusters in apoB suggested the presence of amphipathic α-helical domains (α) and amphipathic β-strand domains (β) organized along the apoB polypeptide as N-α1-β1-α2-β2-α3-C[53,54]. The α1-cluster and the N-terminal part of the β1-cluster constitute the LLT module. The C-terminal β1-α2-β2-α3-clusters stabilize expansion of the initial lipid core in the LLT module and actually possess most of the lipid-binding capacity[40]. Recent data propose that apoLp-II/I contains a similar, however smaller, lipid-associating segment, comprising one C-terminal amphipathic β-sheet and one α-helical domain (α2), organized along the protein as N-α1-β-α2-C, reminiscent of a truncated form of apoB[55]. The α1-cluster and a small N-terminal part of the β-cluster of this tripartite organization constitute the LLT module. Based on the homology between the LLT modules of apoB and apoLp-II/I, the C-terminal sequences of both apolipoproteins may also share a common evolutionary origin. In this respect, it has been speculated that the β2 and α3-clusters in apoB would have arisen from duplication of the β1 and α2-clusters[55]. At its C-terminal end, apoLp-II/I contains a von Willebrand factor module D[32]. Although the function of this domain remains unclear, it does not appear to be involved in lipid binding[55].

The pathway for lipoprotein biogenesis in mammals has disclosed that the lipids bound to the amphipathic lipid-associating segment of apoB are acquired through the assistance of MTP[47-49]. In view of the similar structural organization of apoB and apoLp-II/I and the recovery of MTP homologues in all available insect genomes, we considered whether this mechanism for lipoprotein biosynthesis is also operative in insect lipoprotein biogenesis. Insect MTP clearly stimulated insect lipoprotein biogenesis, since co-expression of the *Drosophila* MTP homologue (dMTP) and recombinant full-length locust (*Locusta migratoria*) apoLp-II/I cDNA in an insect cell (Sf9) expression system resulted in a several-fold increase in the secretion of apoLp-I and -II, as well as uncleaved apoLp-II/I (Figure 3)[55]. Concomitant with their secretion, dMTP significantly stimulated the lipidation of the apoLp-II/I proteins, since the secreted lipoprotein particles were recovered at a decreased buoyant density compared to control cells lacking the dMTP gene (Figure 4). To determine the amphiphatic region(s) of the apoLp-II/I proteins involved in lipid association, dMTP and a series of C-terminal truncation variants of apoLp-II/I were recombinantly co-expressed in Sf9 cells, revealing that formation of a buoyant high-density lipoprotein particularly requires the amphipathic β-cluster (Figure 5)[55]. These data led to the convergence that, regardless of specific modifications, the assembly of lipoproteins both in mammals and insects requires amphipathic structures in the apolipoprotein carriers as well as MTP. Consequently, it has been proposed that lipoprotein biogenesis in animals relies on structural elements that are of early metazoan origin[55].

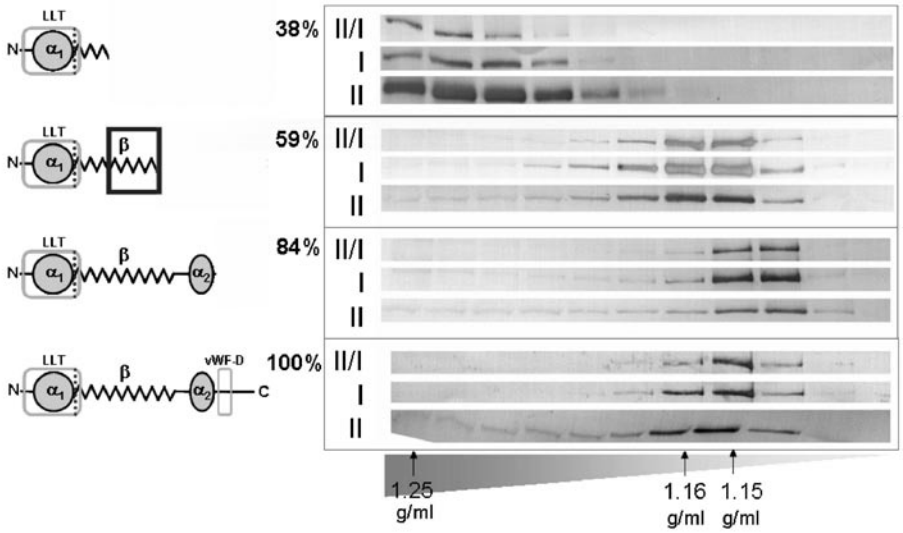

Figure 5. Insect lipoprotein biosynthesis requires the apoLp-II/I amphipathic β-cluster. To determine which amphipathic regions (β-sheet or α-helical) of the apoLp-II/I products are involved in lipid binding, truncated apoLp-II/I cDNA constructs were generated (38, 59, and 84%) in addition to the full-length (100%). Recombinant co-expression of these constructs with dMTP cDNA in Sf9 cells, followed by density gradient ultracentrifugation and subsequent analysis of the buoyant density (g/ml) of the secreted proteins (uncleaved apoLp-II/I (II/I), apoLp-I (I), and apoLp-II (II)) by immunodetection, demonstrates that particularly the β-cluster is required for lipid binding, as indicated by the shift in density (g/ml) when a major portion of the β-sheet region (indicated by β) is present in the apolipoprotein (i.e. apoLp-II/I-59%). The dashed vertical line in the LLT domain indicates location of the site of apoLp-II/I cleavage into apoLp-II and -I. Based on data from[55]. LLT domain: large lipid transfer domain; vWF-D: von Willebrand Factor D-module.

Molecular diversity and evolution of the LLTP superfamily

The above recent discoveries that highlight the common elements in LLTP structure and lipid binding have evoked a comparison of the structural uniformity as well as diversity in this major family of lipid-binding proteins. Analysis of the modular and structural features of the LLTPs known from cloning studies as well as genome sequences was used to reexamine the evolutionary relationships among LLTPs and the nature of their common ancestor, and classify the LLTP superfamily into distinct families[25]. The latter could not be established previously due to a lack of sequence information[23]. Our phylogenetic analyses on the aligned conserved segments in the LLT module yielded a phylogenetic tree that reveals three major families within the superfamily of LLTPs (Figure 6): (1) apoB-like LLTPs, which include vertebrate apoB, insect apoLp-II/I and Vtg from decapod crustaceans; (2) MTPs of vertebrates and invertebrates that range from a nematode and an insect (fruit fly) to zebrafish, human and chicken; and (3) Vtg-like LLTPs (excluding decapodan Vtg), ranging from mollusks and nematodes via insects to chicken and fish like lamprey and zebrafish.

The grouping of a.o. vertebrate apoB, insect apoLp-II/I and decapodan Vtg in the first family (apoB-like LLTPs) is supported by the recognition of a homologous region in these sequences only, the pfam06448 motif [56], that is located just C-terminal to the LLT module. Moreover, at the N-terminal side, members of this family are predicted to contain an amphipathic clustering corresponding to N-α-β-α-C, with a relatively long β-cluster and additional α-cluster. Of the second family (MTPs), the MTP of the fruit fly and particularly of the nematode appear to have diverged strongly, as indicated by their relatively long branch lengths in the phylogenetic tree (Figure 6). Nevertheless, in nematodes, insects and vertebrates, MTP has been reported to stimulate the biosynthesis of other LLTPs[25,55,57,58]. The third family (Vtg-like LLTPs) is highly diverse. The present phylogenetic analysis suggests a closer relation between the Vtgs from nematodes and insects as compared to Vtgs from vertebrates. In addition to multiple (related) Vtgs, insects also have another Vtg-like LLTP, melanin-engaging protein (MEP). In decapodan crustaceans, however, clotting protein (CP) is the only Vtg-like LLTP identified at present. From an evolutionary point of view, the protein that is named Vtg in this taxon actually is an apoB-like LLTP (Figure 6)[25,59].

The emergence of the LLT module appears to be the hallmark event in the origin of the complete superfamily of LLTPs, as it provides the basal structure for the binding of multiple lipid molecules[42,46,60]. The evolution of the LLT module may coincide with the evolution of animal multicellularity, a condition that provoked the need for intercellular lipid transport.

The nature of the earliest LLTP has recently come up for discussion[58]. Previously, the evolutionary progenitor to the present LLTPs has been suggested to function in vitellogenesis, as this ancient process is essential to reproduction even in the oldest animal phyla. More recently, however, an ancient MTP has been proposed to be the predecessor to other LLTPs, in view of the currently recognized importance of MTP-mediated lipid transfer in the biosynthesis of both Vtg-like and apoB-like LLTPs[25,55,57,58,61]. The recent study by Rava *et al.*[61] illustrates the utility of comparative studies in understanding and targeting the role of LLTPs in human disease. The comparison of lipid transfer activity of MTP from fruit fly and man revealed that the transfer of phospholipids and neutral lipids can selectively be inhibited in human MTP. This opens a new perspective on inhibiting MTP activity to specifically control the production of atherogenic apoB lipoproteins, an approach that was severely hampered by aspecific effects.

Insect lipoprotein is endocytosed by the insect LDLR homologue, LpR

Although many structural elements of the lipid transport system of insects are similar to those of mammals, as indicated above, lipoprotein-mediated lipid transport in

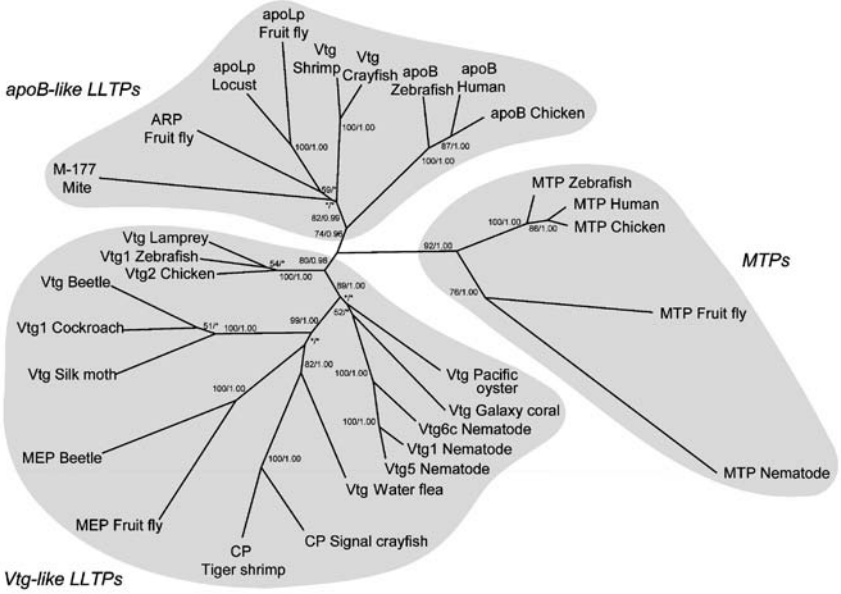

Figure 6. Phylogenetic tree of the LLTP superfamily. Based on all known LLTPs, an unrooted phylogenetic tree was constructed using the aligned segments of the LLT module[25]. The members of the three recognized LLTP families, *i.e.* the MTPs, the Vtg-like LLTPs and the apoB-like LLTPs, are denoted by separate grey backgrounds.

insects was thought to deviate significantly from that in mammals in view of the selective mechanism by which the insect lipoprotein transfers its hydrophobic cargo. Circulating HDLp particles may serve as a lipid donor or acceptor, dependent on the physiological situation, and function as a reusable lipid shuttle without additional synthesis or increased degradation of their apolipoprotein matrix, as discussed above. However, in apparent contrast to this concept of functioning as a shuttle system, receptor-mediated endocytic uptake of HDLp was demonstrated in fat body tissue of larval and young adult locusts[62]. The first lipophorin receptor (LpR) was cloned and sequenced from locust fat body cDNA and identified as a novel member of the LDLR family[29], while presently the LpR sequences of several other species have been elucidated[63-68]. The cDNA and genomic structure of LpR from the silkworm, *Bombyx mori*, indicated the presence of four isoforms that originate from a single gene by alternative splicing and are differentially expressed in a tissue- and stage-specific manner[67]. Remarkably, one of these isoforms was expressed specifically in the brain and central nervous system. In addition to the fat body, locust LpR is expressed in brain, midgut and oocyte[29]. In locust fat body, LpR is expressed only in specific developmental stages of the insect (during a few days after ecdysis, both to the next larval stage as to the adult), indicating additional uptake of HDLp by LpR in this

developmental period. Down-regulation of LpR was postponed by experimental starvation of adult locusts immediately after ecdysis. Moreover, by starving adult locusts after down-regulation of LpR, expression of the receptor was re-induced. These data suggest that LpR expression is regulated by the demand of fat body tissue for lipid components[69]. Receptor-mediated endocytosis of HDLp may therefore provide a mechanism for the uptake -or release- of specific lipid components, separate from the mechanism of selective unloading of HDLp lipid cargo at the cell surface.
Domain organization of LpR shows a high similarity to mammalian LDLR[29, 30,70] (Figure 7), and three-dimensional models of the elements representing the ligand-binding domain and the epidermal growth factor (EGF) precursor homology domain of locust LpR bear a striking resemblance to those of mammalian LDLR[16]. Despite their pronounced structural similarity, however, the specificity of LpR and LDLR for their ligands (HDLp and LDL, respectively) is mutually exclusive[30]. Additionally, the functioning of both receptors in lipid transport in insects and mammals appears to be intriguingly different (ligand recycling versus ligand degradation), as is discussed in more detail below. Possibly, these specific properties may be attributable to relatively small structural differences governing different properties of ligand binding and/or release.
The ligand-binding domain of LpR contains one additional cysteine-rich LDLR class A (LA) repeat compared to the cluster of seven repeats in LDLR (see Figure 7) and therefore counts the same number of LA-repeats as the human VLDL receptor (VLDLR)[29,30]. Another eight LA-repeat-containing LpR was identified in mosquito oocytes and shown to bind HDLp[63]. However, eight LA-repeat clusters in vertebrate and insect lipoprotein receptors do not indicate that they are directly homologous with one another[71] and based on the additional similarity in structure and composition of HDLp and LDL (see above), LpR is considered as an LDLR homologue rather than a homologue of VLDLR[30]. In addition to the extended ligand-binding domain, the amino acid sequence of the intracellular domain of LpR is longer, and unique for insect HDLp receptors: the twelve C-terminal amino acid residues of LDLR are completely different from those of LpR, whereas the C-terminal tail of LpR contains an additional 10 amino acid residues[30,72]. Since LpRs constitute newly discovered LDLR family members, we used the LDLR family members across the entire animal kingdom to reexamine their classification by performing a sequence comparison analysis in combination with a phylogenetic tree analysis[72]. In contrast to the two N-terminal domains of LDLR family members (involved in ligand binding and dissociation, respectively) that are composed of a mosaic of multiple repeats, the three C-terminal domains (i.e. O-linked glycosylation domain, transmembrane domain and intracellular domain, see Figure 7) are of a non-repetitive sequence. Intracellular trafficking and cellular signal transmission often involve the transmembrane domain and/or intracellular domain of membrane proteins, and for LDLR family members also the O-linked glycosylation domain has been implicated in a

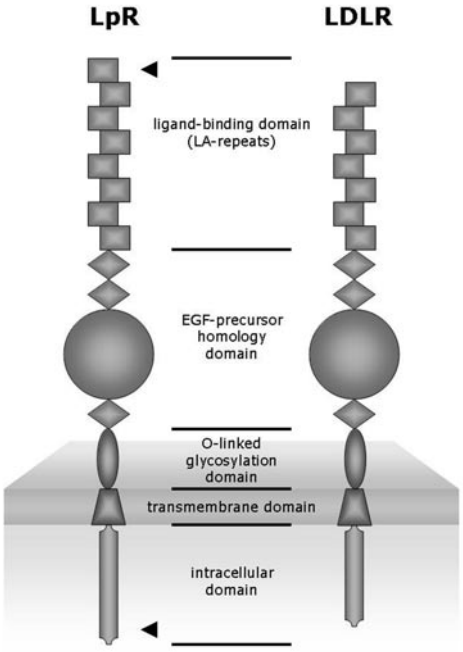

Figure 7. Domain organization of insect LpR and mammalian LDLR. Schematic representation of the insect lipophorin receptor (LpR) and the mammalian LDL receptor (LDLR), indicating an identical domain organization. Each receptor contains a ligand-binding domain composed of LA-repeats (squares), an EGF precursor homology domain composed of two EGF-repeats (diamonds) that are separated from a third one by a β-propeller containing YWTD-repeats (circle), an O-linked glycosylation domain (oval), a transmembrane domain (trapezium), and an intracellular C-terminal domain (stick). The ligand-binding domain of the LpR has one repeat more, and the intracellular domain of LpR is longer, as indicted by the arrowheads in LpR. EGF: epidermal growth factor. Based on data reviewed in[17,45].

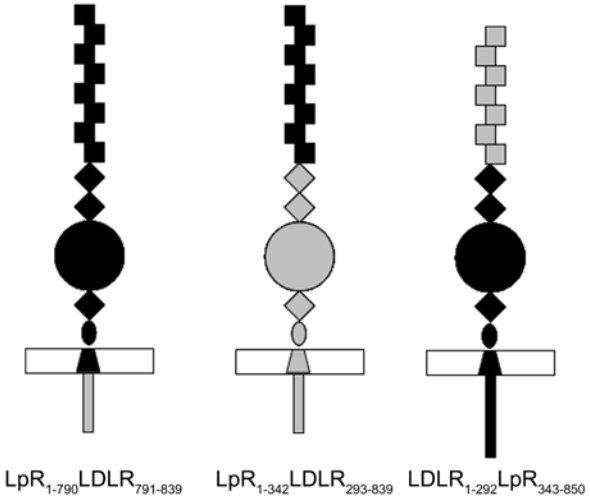

Figure 8. Schematic models of the hybrid receptors. LDLR domains are depicted in grey and LpR domains in black. For more details see Figure 7. The names of the hybrid receptors are indicated below the representations and denoted in an N- to C-terminal fashion. The numbers in the hybrid names refer to the amino acid residues of the mature proteins.

sequence of intracellular events[73,74]. Therefore, as a novel approach, we used the amino acid sequences of these three C-terminal domains of the LDLR family members for our analysis and classification. LpRs appeared to segregate into a specific group distinct from the groups encompassing the other family members, and each of the three C-terminal domains of the insect receptors is composed of a unique set of sequence motifs. Based on conservation of sequence motifs and organization of these motifs in the domains, LpR resembles most the groups of the LDLR, VLDLR, and Vtg receptors. In sequence aspects in which LpR deviates from these three receptor groups, the insect receptors resemble the LDLR-related protein 2 (LRP2) group, the most striking similarity being the presence of a C-terminal PDZ domain interacting motif[72]. PDZ domains are known to be involved in the intracellular trafficking of proteins and their receptors[75]. Therefore, these features might explain the functional differences disclosed between insect and mammalian lipoprotein receptors. However, studies involving hybrid lipoprotein receptors to determine the fate of lipoprotein ligands after endocytosis demonstrated that generation of a hybrid LpR of which the intracellular tail was replaced with that of LDLR ($LpR_{1\text{-}790}LDLR_{791\text{-}839}$, Figure 8) did not significantly affect the ligand recycling properties of the receptor[70]. The relatively unique sequence motifs in the intracellular domain of LpR[72] will therefore most likely be involved in other hitherto unidentified facets of receptor function.

LpR-mediated recycling of insect lipoprotein

While endocytosis of HDLp mediated by the insect LDLR homologue seems to conflict with the selective process of lipid transport between HDLp and fat body cells without degradation of the lipophorin matrix, the pathway followed by the internalized HDLp appeared to be different from the classical receptor-mediated lysosomal pathway typical of LDLR-internalized ligands. In mammalian cells, LDL and di-ferric transferrin have been used extensively to study intracellular transport of ligands that are internalized by receptor-mediated endocytosis. Whereas LDL dissociates from its receptor and is completely degraded in lysosomes[3], transferrin remains attached to its receptor and is eventually resecreted from the cells[76,77]. When the endocytic uptake of locust HDLp was studied simultaneously with human LDL in an LDLR-expressing Chinese hamster ovary (CHO) cell line transfected with LpR cDNA, fluorescently-labeled HDLp and LDL (labeled with different dyes) appeared to colocalize to the same early endocytic vesicle structures, as determined by using confocal laser scanning microscopy (CLSM)[30]. However, when the lipoproteins were allowed to proceed their intracellular routing in pulse-chase experiments, the insect and mammalian lipoproteins followed different routes in the cell. In contrast to LDL, which is degraded in lysosomes after dissociating from its receptor, HDLp remained colocalized with LpR and was transported to the endocytic recycling compartment

(ERC)[30]. From the latter compartment, which was identified by the colocalization of HDLp with transferrin, the insect lipoprotein was eventually resecreted ($t_{½}$ ~ 13 min) in a manner that is similar to the transferrin recycling pathway, and thus escaped from lysosomal degradation[30]. This data indicates that, in mammalian cells, endocytosed insect HDLp, in contrast to human LDL, follows a recycling pathway mediated by LpR.

Although this behavior of LpR in mammalian cells proposes new aspects of LDLR family functions, recycling of endocytosed HDLp in insect fat body cells remained to be shown. Since a locust fat body cell line is not available, fat body tissue from young adults (endogenously expressing LpR) was used to probe ligand recycling[78]. The first step in this process, the endocytosis of HDLp, has been characterized in considerable detail[69,79,80]. Following incubation with fluorescently labeled HDLp, tracking the intracellular pathway of the ligand in the fat body cells indicated that the lipoprotein was not transported to a recognizable ERC-like compartment, but remained in vesicles in the periphery of the cell. During a 2 h chase, the cells became almost completely depleted of their internalized labeled HDLp[78]. Since earlier data from our laboratory had shown the absence of substantial HDLp degradation by fat body cells of young adult animals[62], this depletion of internalized HDLp from fat body cells is indicative of resecretion of the ligand and supports the concept of ligand recycling that was demonstrated for LpR-transfected CHO cells[30]. The above concept, implying that insect lipoprotein endocytosed by an LDLR family member is eventually recycled, conflicts with the generally accepted concept of the fate of ligands endocytosed by all other LDLR family members, which are targeted to lysosomal degradation. Therefore, an intriguing question addresses the mechanism underlying the ability of LpR to recycle HDLp[30]. To obtain more experimental evidence on the contribution of the individual domains in LpR-mediated ligand recycling, we constructed hybrid receptor molecules composed of domains of LpR and LDLR (Figure 8)[70]. As mentioned before, a hybrid receptor in which the intracellular domain of LpR was replaced with that of LDLR ($LpR_{1-790}LDLR_{791-839}$) showed a ligand recycling property identical to that of LpR, indicating that this property is not dictated by the intracellular domain. Changing the complete ligand-binding domain of LDLR for that of LpR ($LpR_{1-342}LDLR_{293-839}$) resulted in a hybrid receptor that bound and endocytosed HDLp, but did not recycle the lipoprotein. The reciprocal receptor, containing the ligand-binding domain of LDLR and the complementary domains of LpR ($LDLR_{1-292}LpR_{343-850}$) did not recycle its ligand (LDL) either. Instead, these hybrid receptors and their respective ligands were targeted to lysosomes, leading to the degradation of ligand and receptor, indicating that ligand recycling by LpR is mediated by the cooperation of the ligand-binding domain and EGF domain[70].

Scope of this thesis

During cellular trafficking, both endocytosed HDLp and LpR are sorted to the ERC and recycled to the plasma membrane in a manner similar to that operative in the transferrin recycling pathway. This mechanism of HDLp recycling by LpR implies that during its intracellular itinerary, the LpR-HDLp complex is not dissociated. Notably, it entails that the integrity of the complex between HDLp and LpR is retained at endosomal conditions. Therefore, a novel, flow cytometric binding assay was developed to analyze the stability of the LpR-HDLp complex. The results indicate the complex to be resistant to pertinent conditions prevailing in the endosome, such as low pH and a decrease in Ca^{2+} concentration as mimicked by EDTA treatment of the complex (**Chapter 2**). Together, these data indicate that LpR and HDLp travel in complex to the ERC, which constitutes a key determinant in the mechanism of ligand recycling by LpR. However, the rationale for LpR expression limited to specific developmental periods, as well as the function of ligand recycling occurring during these periods, remained unclear. Since previous studies suggested that LpR expression is regulated by the demand of fat body tissue for lipid components[69], it was investigated whether the lipid content of HDLp affects binding and subsequent endocytosis by LpR. To this end, HDLp (buoyant density 1.11 g/ml) was partially delipidated in vitro by incubation with α-cyclodextrin, yielding a particle of which the buoyant density had increased to 1.17 g/ml (HDLp-1.17) (**Chapter 3**). Contrary to our expectations, however, LpR appeared to bind HDLp-1.17 with a substantially higher affinity than HDLp, suggesting that, in the physiological system, LpR may function to endocytose low lipid-loaded particles from the circulation and resecrete them after reloading. In concurrence with a higher affinity for LpR, delipidation of HDLp led to the exposure of the cleavage site of apoLp-II/I. Since the cleavage site and its flanking amino acid sequence are rich in lysine and arginine residues, which were shown to mediate the binding of ligands to LDLR family members, the involvement of the cleavage site in high-affinity binding of delipidated HDLp to LpR was examined (**Chapter 4**). One of the findings described in Chapter 2 is that the LpR-HDLp complex is EDTA-resistant, in contrast to that of LDLR and LDL. However, ligand binding to LDLR family members is known to depend on Ca^{2+}, and sequence comparison of the LA-repeats of LpR with those of other LDLR family members suggests that the structure of the Ca^{2+} cage is conserved in the LA-repeats of LpR. Therefore, the Ca^{2+} dependence of LpR for folding and ligand binding was investigated further (**Chapter 5**). Finally, in **Chapter 6** the findings are summarized and discussed from a broader view on lipid metabolism in mammals and insects.

References

1. Brown MS & Goldstein JL (1979) Receptor-mediated endocytosis: insights from the lipoprotein receptor system. Proc Natl Acad Sci USA 76, 3330-3337.
2. Mahley RW & Innerarity TL (1983) Lipoprotein receptors and cholesterol homeostasis. Biochim Biophys Acta 737, 197-222.
3. Goldstein JL, Brown MS, Anderson RG, Russell DW & Schneider WJ (1985) Receptor-mediated endocytosis: concepts emerging from the LDL receptor system. Annu Rev Cell Biol 1, 1-39.
4. Brown MS & Goldstein JL (1986) A receptor-mediated pathway for cholesterol homeostasis. Science 232, 34-47.
5. Havel RJ (1987) Lipid transport function of lipoproteins in blood plasma. Am J Physiol Endocrinol Metab 253, E1-5.
6. Gotto AM, Jr. (1990) Interrelationship of triglycerides with lipoproteins and high-density lipoproteins. Am J Cardiol 66, 20A-23A.
7. Hussain MM, Strickland DK & Bakillah A (1999) The mammalian low-density lipoprotein receptor family. Annu Rev Nutr 19, 141-172.
8. Willnow TE (1999) The low-density lipoprotein receptor gene family: multiple roles in lipid metabolism. J Mol Med 77, 306-315.
9. Herz J & Bock HH (2002) Lipoprotein receptors in the nervous system. Annu Rev Biochem 71, 405-434.
10. Tulenko TN & Sumner AE (2002) The physiology of lipoproteins. J Nucl Cardiol 9, 638-649.
11. Zannis VI, Chroni A, Kypreos KE, Kan HY, Cesar TB, Zanni EE & Kardassis D (2004) Probing the pathways of chylomicron and HDL metabolism using adenovirus-mediated gene transfer. Curr Opin Lipidol 15, 151-166.
12. Jeon H & Blacklow SC (2005) Structure and physiologic function of the low-density lipoprotein receptor. Annu Rev Biochem 74, 535-562.
13. Arrese EL, Canavoso LE, Jouni ZE, Pennington JE, Tsuchida K & Wells MA (2001) Lipid storage and mobilization in insects: current status and future directions. Insect Biochem Mol Biol 31, 7-17.
14. Canavoso LE, Jouni ZE, Karnas KJ, Pennington JE & Wells MA (2001) Fat metabolism in insects. Annu Rev Nutr 21, 23-46.
15. Van der Horst DJ, Van Marrewijk WJ & Diederen JH (2001) Adipokinetic hormones of insect: release, signal transduction, and responses. Int Rev Cytol 211, 179-240.
16. Van der Horst DJ, Van Hoof D, Van Marrewijk WJ & Rodenburg KW (2002) Alternative lipid mobilization: the insect shuttle system. Mol Cell Biochem 239, 113-119.
17. Van der Horst DJ & Ryan RO (2005) Lipid transport. In Comprehensive molecular insect science (Gilbert LI, Iatrou K & Gill SS, editors), 4, pp. 225-246. Elsevier, New York, NY, USA.
18. Van der Horst DJ (2003) Insect adipokinetic hormones: release and integration of flight energy metabolism. Comp Biochem Physiol B Biochem Mol Biol 136, 217-226.
19. Ryan RO & Van der Horst DJ (2000) Lipid transport biochemistry and its role in energy production. Annu Rev Entomol 45, 233-260.

20. Narayanaswami V & Ryan RO (2000) Molecular basis of exchangeable apolipoprotein function. Biochim Biophys Acta 1483, 15-36.
21. Weers PM & Ryan RO (2003) Apolipophorin III: a lipid-triggered molecular switch. Insect Biochem Mol Biol 33, 1249-1260.
22. Weers PMM & Ryan RO (2006) Apolipophorin III: Role model apolipoprotein. Insect Biochem Mol Biol 36, 231-240.
23. Babin PJ, Bogerd J, Kooiman FP, Van Marrewijk WJ & Van der Horst DJ (1999) Apolipophorin II/I, apolipoprotein B, vitellogenin, and microsomal triglyceride transfer protein genes are derived from a common ancestor. J Mol Evol 49, 150-160.
24. Mann CJ, Anderson TA, Read J, Chester SA, Harrison GB, Kochl S, Ritchie PJ, Bradbury P, Hussain FS, Amey J, Vanloo B, Rosseneu M, Infante R, Hancock JM, Levitt DG, Banaszak LJ, Scott J & Shoulders CC (1999) The structure of vitellogenin provides a molecular model for the assembly and secretion of atherogenic lipoproteins. J Mol Biol 285, 391-408.
25. Smolenaars MM, Madsen O, Rodenburg KW & Van der Horst DJ (2007) Molecular diversity and evolution of the large lipid transfer protein superfamily. J Lipid Res 48, 489-502.
26. Van Antwerpen R, Linnemans WA, Van der Horst DJ & Beenakkers AM (1988) Immunocytochemical localization of lipophorins in the flight muscles of the migratory locust (*Locusta migratoria*) at rest and during flight. Cell Tissue Res 252, 661-668.
27. Valentijn KM, Koning R, Derks Y, van Doorn JM, Van der Krift TP, Schouten A, Koerten HK, Van der Horst DJ, Gros P, Koster AJ & Rodenburg KW (2004) Preliminary three-dimensional model of insect lipoprotein HDLp by using electron miscroscopy and X-ray cristallography. In Proc Microsc Microanal (Anderson IM, Price R, Hall E, Clark E & McKernan S, editors), pp. 1514-1515, Savannah, GA, USA.
28. Orlova EV, Sherman MB, Chiu W, Mowri H, Smith LC & Gotto AM, Jr. (1999) Three-dimensional structure of low density lipoproteins by electron cryomicroscopy. Proc Natl Acad Sci USA 96, 8420-8425.
29. Dantuma NP, Potters M, De Winther MP, Tensen CP, Kooiman FP, Bogerd J & Van der Horst DJ (1999) An insect homolog of the vertebrate very low density lipoprotein receptor mediates endocytosis of lipophorins. J Lipid Res 40, 973-978.
30. Van Hoof D, Rodenburg KW & Van der Horst DJ (2002) Insect lipoprotein follows a transferrin-like recycling pathway that is mediated by the insect LDL receptor homologue. J Cell Sci 115, 4001-4012.
31. Weers PM, Van Marrewijk WJ, Beenakkers AM & Van der Horst DJ (1993) Biosynthesis of locust lipophorin. Apolipophorins I and II originate from a common precursor. J Biol Chem 268, 4300-4303.
32. Bogerd J, Babin PJ, Kooiman FP, Andre M, Ballagny C, Van Marrewijk WJ & Van der Horst DJ (2000) Molecular characterization and gene expression in the eye of the apolipophorin II/I precursor from *Locusta migratoria*. J Comp Neurol 427, 546-558.
33. Van der Horst DJ (1993) Lipoproteins and lipid transport. In Insect lipids: Chemistry, biochemistry and biology (Stanley-Samuelson DW & Nelson DR, editors), pp. 1-24, Lincoln, NE, USA.

34. Kutty RK, Kutty G, Kambadur R, Duncan T, Koonin EV, Rodriguez IR, Odenwald WF & Wiggert B (1996) Molecular characterization and developmental expression of a retinoid- and fatty acid-binding glycoprotein from *Drosophila*. A putative lipophorin. J Biol Chem 271, 20641-20649.
35. Sundermeyer K, Hendricks JK, Prasad SV & Wells MA (1996) The precursor protein of the structural apolipoproteins of lipophorin: cDNA and deduced amino acid sequence. Insect Biochem Mol Biol 26, 735-738.
36. Van Heusden MC, Thompson F & Dennis J (1998) Biosynthesis of *Aedes aegypti* lipophorin and gene expression of its apolipoproteins. Insect Biochem Mol Biol 28, 733-738.
37. Adams MD *et al*. (2000) The genome sequence of *Drosophila melanogaster*. Science 287, 2185-2195.
38. Holt RA *et al*. (2002) The genome sequence of the malaria mosquito *Anopheles gambiae*. Science 298, 129-149.
39. Segrest JP, Jones MK & Dashti N (1999) N-terminal domain of apolipoprotein B has structural homology to lipovitellin and microsomal triglyceride transfer protein: a "lipid pocket" model for self-assembly of apoB-containing lipoprotein particles. J Lipid Res 40, 1401-1416.
40. Segrest JP, Jones MK, De Loof H & Dashti N (2001) Structure of apolipoprotein B-100 in low density lipoproteins. J Lipid Res 42, 1346-1367.
41. Manchekar M, Richardson PE, Forte TM, Datta G, Segrest JP & Dashti N (2004) Apolipoprotein B-containing lipoprotein particle assembly: lipid capacity of the nascent lipoprotein particle. J Biol Chem 279, 39757-39766.
42. Richardson PE, Manchekar M, Dashti N, Jones MK, Beigneux A, Young SG, Harvey SC & Segrest JP (2005) Assembly of lipoprotein particles containing apolipoprotein-B: structural model for the nascent lipoprotein particle. Biophys J 88, 2789-2800.
43. Smolenaars MM, Kasperaitis MA, Richardson PE, Rodenburg KW & Van der Horst DJ (2005) Biosynthesis and secretion of insect lipoprotein: involvement of furin in cleavage of the apoB homolog, apolipophorin-II/I. J Lipid Res 46, 412-421.
44. Shelness GS, Hou L, Ledford AS, Parks JS & Weinberg RB (2003) Identification of the lipoprotein initiating domain of apolipoprotein B. J Biol Chem 278, 44702-44707.
45. Rodenburg KW & Van der Horst DJ (2005) Lipoprotein-mediated lipid transport in insects: analogy to the mammalian lipid carrier system and novel concepts for the functioning of LDL receptor family members. Biochim Biophys Acta 1736, 10-29.
46. Thompson JR & Banaszak LJ (2002) Lipid-protein interactions in lipovitellin. Biochemistry 41, 9398-9409.
47. Hussain MM, Kedees MH, Singh K, Athar H & Jamali NZ (2001) Signposts in the assembly of chylomicrons. Front Biosci 6, D320-331.
48. Shelness GS & Sellers JA (2001) Very-low-density lipoprotein assembly and secretion. Curr Opin Lipidol 12, 151-157.
49. Ledford AS, Weinberg RB, Cook VR, Hantgan RR & Shelness GS (2006) Self-association and lipid binding properties of the lipoprotein initiating domain of apolipoprotein B. J Biol Chem 281, 8871-8876.

50. Sellers JA, Hou L, Athar H, Hussain MM & Shelness GS (2003) A *Drosophila* microsomal triglyceride transfer protein homolog promotes the assembly and secretion of human apolipoprotein B. Implications for human and insect transport and metabolism. J Biol Chem 278, 20367-20373.
51. Molloy SS, Anderson ED, Jean F & Thomas G (1999) Bi-cycling the furin pathway: from TGN localization to pathogen activation and embryogenesis. Trends Cell Biol 9, 28-35.
52. Sappington TW & S. Raikhel A (1998) Molecular characteristics of insect vitellogenins and vitellogenin receptors. Insect Biochem Mol Biol 28, 277-300.
53. Segrest JP, Jones MK, Mishra VK, Anantharamaiah GM & Garber DW (1994) ApoB-100 has a pentapartite structure composed of three amphipathic alpha-helical domains alternating with two amphipathic beta-strand domains. Detection by the computer program LOCATE. Arterioscler Thromb 14, 1674-1685.
54. Segrest JP, Jones MK, Mishra VK, Pierotti V, Young SH, Boren J, Innerarity TL & Dashti N (1998) Apolipoprotein B-100: conservation of lipid-associating amphipathic secondary structural motifs in nine species of vertebrates. J Lipid Res 39, 85-102.
55. Smolenaars MM, De Morrée A, Kerver J, Van der Horst DJ & Rodenburg KW (2007) Insect lipoprotein biogenesis depends on an amphipathic beta cluster in apolipophorin II/I and is stimulated by microsomal triglyceride transfer protein. J Lipid Res 48, 1955-1965.
56. Marchler-Bauer A, Anderson JB, Cherukuri PF, DeWeese-Scott C, Geer LY, Gwadz M, He S, Hurwitz DI, Jackson JD, Ke Z, Lanczycki CJ, Liebert CA, Liu C, Lu F, Marchler GH, Mullokandov M, Shoemaker BA, Simonyan V, Song JS, Thiessen PA, Yamashita RA, Yin JJ, Zhang D & Bryant SH (2005) CDD: a Conserved Domain Database for protein classification. Nucleic Acids Res 33, D192-196.
57. Sellers JA, Hou L, Schoenberg DR, Batistuzzo de Medeiros SR, Wahli W & Shelness GS (2005) Microsomal triglyceride transfer protein promotes the secretion of *Xenopus laevis* vitellogenin A1. J Biol Chem 280, 13902-13905.
58. Shelness GS & Ledford AS (2005) Evolution and mechanism of apolipoprotein B-containing lipoprotein assembly. Curr Opin Lipidol 16, 325-332.
59. Avarre JC, Lubzens E & Babin PJ (2007) Apolipocrustacein, formerly vitellogenin, is the major egg yolk precursor protein in decapod crustaceans and is homologous to insect apolipophorin II/I and vertebrate apolipoprotein B. BMC Evol Biol 7, 3.
60. Anderson TA, Levitt DG & Banaszak LJ (1998) The structural basis of lipid interactions in lipovitellin, a soluble lipoprotein. Structure 6, 895-909.
61. Rava P, Ojakian GK, Shelness GS & Hussain MM (2006) Phospholipid transfer activity of microsomal triacylglycerol transfer protein is sufficient for the assembly and secretion of apolipoprotein B lipoproteins. J Biol Chem 281, 11019-11027.
62. Dantuma NP, Pijnenburg MA, Diederen JH & Van der Horst DJ (1997) Developmental down-regulation of receptor-mediated endocytosis of an insect lipoprotein. J Lipid Res 38, 254-265.
63. Cheon H-M, Seo S-J, Sun J, Sappington TW & Raikhel AS (2001) Molecular characterization of the VLDL receptor homolog mediating binding of lipophorin in oocyte of the mosquito *Aedes aegypti*. Insect Biochem Mol Biol 31, 753-760.

64. Lee CS, Han JH, Kim BS, Lee SM, Hwang JS, Kang SW, Lee BH & Kim HR (2003) Wax moth, *Galleria mellonella*, high density lipophorin receptor: alternative splicing, tissue-specific expression, and developmental regulation. Insect Biochem Mol Biol 33, 761-771.
65. Lee CS, Han JH, Lee SM, Hwang JS, Kang SW, Lee BH & Kim HR (2003) Wax moth, *Galleria mellonella* fat body receptor for high-density lipophorin (HDLp). Arch Insect Biochem Physiol 54, 14-24.
66. Seo S-J, Cheon H-M, Sun J, Sappington TW & Raikhel AS (2003) Tissue- and stage-specific expression of two lipophorin receptor variants with seven and eight ligand-binding repeats in the adult mosquito. J Biol Chem 278, 41954-41962.
67. Gopalapillai R, Kadono-Okuda K, Tsuchida K, Yamamoto K, Nohata J, Ajimura M & Mita K (2006) Lipophorin receptor of *Bombyx mori*: cDNA cloning, genomic structure, alternative splicing, and isolation of a new isoform. J Lipid Res 47, 1005-1013.
68. Ciudad L, Belles X & Piulachs MD (2007) Structural and RNAi characterization of the German cockroach lipophorin receptor, and the evolutionary relationships of lipoprotein receptors. BMC Mol Biol 8, 53.
69. Van Hoof D, Rodenburg KW & Van der Horst DJ (2003) Lipophorin receptor-mediated lipoprotein endocytosis in insect fat body cells. J Lipid Res 44, 1431-1440.
70. Van Hoof D, Rodenburg KW & Van der Horst DJ (2005) Intracellular fate of LDL receptor family members depends on the cooperation between their ligand-binding and EGF domains. J Cell Sci 118, 1309-1320.
71. Sappington TW & Raikhel AS (1998) Ligand-binding domains in vitellogenin receptors and other LDL-receptor family members share a common ancestral ordering of cysteine-rich repeats. J Mol Evol 46, 476-487.
72. Rodenburg KW, Smolenaars MM, Van Hoof D & Van der Horst DJ (2006) Sequence analysis of the non-recurring C-terminal domains shows that insect lipoprotein receptors constitute a distinct group of LDL receptor family members. Insect Biochem Mol Biol 36, 250-263.
73. May P, Bock HH & Herz J (2003) Integration of endocytosis and signal transduction by lipoprotein receptors. Sci STKE 2003, PE12.
74. May P, Bock HH, Nimpf J & Herz J (2003) Differential glycosylation regulates processing of lipoprotein receptors by gamma-secretase. J Biol Chem 278, 37386-37392.
75. Sheng M & Sala C (2001) PDZ domains and the organization of supramolecular complexes. Annu Rev Neurosci 24, 1-29.
76. Ghosh RN, Gelman DL & Maxfield FR (1994) Quantification of low density lipoprotein and transferrin endocytic sorting HEp2 cells using confocal microscopy. J Cell Sci 107, 2177-2189.
77. Maxfield FR & McGraw TE (2004) Endocytic recycling. Nat Rev Mol Cell Biol 5, 121-132.
78. Van Hoof D, Rodenburg KW & Van der Horst DJ (2005) Receptor-mediated endocytosis and intracellular trafficking of lipoproteins and transferrin in insect cells. Insect Biochem Mol Biol 35, 117-128.
79. Dantuma NP, Pijnenburg MA, Diederen JH & Van der Horst DJ (1998) Multiple interactions between insect lipoproteins and fat body cells: extracellular trapping and endocytic trafficking. J Lipid Res 39, 1877-1888.

80. Dantuma NP, Pijnenburg MA, Diederen JH & Van der Horst DJ (1998) Electron microscopic visualization of receptor-mediated endocytosis of DiI-labeled lipoproteins by diaminobenzidine photoconversion. J Histochem Cytochem 46, 1085-1089.

2

The complex of the insect LDL receptor homologue, LpR, and its lipoprotein ligand does not dissociate under endosomal conditions

Sigrid D. Roosendaal[1], Jana Kerver[1], Maria Schipper[2], Kees W. Rodenburg[1] and Dick J. Van der Horst[1]

[1]Division of Endocrinology and Metabolism, Department of Biology and Institute of Biomembranes, Utrecht University, The Netherlands; and [2]Centre for Biostatistics, Department of Biology, Utrecht University, The Netherlands

FEBS J (2008), 275 (8): 1751-1766

Abstract

The insect low-density lipoprotein (LDL) receptor (LDLR) homologue, LpR, mediates endocytic uptake of the single insect lipoprotein, lipophorin (HDLp), which is structurally related to LDL. However, contrary to the fate of LDL endocytosed by LDLR, we previously demonstrated that after endocytosis, HDLp is sorted to the endocytic recycling compartment (ERC) and recycled for resecretion in a transferrin-like manner. This entails that the integrity of the complex between HDLp and LpR is retained at endosomal conditions. Therefore, in this study the ligand binding and dissociation capacities of LpR were investigated by employing a new flow cytometric assay, using LDLR as a control. At pH 5.4, the LpR-HDLp complex remained stable, whereas that of LDLR and LDL dissociated. Hybrid HDLp-binding receptors, containing either the β-propeller or both the β-propeller and the hinge region of LDLR, appeared unable to release ligand at endosomal pH, revealing that the stability of the complex is imparted by the ligand-binding domain of LpR. The LpR-HDLp complex additionally appeared EDTA-resistant, excluding low Ca^{2+} concentration appearing in the endosome as an alternative trigger for complex dissociation. From binding of HDLp to the above hybrid receptors was inferred that the stability upon EDTA treatment is confined to ligand-binding (LA-) repeats 1-7. Additional (competition) binding experiments indicated that the binding site of LpR for HDLp most likely involves LA-2-7. It is therefore proposed that the remarkable stability of the LpR-HDLp complex is attributable to this binding site. Together, these data indicate that LpR and HDLp travel in complex to the ERC, which constitutes a key determinant for ligand recycling by LpR.

Introduction

Lipoproteins are used to transport lipids in the circulation of vertebrates as well as invertebrates. Whereas mammals employ an array of different lipoproteins, insects rely on one single multifunctional lipoprotein, high-density lipophorin (HDLp), which is synthesized in the fat body and released into the blood (hemolymph). In addition to lipid, the particle harbors two non-exchangeable apolipoproteins, apolipophorin I and apolipophorin II (apoLp-I and apoLp-II), that are derived from the post-translational cleavage of their common precursor, apoLp-II/I[1,2]. ApoLp-II/I was demonstrated to be a homologue of apoB-100[3,4], the non-exchangeable apolipoprotein of mammalian lipoproteins such as very-low-density lipoprotein (VLDL) and low-density lipoprotein (LDL)[5,6]. Despite this homology, HDLp appears to function differentially from these mammalian lipoproteins, since upon conversion of VLDL to LDL, the latter is being endocytosed by the LDL receptor (LDLR) and subsequently lysosomally degraded[7], whereas the insect lipoprotein iteratively loads and unloads lipid at various target tissues without being internalized or degraded, and thus acts as a reusable shuttle[8-11]. However, in apparent contrast to this concept of HDLp as a reusable shuttle, receptor-mediated endocytic uptake of HDLp was uncovered in fat body tissue of larval and young adult locusts[12], which was shown to be mediated by an LDLR homologue[13]. This first lipophorin receptor (LpR) was molecularly and functionally characterized[13-18] while afterwards the LpR sequences of several other insect species have been reported[19-24]. Sequence analysis showed that LpR is a classic LDLR family member, encompassing all the typical domains in an LDLR-like sequential manner[13]: (i) ligand-binding domain consisting of LDLR type A (LA-) repeats; (ii) epidermal growth factor (EGF) precursor homology domain composed of two EGF-repeats (EGF-A and EGF-B), a β-propeller containing YWTD-repeats, and a third EGF-repeat (EGF-C); (iii) O-linked glycosylation domain; (iv) transmembrane domain; and (v) intracellular C-terminal domain[25]. Three-dimensional models of the elements representing the ligand-binding domain and EGF precursor homology domain of locust LpR bear a striking resemblance to those of mammalian LDLR[10]. On the other hand, the ligand-binding domain of LpR contains one additional LA-repeat compared to the cluster of seven repeats in LDLR[13,14] while despite their pronounced structural similarity, the specificity of LpR and LDLR for their ligands (HDLp and LDL, respectively) is mutually exclusive[14].

Remarkably, however, when the functioning of LpR was compared directly with that of LDLR in a mammalian cell line (CHO cells transfected with LpR), the insect lipoprotein, in contrast to LDL, was shown to remain colocalized with its receptor and was targeted to the endocytic recycling compartment (ERC). From the latter compartment HDLp is resecreted, following a recycling pathway similar to that of transferrin[14]. In the insect system, LpR appeared to function similarly. Although an

insect fat body cell line is not available, HDLp internalized by fat body tissue from young adult locusts endogenously expressing LpR is also resecreted, consistent with the above concept of ligand recycling in LpR-transfected CHO cells[12,18]. Trafficking of ligand to the ERC constitutes a highly unusual property among LDLR family members while in addition, LDLR mutants that remain in complex with LDL are targeted to lysosomes[17,26].

During LDLR-mediated endocytosis of LDL, the receptor-ligand complex ends up in early endosomes that have a lumenal pH of 6-6.5[27]. At this acidic pH, the ectodomain of LDLR, composed of the ligand-binding domain, EGF precursor homology domain and glycosylation domain, is proposed to undergo a conformational change, resulting in the release of bound LDL. In this model, the ligand-binding domain is hypothesized to fold onto the β-propeller after protonation of histidine residues located at the interface of LA-4, LA-5 and the β-propeller[28], while other residues at this interface, i.e. Gln-540, Glu-581 and Lys-582, are important for docking of the ligand-binding domain onto the β-propeller[29]. In addition, the linker between LA-7 and EGF-A was demonstrated to constitute a rigid structure stabilized by a cluster of hydrophobic residues that includes Phe-261, Val-274 and Ile-313[29]. Because of the rigidity of this linker as well as that between EGF-A and EGF-B, the three repeats serve as a rigid scaffold, setting a favorable overall topology that permits the ligand-binding domain to fold over the β-propeller[29,30]. As a result of this conformational change, the β-propeller displaces bound LDL[28,31]. In addition to the low pH, a drop in Ca^{2+} concentration in the endosome is appearing[32], which is predicted to destabilize the Ca^{2+}-binding properties of the LA-repeats and of EGF-A and EGF-B, and thus might additionally contribute to the pH-dependent ligand release[25,33-35]. In the LA-repeats that consist of approximately 40 amino acids and are organized in a two-loop conformation stabilized by three disulfide bonds, a Ca^{2+} ion is chelated by a conserved stretch of acidic amino acids (DCxDxSDE) and essential to stabilize the C-terminal fold of the repeat[34,36-39]. Consequently, removal of Ca^{2+} abolishes ligand binding by LDLR[40]. Whereas the released LDL is targeted to lysosomes for degradation[31], LDLR is directed to the ERC, and from there efficiently recycled to the plasma membrane for another round of endocytosis[7,41].

Since contrary to the different fate of LDLR and LDL, LpR and HDLp are both directed to the ERC, functional studies with LpR-LDLR hybrid receptors were performed to disclose the molecular mechanism of LpR-mediated ligand sorting and subsequent recycling. The data obtained indicate that the property of LpR to deliver HDLp to the ERC is not attributable to the C-terminal intracellular domain, both the length and sequence of which are very different from that of LDLR, but appeared to be a function of the ectodomain[16]. The mechanism of HDLp recycling by LpR implies that during its intracellular itinerary, the LpR-HDLp complex is not dissociated.

Therefore, in this study, a novel binding assay using flow cytometry was used to demonstrate that, in contrast to control experiments involving LDLR and LDL, LpR and HDLp remain in complex at endosomal pH. This remarkable stability of the receptor-ligand complex appeared to be accounted for by the ligand-binding domain. In addition, treatment of the LpR-HDLp complex with an EDTA-containing buffer to mimic the effect of the low Ca^{2+} concentration in the endosome did not induce complex dissociation either, once again in contrast to the LDLR-LDL complex. Together, our new findings provide ample evidence that endosomal conditions fail to result in dissociation of the complex, signifying that HDLp and LpR travel in complex to the ERC. Experiments using an LpR-LDLR hybrid receptor containing LA-1-7 of LpR and the complementary part of LDLR suggest that the stability of the complex is imparted by LA-1-7, which were shown to comprise the binding site for HDLp. The data accumulated implies that the stability of the complex is engendered by the specific interaction between LpR and HDLp.

Materials and Methods

Proteins and antibodies

Insect HDLp was isolated from locust hemolymph by density gradient ultracentrifugation as described earlier[14]. Human LDL was isolated from blood plasma (Bloedbank Midden Nederland, The Netherlands) as described by Redgrave[42] with minor adaptations to the original protocol. The salt solutions of different densities used in the procedure contained 86.89 g/ml KBr (density 1.063 g/ml), 18.36 g/ml KBr (density 1.019 g/ml) and 8.69 g/ml KBr (density 1.006 g/ml). Polyclonal rabbit-anti-LpR 2189/90 antibody was raised against a synthetic peptide representing the unique very N-terminal 20 amino acids (34-53) of LA-1 of LpR[15]. Mouse-anti-LDLR antibody C7 was a generous gift from Dr. Ineke Braakman (Utrecht University, Utrecht, The Netherlands). Human his-tagged RAP (RAP-his) was a generous gift from Dr. Michael Etzerodt (IMSB, Aarhus University, Århus, Denmark).

Construction of expression vectors encoding lipoprotein receptor cDNA

The cloning of the expression vectors was performed according to standard laboratory procedures and performed according to the protocols supplied with enzymes and kits. Site specific mutations were generated with QuickChange site directed mutagenesis using PfuTurbo DNA polymerase (Stratagene, Amsterdam, The Netherlands) according to the manufacturer's protocol. PCR fragments were generated

using PfuTurbo DNA polymerase and synthetic oligonucleotide primers (Biolegio, Nijmegen, The Netherlands). Endonucleases were from New England BioLabs (Westburg B.V., Leusden, The Netherlands) and Fermentas (St. Leon-Rot, Germany). Plasmid pcDNA3-LpR$_{1\text{-}297}$LDLR$_{248\text{-}839}$ was made as follows. First, by mutagenesis a unique *Age*I site was introduced in pcDNA3-LpR (piLR-e[13]) causing a silent mutation in the Pro-301 codon (CCA→ CCG; the first amino acid is that of the mature protein) using the oligonucleotide 5′ gagaattgcacatcaccggtgccaaagtgtgaccc 3′ (forward primer), and 5′ gggtcacactttggcaccggtgatgtgcaattctc 3′ (reverse primer), yielding the construct pcDNA3-LpR(*Age*I). Subsequently, to replace the sequence encoding LA-8 of LpR with that of LA-7 of human LDLR, a 1668 bp fragment containing the 5′ flanking *Age*I and 3′ flanking *Acc*III sites was generated by PCR from pGEM-T-LDLR$_{1\text{-}292}$ LpR$_{343\text{-}850}$[16] using the oligonucleotides 5′ggccgcaccggtgacactctgcgagggaccc 3′ (forward primer), and 5′gcggccgcttatacataatcatttgtccc3′ (reverse primer). The *Age*I-*Acc*III fragment encoding at the 5′ end LA-7 of LDLR obtained by PCR was cloned in pcDNA3-LpR(*Age*I) using the enzymes *Age*I and *Acc*III, thereby replacing the sequence encoding LA-8 of LpR to yield the mosaic receptor construct pcDNA3-LpR$_{1\text{-}301}$LDLR$_{252\text{-}292}$LpR$_{343\text{-}850}$. Subsequently, the 1267 bp *Eco*RI-*Kpn*I fragment[16] from the mosaic receptor construct was isolated and cloned into pGEM-T-LpR$_{1\text{-}342}$LDLR$_{293\text{-}839}$ digested with the same two endonucleases to replace the sequence encoding LA-1 through LA-8 of LpR, with that of the LA-1 through LA-7 of LpR combined with LA-7 of human LDLR, thereby generating pGEM-T-LpR$_{1\text{-}301}$LDLR$_{252\text{-}839}$. Finally, the *Eco*RI-*Not*I fragment encoding the LpR$_{1\text{-}301}$LDLR$_{252\text{-}839}$ sequence was cloned in pcDNA3 digested with the same enzymes to yield pcDNA3-LpR$_{1\text{-}301}$LDLR$_{252\text{-}839}$.

Plasmid pcDNA3-LDLR$_{1\text{-}251}$LpR$_{302\text{-}850}$ was constructed similarly. First, a unique *Hpa*I site was introduced in pcDNA3-LDLR[16] causing a silent mutation in the Asn-251codon (AAT→AAC) using the oligonucleotide 5′ggctgcgttaacgtgacactctgcgag 3′ (forward primer), and 5′ctcgcatgtcaggttaacgcagcc 3′ (reverse primer), yielding the construct pBS-LDLR(*Hpa*I). Subsequently, to replace the sequence encoding LA-7 of human LDLR with that of LA-8 of LpR, a 1790 bp fragment, containing the unique *Hpa*I and *Bsu*361 sites, was generated from pcDNA3-LpR$_{1\text{-}342}$LDLR$_{293\text{-}839}$ by PCR using the oligonucleotide primers 5′cccggggttaacgtgccaaagtgtgacccc 3′ (forward primer), and 5′atttaaattcacgccagctcatcctcc 3′ (reverse primer). The 473 bp *Hpa*I-*Bsu*361 fragment, at the 5′ end encoding LA-8, obtained by PCR, was then cloned in pBS-LDLR(*Hpa*I) using the enzymes *Hpa*I and *Bsu*361 replacing the sequence encoding LA-7 of LDLR with that of LA-8 of LpR, to yield the mosaic receptor pBS-LDLR$_{1\text{-}251}$LpR$_{301\text{-}342}$LDLR$_{293\text{-}839}$. To obtain the construct pcDNA3-LDLR$_{1\text{-}251}$LpR$_{301\text{-}342}$LDLR$_{293\text{-}839}$ the sequence encoding the mosaic receptor was cloned in pcDNA3using the *Xba*I restriction enzyme. Subsequently, the 225 bp *Eco*RI-*Kpn*I fragment from the mosaic receptor construct was isolated and cloned into pGEM-T-LDLR$_{1\text{-}292}$LpR$_{343\text{-}850}$ digested

with the same two endonucleases to replace the sequence encoding the seven LA-repeats of LDLR with that of the LA-1-6 of LDLR followed by LA-8 of LpR, thereby generating pGEM-T-LDLR$_{1-251}$LpR$_{301-850}$. Finally, the *Hind*I-*Not*I fragment encoding the LDLR$_{1-251}$LpR$_{301-850}$ sequence was cloned in pcDNA3 digested with the same enzymes to yield pcDNA3-LDLR$_{1-251}$LpR$_{301-850}$. All PCR and mutagenesis generated LpR fragments were sequenced and their sequence, apart from the intended mutations, confirmed to be identical to that of LpR as indicated in the EMBL sequence database (accession number AJ000010).

Cell culture

Chinese hamster ovary (CHO) cells were cultured in 25 cm^2 polystyrene culture flasks in growth medium (Ham F-10 nutrient mixture (GibcoBRL, Invitrogen, Breda, The Netherlands) supplemented medium, containing 5% heat inactivated fetal bovine serum (FBS, GibcoBRL) and 100 U/ml penicillin G sodium and 100 µg/ml streptomycin sulfate in 85% saline (GibcoBRL)). The cells were maintained at 37°C and 5% CO_2.

Transfections

LDLR-deficient CHO(*ldlA*) cells[43] were grown up to 40% confluency in 12-well multi-dishes (Costar). After washing the cells once, the growth medium was replaced with 500 µl of fresh growth medium. Subsequently, 2 µg DNA and 4 µg polyethylenimine (PEI, Polysciences, Eppelheim, Germany) in 50 µl serum-free medium (Ham F-10 nutrient mixture supplemented medium with 100 U/ml penicillin G sodium and 100 µg/ml streptomycin sulfate in 85% saline) was administered to the cells. After 4 h, 500 µl growth medium was added and cells were cultured overnight. The next day, cells were detached from dishes and cultured in 25 cm^2 culture flasks in growth medium supplemented with 400 µg/ml geneticin (GibcoBRL) or 400 µg/ml zeocin (Cayla, Toulouse, France). Ten days after transfection, cells were used for experiments.

Fluorescence labeling of LDL and HDLp

LDL and HDLp were covalently labeled with Oregon green (OG) 488 carboxylic acid (Molecular Probes, Leiden, The Netherlands) as described previously[14].

Binding experiments using flow cytometry

The cells were grown until a confluency of 70%. 16 h before the experiment, the growth medium was replaced by serum-free medium. At the start of the experiment

the cells were placed on ice. Subsequently, the cells were washed with ice-cold binding buffer (50 mM Tris-HCl, 2 mM $CaCl_2$, 150 mM NaCl, pH 7.4, 4°C) and incubated with OG-labeled LDL (35 µg/ml) or HDLp (25 µg/ml) in binding buffer for 30 min. After binding, the cells were washed once with either ice-cold binding buffer, or low-pH buffer (25 mM Tris, 25 mM sodium succinate, 2 mM $CaCl_2$, 150 mM NaCl, pH 5.4 or pH 4.0, 4°C) or EDTA-containing buffer (50 mM Tris-HCl, 150 mM NaCl, 5 mM EDTA, pH 7.4, 4°C). Then the cells were incubated with the buffer for 30 min. After washing of the cells, the cells were incubated for 5 min at 37°C in serum-free medium, to allow the cells to endocytose bound ligand. After endocytosis, the cells were detached using trypsin-EDTA (Invitrogen) according to manufacturer's conditions and resuspended in growth medium. Resuspended cells were fixed in 0.5% paraformaldehyde (PFA) in PBS at 4°C for at least 30 min to overnight.
The receptor on the plasma membrane was detected using the same protocol as for ligand binding. However, the cells were incubated with an antibody against the first LA-repeat (C7[44] for LDLR and 2189/90[15] for LpR), for 30 min in binding buffer. After washing with binding buffer, the cells were incubated for 30 min with a fluorescein isothiocyanate (FITC)-labeled secondary anti-IgG antibody (Jackson Immuno-Research Laboratories Inc, Brunschwig, Amsterdam, The Netherlands). Then, the complex was endocytosed, and cells were detached and fixed as described above.

Competition binding experiments

Competition experiments were performed similarly to the binding experiments. However, the cells were first incubated for 30 min with primary antibody 2189/90, followed by 30 min incubation with OG-HDLp, or vice versa. The degree of binding was compared to the degree of binding without the antibody incubation. For competition experiments with RAP, RAP-his (3.6 µg/ml) was added simultaneously with (OG)-HDLp or primary antibody 2189/90. Then bound OG-HDLp or 2189/90 was detected as described previously. RAP-his was detected by subsequent washing and incubation of mouse-anti-his antibody (Amersham Biosciences, Roosendaal, The Netherlands) in binding buffer, followed by washing and incubation with a FITC-labeled secondary anti-IgG antibody (Jackson ImmunoResearch Laboratories Inc).

Flow cytometry data analysis

Samples were measured using a fluorescence-activated cell sorter (FACS, Becton Dickinson FACS Calibur). Flow cytometry data were collected using Cell Quest (Becton Dickinson) and downloaded into the program WinMDI (TSRI FACS Core Facility, La Jolla, CA) for analysis. For each sample (~ 100.000 cells) the fluorescence was plotted against the forward scatter (FSC). Based on samples of untransfected cells, for each series of experiments region R1 was defined to exclude cells of which

the fluorescence did not exceed that of untransfected cells from the analysis. Then the number of cells and the mean fluorescence (y-mean) in R1 were determined. If the number of cells in R1 decreases by the different treatments of the cells, the y-mean in R1 is overestimated. Therefore, for each cell line, the number of cells in R1 after different treatments was compared by a t-test for paired samples performed on the logarithms of the number of cells. In case of a significant ($p \leq 0.05$) difference in sample size due to the different treatments, the y-mean was corrected by using random values of the missing number of cells from the population of lower intensity (outside R1). After correction, for each sample the relative amount of fluorescence as compared to control samples was determined. Data presented as means ± s.e.m. were obtained from at least three independent experiments. To test whether samples were significantly different from control samples, a t-test for paired samples was performed on the logarithms of the y-means.

Results

Measurement of ligand binding and subsequent endocytosis by flow cytometry

To asses the binding of HDLp to LpR, a flow cytometric assay was developed in which living, attached LDLR-deficient CHO cells[43] transfected with LpR were incubated with Oregon green-labeled HDLp (OG-HDLp). The analysis of bound ligand was performed using flow cytometry, which requires cells in suspension. Therefore, a three-step procedure was used. The first step involved the binding of ligand at 4°C to prevent endocytosis, allowing the binding to reach equilibrium. Second, the cells were incubated at 37°C for 5 min in serum-free medium to mediate endocytosis of bound ligand by LpR[14], protecting bound ligand from the trypsin treatment applied in the next step. The third step involved resuspension of the cells by trypsinization and measurement of the fluorescence by flow cytometry. Latter measurement resulted in a dotplot displaying two populations of cells with different fluorescence intensities (Figure 1A): first, a small population with a relatively high fluorescence intensity (Figure 1A, population 1), representing LpR-transfected cells that bound and subsequently endocytosed HDLp, and second, a population of LpR-transfected cells of a lower fluorescence intensity (Figure 1A, population 2). The second population is located at the same position as the negative control cells (Figure 1B), indicating that these cells did not bind HDLp. Detection of the receptor on the plasma membrane, enabled by the use of antibody 2189/90, yielded a similar distribution of the two populations (Figure 1C, cf. Figure 1A). Quantification of the number of cells in population 1 revealed that the number of cells that bound ligand was 91.5 ± 6.3% of the number that bound antibody, indicating that binding of HDLp was proportional to the amount of receptor on the plasma membrane.

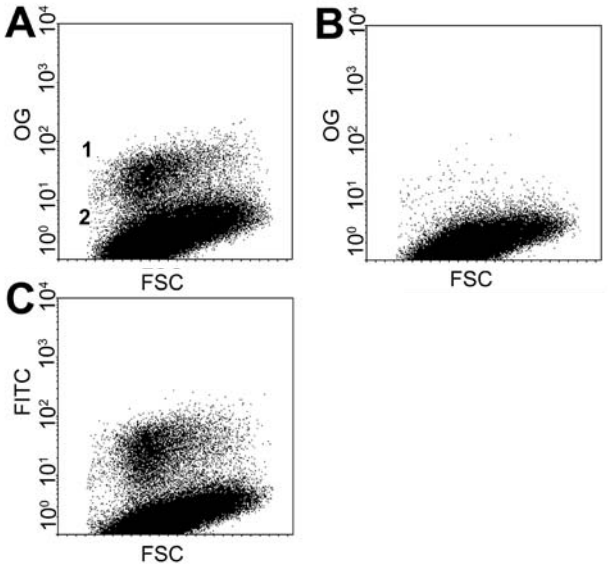

Figure 1. FACS analysis of HDLp binding by LpR. After binding and subsequent endocytosis of OG-HDLp, the cells were trypsinized and analyzed by flow cytometry (A). The amount of fluorescence is plotted on the y-axis (relative values), and the forward scatter (FSC, relative values) on the x-axis. Cells in the population indicated by 1 (population 1) are transfected cells with a higher fluorescence intensity than the cells in the population indicated by 2 (population 2). In plot B a similar experiment using untransfected cells is shown. Plot C represents measurements of cells that were incubated at 4°C with antibody 2189/90, followed by incubation with a FITC-labeled secondary antibody at 4°C, and then incubated at 37°C for 5 min before trypsinization and analysis. The data shown in the plots are representative of four independent experiments.

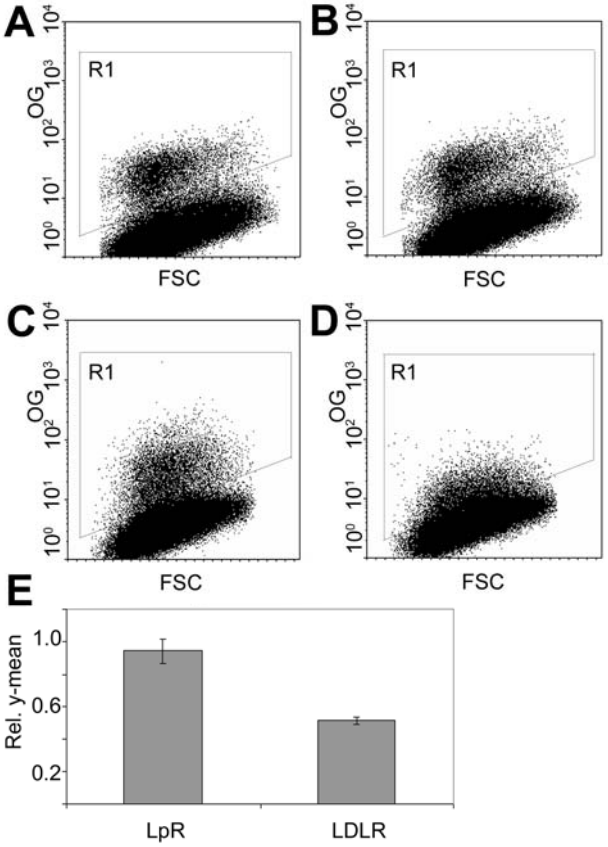

Figure 2. LpR and HDLp remain in complex at endosomal pH. CHO(LpR) cells were incubated with OG-HDLp and washed with buffer of pH 7.4 (A) or pH 5.4 (B). Plot C and D show a similar experiment for binding of OG-LDL to cells transfected with LDLR, and washed with pH 7.4 (C) or pH 5.4 (D). Plots are representative of at least eight independent experiments performed on cell lines created by four different transfections. E: Amount of bound ligand after washing with buffer of pH 5.4. The mean fluorescence (y-mean) in R1 (Figs. 2A, B, C, D) was determined for each sample. The relative y-mean (Rel. y-mean) after washing at pH 5.4 was calculated by the formula: $\text{y-mean}_{pH5.4}/\text{y-mean}_{pH7.4}$, and is plotted on the y-axis. Data represented are the means of at least eight independent experiments. Error bars indicate the s.e.m. See the legend to Figure 1 for more details.

HDLp and LpR remain in complex at endosomal pH

To investigate whether the LpR-HDLp complex dissociates upon exposure to endosomal pH, OG-HDLp was bound at neutral pH (7.4) to LpR-transfected cells, after which the cells were washed at 4°C with a buffer of low pH (5.4). After endocytosis of bound ligand, the fluorescence of the cells appeared to be not affected when compared to cells that had been washed with pH 7.4 (Figures 2A, B). By contrast, similar experiments performed with cells transfected with LDLR cDNA, that were incubated with OG-LDL and subsequently washed at pH 5.4, resulted in a decrease in fluorescence in comparison to cells that had been washed at pH 7.4 (Figures 2C, D). After washing at pH 5.4 the population of low fluorescence intensity was located at the same position as after washing at pH 7.4, indicating that the different pH of the buffers used in the incubations did not affect the size or the morphology of the cells, and thereby the amount of fluorescence. The population of low intensity was excluded from the analysis by setting region R1 (Figures 2A-D). To quantify the amount of bound ligand, the mean fluorescence in R1 was determined and compared to the mean fluorescence in R1 after washing with pH 5.4 (Figure 2). In the case of LpR, the fluorescence of cells washed at pH 5.4 was 94.3 ± 7.6% of the fluorescence of cells washed at pH 7.4, indicating that OG-HDLp remained bound to LpR upon exposure to pH 5.4. As expected, in the case of LDLR, the fluorescence of cells washed at pH 5.4 had decreased significantly and amounted to only 51.4 ± 2.2% of the fluorescence of cells washed at pH 7.4 (Figure 2E). A longer incubation at pH 5.4 (one hour instead of 30 min, data not shown) did not result in further dissociation of both the LDLR-LDL and LpR-HDLp complexes, suggesting that an incubation time of 30 min was sufficient to achieve maximum dissociation. Furthermore, the expression level of receptor, which varied between different cell lines and thus between different experiments, did not influence the relative amount of dissociation (data not shown).

Exposure of the LpR-HDLp complex to pH values between 4.0 and 5.0 resulted in a substantial decrease in fluorescence of the cells (data not shown). However, at this pH, HDLp appeared to be precipitated (data not shown). Moreover, since in LpR-transfected CHO cells HDLp is transported from the early endosome to the ERC and from there is returned to the plasma membrane[14], it is unlikely that the LpR-HDLp complex encounters a pH lower than 5.4. Additionally, it should be noted that the pH of endosomes in the insect fat body is similar to that of mammalian cells[45], indicating that also after LpR-mediated uptake of HDLp in insect fat body tissue the LpR-HDLp complex does not encounter a pH lower than 5.4.

Table 1. LDLR amino acid residues that are essential for LDL release and the corresponding amino acid of LpR.

Residue LDLR	Corresponding residue LpR	Location	Function	Reference
His-190	His-270	LA-5	Interaction with β-propeller	29, 46
Phe-261	Phe-344	LA-7	Required for rigidity of the hinge region	29
His-264	Gly-346	LA-7	Unknown	http://www.ucl.ac.uk/fh/
Ser-265	Gly-347	LA-7	Unknown	http://www.ucl.ac.uk/fh/
Val-274	Val-357	LA-7	Required for rigidity of the hinge region	29
Ile-313	Ala-395	EGF-A	Anchorage of EGF-A and -B with LA-7	29, 51
Gln-540	Lys-621	β-propeller	Interaction with ligand-binding domain	29, 51
His-562	Asn-643	β-propeller	Inducement conformational change	29
Glu-581	Pro-662	β-propeller	Interaction with ligand-binding domain	29, 51
Lys-582	Glu-663	β-propeller	Interaction with ligand-binding domain	29
His-586	His-667	β-propeller	Interaction with ligand-binding domain	29, 46

The lack of LpR-HDLp complex dissociation is caused by the ligand-binding domain

Sequence alignment of the amino acid sequence of LDLR with that of LpR revealed that several of the residues crucial for LDL release by LDLR are not conserved in LpR (Table 1). To investigate whether the deficiency of these crucial residues in LpR may be responsible for the lack of dissociation of the LpR-HDLp complex, the binding and dissociation capacities of different hybrid receptors (Figure 3A[16]) were assessed. $LDLR_{1\text{-}292}LpR_{343\text{-}850}$ was able to bind LDL, but unable to release this ligand at endosomal pH (Figure 3B), suggesting that the absence of Gln-540, His-562, Glu-581 and Lys-582 in the β-propeller of LpR causes the lack of HDLp release by LpR. However, the reciprocal hybrid, $LpR_{1\text{-}342}LDLR_{293\text{-}839}$ (Figure 3A) appeared to be equally incapable of releasing its ligand, HDLp (Figure 3B). The presence of Gln-540, His-562, Glu-581 and Lys-582 in this hybrid suggests that the β-propeller of this hybrid may be able to interact with the ligand-binding domain. However, although $LpR_{1\text{-}342}LDLR_{293\text{-}839}$ contains Ile-313, it does not contain the complete hinge region of LDLR. The presence of two glycine residues in LpR on the corresponding positions of His-264 and Ser-265 of LDLR (Table 1) might decrease the rigidity of the hinge region of $LpR_{1\text{-}342}LDLR_{293\text{-}839}$, thereby abolishing ligand release. To investigate whether the complete hinge region and β-propeller of LDLR were able to induce HDLp release by LpR, the hybrid receptor $LpR_{1\text{-}301}LDLR_{252\text{-}839}$ (Figure 3A) was created. This hybrid receptor was able to bind HDLp, but similar to wild type LpR, unable to release it (Figure 3B). Since these functional LDLR domains failed to evoke HDLp release, the lack of dissociation of the complex is proposed to result from the specific binding interaction of the ligand-binding domain of LpR with HDLp.

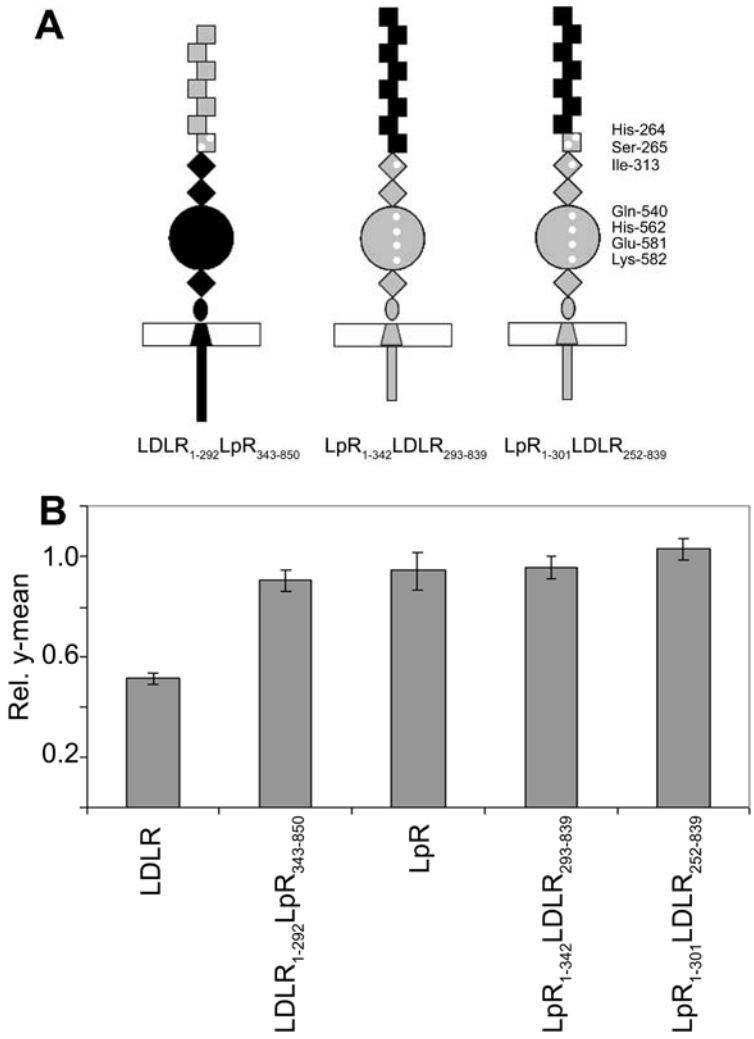

Figure 3. Hybrid receptors and relative amount of pH-dependent ligand dissociation. A: Schematic models of the hybrid receptors. LDLR domains are depicted in grey and LpR domains in black. Each receptor contains a ligand-binding domain composed of LA-repeats (squares), an EGF-precursor homology domain composed of two EGF-repeats (diamonds) that are separated from a third by a β-propeller containing YWTD-repeats (circle), an O-linked glycosylation domain (oval), a transmembrane domain (trapezoid) and an intracellular C-terminal domain (long rectangle). The wide and open rectangle represents the plasma membrane. The numbers indicate the amino acid residues of the mature proteins. Amino acids that are important for LDL release and not conserved in LpR are indicated by white dots. B: Amount of bound ligand to different hybrid receptors after incubation at pH 5.4. CHO cells transfected with the different hybrid receptors were incubated with OG-LDL (LDLR and $LDLR_{1\text{-}292}LpR_{343\text{-}850}$) or OG-HDLp (LpR, $LpR_{1\text{-}342}LDLR_{293\text{-}839}$, $LpR_{1\text{-}301}LDLR_{252\text{-}839}$) and washed with buffer of pH 7.4 or pH 5.4. The fluorescence was measured by flow cytometry. The mean fluorescence (y-mean) in R1 was determined for each sample. The relative y-mean (Rel. y-mean) after a wash at pH 5.4 was calculated by the formula: $y\text{-}mean_{pH5.4}/y\text{-}mean_{pH7.4}$, and is plotted on the y-axis. The values represented are the averages of at least three independent experiments. Error bars indicate the s.e.m. See the legend to Figure1 for more details.

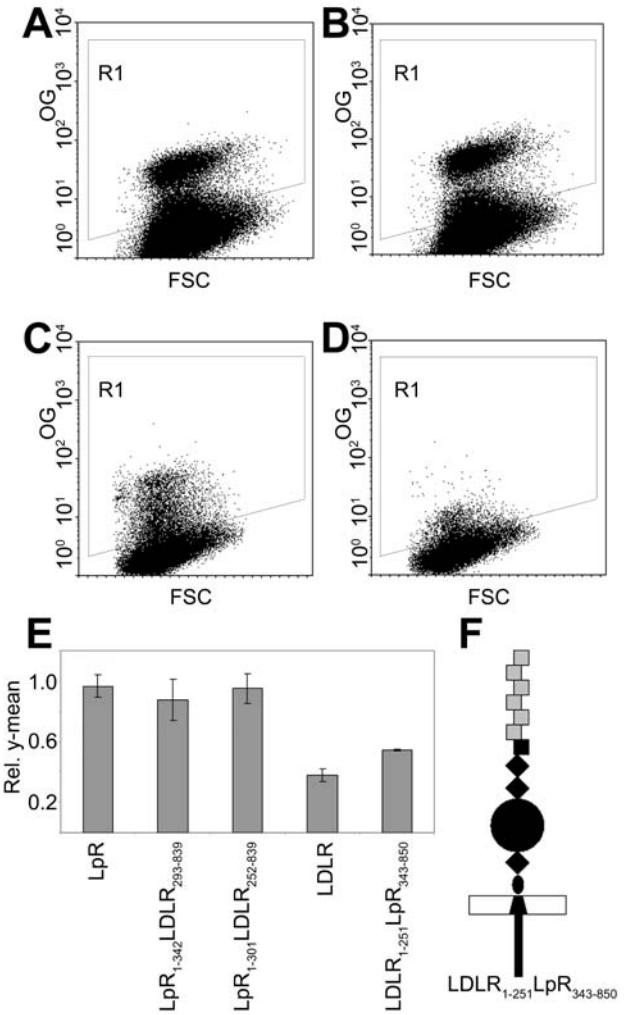

Figure 4. HDLp remains in complex with LA-1-7 of LpR after EDTA treatment. CHO(LpR) cells were incubated with OG-HDLp and washed with buffer of pH 7.4 without (A) or with (B) EDTA. Plot C and D show a similar experiment for binding of OG-LDL to cells transfected with LDLR, washed in the absence (C) and presence (D) of EDTA. E: Amount of bound OG-HDLp to LpR, $LpR_{1-342}LDLR_{293-839}$ or $LpR_{1-301}LDLR_{252-839}$ or of bound OG-LDL to LDLR (control) and $LDLR_{1-251}LpR_{302-850}$ after wash with EDTA. The mean fluorescence (y-mean) in R1 was determined for each sample. The relative y-mean (Rel. y-mean) after a wash with an EDTA-containing buffer was calculated by the formula: $y\text{-mean}_{EDTA}/y\text{-mean}_{pH7.4}$, and is plotted on the y-axis. Data represented are the mean of at least six independent experiments. Error bars indicate the s.e.m. See for more details the legend to Figure 1. F: Schematic model of $LDLR_{1-251}LpR_{302-850}$. LDLR domains are depicted in grey and LpR domains in black. See for more details the legend to Figure 3.

HDLp binding to LpR is not sensitive to EDTA

Ligand binding by LDLR family members is known to be dependent on Ca^{2+} [33,46], and the removal of Ca^{2+} from LDLR, e.g. by EDTA, prevents ligand binding[40]. To investigate whether the drop in Ca^{2+}-level that occurs in the early endosome could result in a disruption of the interaction between LpR and HDLp, LpR-transfected cells that had bound OG-HDLp were exposed to an EDTA-containing buffer (Figures 4A, B). After washing and subsequent endocytosis of bound ligand, the fluorescence of the cells was measured by flow cytometry. The mean fluorescence of cells that bound OG-HDLp did not change upon EDTA treatment, as 96.6 ± 7.5% of OG-HDLp remained bound to the receptor (Figure 4E), demonstrating that the complex was not disrupted. By contrast, when the same experimental approach was employed using the LDLR-LDL

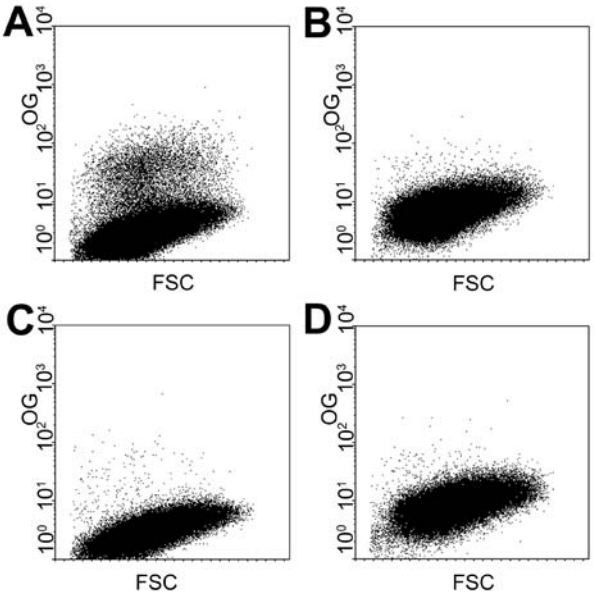

Figure 5. RAP competes with OG-HDLp for binding. CHO(LpR) cells were incubated with OG-HDLp (A) or OG-HDLp in the presence of RAP (B). Plots C and D were obtained by a similar experiment using untransfected cells incubated with OG-HDLp in the absence (C) or presence (D) of RAP. Plots are representative of three independent experiments. See for more details the legend of Figure 1.

complex as a control this resulted, as expected, in a significant decrease of receptor-bound LDL fluorescence (Figures 4C, D). Only 37.8 ± 4.1% of OG-LDL remained bound to the receptor (Figure 4E). This indicates that the low Ca^{2+} concentration in the early endosome is not able to induce dissociation of the LpR-HDLp complex. To determine whether the stability of the complex upon EDTA treatment is caused by the LA-repeats or by the two N-terminal EGF-repeats (EGF-A and EGF-B), that also contain a Ca^{2+} ion, similar experiments were executed with the hybrid receptors (Figure 3A). The interaction between HDLp and $LpR_{1\text{-}342}LDLR_{293\text{-}839}$ was not abrogated by EDTA treatment (Figure 4E). Since this receptor contains EGF-A and EGF-B of LDLR, this suggests that the stability results from the ligand-binding domain of LpR. In addition, the binding of HDLp to $LpR_{1\text{-}301}LDLR_{252\text{-}839}$ was shown to be EDTA-resistant, indicating that the resistance resides in the first seven LA-repeats of LpR. By contrast, the binding of LDL to the reciprocal hybrid receptor $LDLR_{1\text{-}251}LpR_{302\text{-}850}$ (Figure 4F), the ligand-binding domain of which is composed of the six most N-terminal LA-repeats of LDLR and LA-8 of LpR, was not EDTA-resistant (Figure 4E). Collectively, these results indicate that the EDTA resistance of the binding of HDLp to LpR is imparted by LA-1-7.

HDLp binding by LpR is similar to ligand binding by other LDLR family members

Since neither treatment with EDTA nor endosomal pH was able to disrupt the complex, the issue was addressed whether LpR binds HDLp in a different manner than other LDLR family members bind their ligands. Therefore, the ability of RAP,

Table 2. Binding efficiency of expressed receptors. CHO cells transfected with the different (hybrid) receptors were incubated with OG-LDL (LDLR, $LDLR_{1-251}LpR_{302-850}$) or with OG-HDLp (LpR, $LpR_{1-301}LDLR_{252-839}$, LpR_{splice}) or a primary antibody detected by a FITC-labeled secondary antibody. The percentage of cells that bound ligand relative to the percentage of cells that bound antibody was determined. The percentages shown are the means ± s.e.m. of at least five independent experiments.

Receptor	Binding efficiency
LDLR	96.1 ± 7.0%
$LDLR_{1-251}LpR_{302-850}$	58.7 ± 4.2%
LpR	91.5 ± 6.3%
$LpR_{1-301}LDLR_{252-839}$	84.4 ± 7.5%
LpR_{splice}	57.3 ± 5.9%

Figure 6. Sequence of LA-3 of a putative splice variant in LpR. Alignment of the sequences of LA-3 of wt LpR and LpR_{splice}. Amino acids are indicated by the single letter code, identical residues are boxed in black, conserved residues are shaded in grey. The arrow indicates the position of the central Trp (W) in the sequence of wt LpR.

a general ligand for LDLR family members[47-49], to compete with HDLp binding to LpR was assayed. LpR-transfected cells incubated with OG-HDLp in the presence of an equimolar concentration of RAP displayed a fluorescence similar to that of untransfected cells incubated with OG-HDLp and RAP (Figure 5), indicating that RAP completely blocked the binding of OG-HDLp to LpR. Thus, RAP and HDLp apparently use the same binding site. Therefore, LpR probably binds HDLp using the general concept for binding of ligands by LDLR family members[50,51].

LA-8 and EGF-A of LpR are not involved in the binding site of LpR for HDLp

To characterize the binding site for HDLp in LpR, the binding of OG-ligand by wt LpR was compared with the binding of OG-HDLp by $LpR_{1-301}LDLR_{252-839}$. To exclude that differences in ligand binding were caused by differences in receptor expression, binding of antibody to the receptor was used as a measure for the amount of receptor on the plasma membrane. After binding, cells were allowed to endocytose bound

ligand or antibody, by incubation of the cells at 37°C. Following endocytosis, the cells were trypsinized and the fluorescence analyzed by flow cytometry. As a control, the binding of OG-LDL to LDLR was compared to the binding of OG-LDL to $LDLR_{1-251}$ $LpR_{302-850}$. For wt LDLR, both ligand binding and antibody binding yielded similar numbers of fluorescent cells in R1 (Table 2), indicating that the amount of LDL binding was proportional to the amount of LDLR on the plasma membrane. However, in the case of the hybrid receptor $LDLR_{1-251}LpR_{302-850}$ (Figure 4F) of which the ligand-binding domain is composed of the six most N-terminal LA-repeats of LDLR and LA-8 of LpR, the number of cells that bound ligand was only 58.7 ± 4.2% of the number of cells that bound antibody. This suggests a reduction in affinity of the hybrid receptor for LDL, which may be expected since the binding site of LDLR for LDL encompasses LA-3-7 and EGF-A[52,53]. Despite the presence of LA-8 of LpR in this receptor, $LDLR_{1-251}LpR_{302-850}$ was not able to bind HDLp. Moreover, as was previously found for ligand binding to LpR and LDLR[14], also for binding to the other hybrid receptors the ligands are not interchangeable (data not shown[16]). Applied to the binding of HDLp to LpR, the number of cells that bound ligand was 91.5 ± 6.3% of the number of cells that bound antibody, showing that also for LpR the binding of HDLp is proportional to LpR expression. As for the hybrid receptor $LpR_{1-301}LDLR_{252-839}$, that contains LA-1-7 of LpR, followed by LA-7 of LDLR, the binding of HDLp yielded 84.4 ± 7.5% of fluorescent cells compared to the number of cells that bound antibody (Table 2). Since 84.4 ± 7.5% is not significantly lower than 91.5 ± 6.3% measured for LpR, this suggests that $LpR_{1-301}LDLR_{252-839}$ binds HDLp with a similar affinity as wt LpR. These results indicate that LA-7 and EGF-A of LDLR were able to replace the corresponding region of LpR (LA-8 and EGF-A) without disrupting the binding site for HDLp. This suggests that these repeats of LpR are not involved in the ligand-binding site of LpR, in contrast to the same structure (LA-7 and EGF-A) in LDLR.

LA-3 is involved in the binding site of LpR for HDLp

Recently a putative splice variant of LpR, LpR_{splice}, has been identified in ovaries of young animals (Kerver J. and Rodenburg K. W., unpublished results), in which the sequence of LA-3 is altered. Although sequence alignment revealed a high similarity between LA-3 of the two variants, the central tryptophan (Trp) present in LA-3 of wt LpR is absent in LA-3 of LpR_{splice} (Figure 6). Since the central Trp plays an important role in the interaction between LDLR family members and its ligands[51], it was investigated whether the binding of OG-HDLp to LpR_{splice} deviates from that to wt LpR. The binding of OG-HDLp to LpR_{splice} yielded only 57.3 ±6.9% of fluorescent cells compared to the number of cells that bound antibody (Table 2), implying that LpR_{splice} binds HDLp with a lower affinity than wt LpR. This indicates that LA-3 is involved in the binding of HDLp to wt LpR, suggesting that the Trp in wt LpR may be involved in the interface between HDLp and LpR.

LA-1 is not essential for binding of ligand to LpR

To further investigate which LA-repeats are involved in HDLp binding, it was tested whether the antibody 2189/90, directed against the first LA-repeat of LpR, was able to compete with HDLp for binding by LpR. After a pre-incubation with OG-HDLp at 4°C, followed by incubation with 2189/90 at 4°C, the fluorescence after uptake of the bound OG-HDLp appeared to be 73.2 ± 6.3% of the fluorescence of the cells in such an experiment without incubation with 2189/90. In a similar experiment in which the order of the incubations with OG-HDLp and 2189/90 was reversed, the fluorescence of the cells was 78.9 ± 7.0% of the fluorescence of cells incubated with OG-HDLp alone. Although the presence of antibody resulted in a significant decrease in fluorescence of the cells compared to cells that were incubated with OG-HDLp only, these results indicate that LpR is still able to efficiently bind a major amount of OG-HDLp in the presence of the antibody. Moreover, the amount of competition is similar to that in the corresponding control experiment using LDLR and C7, an antibody against the first repeat of LDLR (data not shown[54,55]). Since LA-1 of LDLR is not involved in LDL binding[53], the inhibition of binding measured is probably resulting from sterical hindrance due to the size of the antibody and not from competition for the same binding site. No competition was observed between RAP and the antibody (data not shown), suggesting that LA-1 is not involved in the binding of LpR to RAP or HDLp.

Discussion

Previous studies have demonstrated that in a mammalian model (CHO) cell line transfected with insect LpR, the receptor recycles its ligand, HDLp, in a transferrin-like manner, in contrast to endogenously expressed LDLR, the ligand of which (LDL) is released and undergoes intracellular degradation[14]. Also during insect development LpR appeared to function similarly, since HDLp internalized by fat body tissue from young adult locusts endogenously expressing LpR appeared to be resecreted, supporting the concept of LpR-mediated ligand recycling[12,18]. To investigate the mechanism underlaying the highly unusual behavior of this insect LDLR family member, we examined the stability of the binding of HDLp to LpR in direct comparison to that of LDL to LDLR and additionally explored the subset of structural features in LpR that may allow for the occurrence of the difference in ligand delivery compared to that in mammals.

Our present studies provide the new findings that the complex of LpR and HDLp is stable at endosomal pH and EDTA-resistant, both in contrast to the complex of LDLR and LDL. This stability of the LpR-HDLp complex is proposed to be caused by the specific interaction between HDLp and LA-repeats 2-7. Together, our data indicate that the complex of LpR and HDLp remains intact during its intracellular itinerary, which is in complete agreement with the occurrence of ligand recycling[14,16-18] and may provide a vital determinant to the ligand recycling capacity of LpR.

In several studies, flow cytometry has been used to quantify lipoprotein binding and uptake[29,55-61]. In most cases the experiments were performed on blood cells. Since these cells are already in suspension, they can be easily measured by flow cytometry. In the case of attached cells, resuspending the cells may destroy the interaction between receptor and ligand or antibody. For this reason the actual binding experiment was performed at 4°C to prevent endocytosis, so that equilibrium binding was achieved. After binding, the cells were allowed to endocytose bound ligand to protect it from the subsequent trypsin treatment. Fluorescence images of the cells after binding at 4°C and after endocytosis at 37°C showed that the bound ligand or antibodies were efficiently endocytosed, indicating that the amount of intracellular fluorescence was proportional to the amount of bound ligand at equilibrium (data not shown). For these experiments, stably transfected polyclonal cell lines were used to provide heterogeneous samples of cells that express the receptor. This resulted in flow cytometry plots containing at least two populations, one of which comprised cells of which the fluorescence did not exceed that of untransfected cells (Figure 1). In order to analyze only the cells that expressed the receptor, region 1 (R1) was defined to exclude the population of lower fluorescence intensity from the analysis (Figures 2 and 4). However, for LDLR, the decrease in fluorescence after treatment with pH 5.4 or EDTA resulted in a decrease of the number of cells in R1. Since this reduction in sample size introduced a bias in the analysis, the number of cells in the analysis was restored by using random measurements from the population of low intensity. After correction of the mean fluorescence, similar values for LDL release by LDLR were obtained as measured by Blacklow and colleagues for monoclonal cell lines[29]. The relative amount of dissociation was not affected by differences in receptor expression; we therefore conclude that the results obtained with the flow cytometric assay represent physiologically relevant receptor properties.

Our data indicate that, unlike the complex of LDLR and LDL, the complex of LpR and HDLp remains stable at a pH as low as 5.4 that is significantly lower than that encountered in endosomal pH (pH 6-6.5)[27]. This indicates that despite the substantial sequence similarity between LpR and LDLR, LpR is unable to release HDLp in the early endosome. LDLR is hypothesized to release LDL at endosomal pH by undergoing a conformational change in which the β-propeller displaces LDL[31]. Blacklow and colleagues elegantly identified domains and residues that are important for LDL release by LDLR[29,61] (Table 1). In agreement with these results, the β-propeller of LpR, lacking the important residues Gln-540, His-562, Glu-581 and Lys-582, was incapable of inducing LDL release. Similar results were obtained for the swap of the β-propeller of LDLR with β-propeller 4 of LDLR related protein 6 (LRP6), in which two Lys residues and one His residue are not conserved. However, when β-propeller 2 of LRP6 was introduced, containing these residues, the receptor was able to release LDL, indicating that a different β-propeller is able to substitute for the wt propeller of LDLR[29]. However, introducing the β-propeller of LDLR into LpR did not lead to HDLp release by the hybrid receptor $LpR_{1-342}LDLR_{293-839}$, implying that other domains

produce the remarkable stability of the complex. In LDLR, also the interface between LA-7 and EGF-A, the hinge region, plays an important role in LDL release, since this region functions as a rigid scaffold allowing the β-propeller to fold over the ligand-binding domain. To investigate the importance of this hinge region for the lack of HDLp release by LpR, both the hinge region and β-propeller of LDLR were introduced into LpR. The resulting hybrid receptor, $LpR_{1\text{-}301}LDLR_{252\text{-}839}$, did not release HDLp, despite the fact that this hybrid contains all the essential domains of LDLR for LDL release. This suggests that the β-propeller of LDLR is not able to compete with HDLp for binding to the ligand-binding domain of LpR, implying that the lack of HDLp release is mainly caused by the interaction between HDLp and the ligand-binding domain of LpR, and suggests that LpR may use a different mechanism to release HDLp, in contrast to the mechanism of LDL release by LDLR in which the β-propeller is of vital importance[28,29,62]. Interestingly, our earlier localization studies of the hybrid receptors revealed that the intracellular fate of the complex is determined by the extracellular domain as a whole[16]. In view of the mechanism of ligand recycling by LpR this implies that for the stability of the complex the ligand-binding domain is sufficient, however, for proper targeting of LpR to the ERC the combination of the ligand-binding domain and β-propeller of LpR is essential[16].

Ligand binding to LDLR family members is known to depend on Ca^{2+}, due to the stabilization of the LA-repeats by a central Ca^{2+} ion[33,34,36-39]. Sequence comparison of the LA-repeats of LpR with that of other LDLR family members, as well as modeling and molecular dynamics studies of LA-4-6 of LpR indicate that this also applies for the LA-repeats of LpR (Roosendaal S.D., Cuesta-López S., Sancho J. and Rodenburg K.W., unpublished results). In addition to a decrease in pH, the Ca^{2+} concentration in the early endosome drops within minutes to the low micromolar range[32], possibly contributing to ligand release by LDLR[33]. Therefore, the LpR-HDLp complex was exposed to a Ca^{2+}-chelating agent (viz. EDTA) to mimic the effect of low Ca^{2+} in the early endosome. In contrast to the binding of LDL to LDLR, the binding of HDLp to LpR appeared resistant to EDTA treatment. A possible explanation for this phenomenon might be that LpR binds HDLp by using a different binding mode than other LDLR family members use for binding of their ligands. For example, a different, Ca^{2+}-independent binding mode is used in the interaction between the single LA-repeat of Tva, the cellular receptor for subgroup A Rous sarcoma virus[63] and its ligand. However, since the ligand bound Tva with an aberrant binding mode, RAP appeared unable to compete with the ligand for binding to Tva[64]. Our studies show that RAP efficiently competes with HDLp for binding to LpR, indicating that HDLp binds LpR using the same binding mode as other ligands for LDLR family members, which again implies the presence of Ca^{2+} in LA-repeats of LpR. Therefore, the resistance of the LpR-HDLp complex may be caused by a higher affinity of the LA-repeats of LpR for Ca^{2+}, or by the ability of HDLp to shield the Ca^{2+} ions from EDTA. Although it is unclear what precisely causes this remarkable stability, our

data emerging from the use of hybrid receptors indicate that the stability of the complex at low pH and upon EDTA-treatment is caused by the interaction between HDLp and LA-1-7 of LpR. The general binding mode of LDLR family members and their ligands consists of an acidic binding pocket present in the LA-repeats that entraps a Lys residue from the ligand. The binding is augmented by an essential aromatic residue, preferentially Trp, of the LA-repeat, positioned next to the binding pocket[47,49,51,65]. To obtain more information about the recognition interface between LpR and HDLp, the LA-repeats of LpR were aligned with those of LDLR. This revealed that only LA-1-6 of LpR contain a central aromatic residue, in all cases Trp (data not shown). Since LA-1 appeared not to be involved in the binding site for HDLp, this suggests that only LA-2-6 are involved in the interface. LA-3 of wt LpR contains the central Trp, but importantly, in addition to other amino acid changes, LA-3 of LpR_{splice} lacks this Trp (Figure 6). Since LpR_{splice} binds HDLp with a lower affinity, indicating that LA-3 is involved in the interaction with HDLp, it may very well be that the absence of the Trp weakens the interaction between HDLp and LpR. In this respect it is interesting to note that the binding of HDLp to the splice variant is also resistant to low pH and EDTA treatment (data not shown). This suggests that the Trp and the other residues that are different between LA-3 of wt LpR and LpR_{splice} do not importantly determine the stability of the interaction at endosomal conditions. Additionally, from these results, it may be apparent that the stability of the complex at endosomal pH and upon EDTA treatment is not merely the result of the affinity of the interaction, but may require additional contacts or a slightly alternative binding mode of HDLp to LpR. An alternative mechanism for a stable complex at endosomal pH may be provided by the binding of proprotein convertase subtilisin type 9 (PCSK9) to LDLR. PCSK9 has been shown to be involved in the regulation of cell surface LDLR levels. After endocytosis, the LDLR-PCSK9 is not dissociated at endosomal pH. Instead, the affinity of PCSK9 for LDLR is enhanced by the low pH[66,67], possibly by protonation of the abundant His residues on the surface of PCSK9[67,68]. Even though HDLp binds to the LA-repeats of the receptor and PCSK9 to EGF-A of LDLR, similar effects may play a role in the stability of the complex of HDLp and LpR. An important difference is, however, that binding of PCSK9 seems to target LDLR to lysosomes for degradation[69,70], while the complex of HDLp and LpR is transported to the ERC for recycling.

The acidic residues involved in Ca^{2+}-ion binding of specific LA-repeats are proposed to interact with the basic residues of the ligand, in particular one protruding Lys[51]. A consensus sequence containing the protruding Lys was proposed, in which the Lys is surrounded by basic and hydrophobic residues[71,72]. Such sequences are numerously found in both apolipoproteins of HDLp, apoLp-I and apoLp-II. Interestingly, the three-dimensional model of their protein precursor apoLp-II/I reveals that at least one of these motifs is situated at the end of an α-helix[73], as is the case for the binding site of RAP and apoE for LDLR-related protein (LRP)[51]. Furthermore, this

helix is probably exposed on the surface of the HDLp particle, thus being available for interaction with LpR[73]. Because of the multitude of putative binding sites in apoLp-I and -II, it can not excluded that one HDLp particle binds several receptors concomitantly, as is the case for apoE containing lipoproteins[74,75]. In this respect it is important to note that also apoB-100, which is a homologue of apoLp-II/I[3,4] contains multiple of these consensus sequences (data not shown). However, LDL binds to LDLR with a stoichiometry of 1:1. Moreover, RAP is able to efficiently compete at equimolar concentrations with the binding of HDLp. Although several RAP molecules may be able to bind LpR, since RAP binds to two LA-repeats[51,76], competition binding studies indicated that RAP and antibody 2189/90 against LA-1 of LpR do not compete (data not shown), suggesting that RAP does not bind LA-1. Based on the presence of an important acidic residue[76], sequence analysis of the LA-repeats of LpR suggest that RAP may bind either LA-4-5 or LA-5-6, suggesting that the stoichiometry is one RAP molecule per LpR molecule. Therefore, it seems unlikely that LpR binds more than one HDLp molecule.

Conclusively, our results indicate that the interaction between HDLp and LA-2-7 of LpR is stable upon exposure to endosomal pH as well as EDTA treatment, implying that the integrity of the complex is maintained during intracellular trafficking of LpR and HDLp in LpR-transfected CHO cells and most likely also in insect cells. Similar to transferrin recycling, the intracellular transfer of lipid or other hydrophobic compounds from or to the HDLp particle may change its affinity for LpR, thus allowing HDLp resecretion. Indeed, binding studies using a partially delipidated HDLp particle revealed that the affinity of LpR for HDLp is modulated by the amount of lipids (Roosendaal S. D., Van Doorn J. M., Valentijn K. M., Van der Horst D. J., Rodenburg K. W, unpublished), suggesting that changes in lipid content may trigger HDLp resecretion. The stability of the complex and the modulation thereof may be determined by secondary contacts between HDLp and non-conserved residues of LpR. While the function of recycling of endocytosed lipoprotein ligand during insect development remains to be defined, our study uncovers the molecular mechanism underlying the stability of the LpR-HDLp complex that is likely to provide a crucial key to the process of ligand recycling, and might additionally help to explain the ability of LDLR family members to bind a wide range of structurally unrelated ligands.

Acknowledgements

We thank Steve Blacklow, Sander Meijer, Ineke Braakman, Jürgen Gent, Manon Wildenberg and Masja van Oort for stimulating discussions, Ger Arkesteijn for his help with flow cytometry, Wim Busschers for help with quantification of the flow cytometry data, and Santiago Cuesta-López and Javier Sancho for molecular dynamics studies on LA-4-6 of LpR.

References

1. Weers PM, Van Marrewijk WJ, Beenakkers AM & Van der Horst DJ (1993) Biosynthesis of locust lipophorin. Apolipophorins I and II originate from a common precursor. J Biol Chem 268, 4300-4303.
2. Bogerd J, Babin PJ, Kooiman FP, Andre M, Ballagny C, Van Marrewijk WJ & Van der Horst DJ (2000) Molecular characterization and gene expression in the eye of the apolipophorin II/I precursor from *Locusta migratoria*. J Comp Neurol 427, 546-558.
3. Babin PJ, Bogerd J, Kooiman FP, Van Marrewijk WJ & Van der Horst DJ (1999) Apolipophorin II/I, apolipoprotein B, vitellogenin, and microsomal triglyceride transfer protein genes are derived from a common ancestor. J Mol Evol 49, 150-160.
4. Mann CJ, Anderson TA, Read J, Chester SA, Harrison GB, Kochl S, Ritchie PJ, Bradbury P, Hussain FS, Amey J, Vanloo B, Rosseneu M, Infante R, Hancock JM, Levitt DG, Banaszak LJ, Scott J & Shoulders CC (1999) The structure of vitellogenin provides a molecular model for the assembly and secretion of atherogenic lipoproteins. J Mol Biol 285, 391-408.
5. Mahley RW & Innerarity TL (1983) Lipoprotein receptors and cholesterol homeostasis. Biochim Biophys Acta 737, 197-222.
6. Davidson NO & Shelness GS (2000) Apolipoprotein B: mRNA editing, lipoprotein assembly, and presecretory degradation. Annu Rev Nutr 20, 169-193.
7. Brown MS & Goldstein JL (1986) A receptor-mediated pathway for cholesterol homeostasis. Science 232, 34-47.
8. Ryan RO & Van der Horst DJ (2000) Lipid transport biochemistry and its role in energy production. Annu Rev Entomol 45, 233-260.
9. Van der Horst DJ, Van Marrewijk WJ & Diederen JH (2001) Adipokinetic hormones of insect: release, signal transduction, and responses. Int Rev Cytol 211, 179-240.
10. Van der Horst DJ, Van Hoof D, Van Marrewijk WJ & Rodenburg KW (2002) Alternative lipid mobilization: the insect shuttle system. Mol Cell Biochem 239, 113-119.
11. Van der Horst DJ, Ryan R.O. (2005) Lipid transport. In Comprehensive Molecular Insect Science (Gilbert L. Iatrou IK, Gill S. S., editors), 4, pp. 225-246. Elsevier, New York, NY, USA.
12. Dantuma NP, Pijnenburg MA, Diederen JH & Van der Horst DJ (1997) Developmental down-regulation of receptor-mediated endocytosis of an insect lipoprotein. J Lipid Res 38, 254-265.
13. Dantuma NP, Potters M, De Winther MP, Tensen CP, Kooiman FP, Bogerd J & Van der Horst DJ (1999) An insect homolog of the vertebrate very low density lipoprotein receptor mediates endocytosis of lipophorins. J Lipid Res 40, 973-978.
14. Van Hoof D, Rodenburg KW & Van der Horst DJ (2002) Insect lipoprotein follows a transferrin-like recycling pathway that is mediated by the insect LDL receptor homologue. J Cell Sci 115, 4001-4012.
15. Van Hoof D, Rodenburg KW & Van der Horst DJ (2003) Lipophorin receptor-mediated lipoprotein endocytosis in insect fat body cells. J Lipid Res 44, 1431-1440.
16. Van Hoof D, Rodenburg KW & Van der Horst DJ (2005) Intracellular fate of LDL receptor family members depends on the cooperation between their ligand-binding and EGF domains. J Cell Sci 118, 1309-1320.

17. Rodenburg KW & Van der Horst DJ (2005) Lipoprotein-mediated lipid transport in insects: analogy to the mammalian lipid carrier system and novel concepts for the functioning of LDL receptor family members. Biochim Biophys Acta 1736, 10-29.
18. Van Hoof D, Rodenburg KW & Van der Horst DJ (2005) Receptor-mediated endocytosis and intracellular trafficking of lipoproteins and transferrin in insect cells. Insect Biochem Mol Biol 35, 117-128.
19. Cheon H-M, Seo S-J, Sun J, Sappington TW & Raikhel AS (2001) Molecular characterization of the VLDL receptor homolog mediating binding of lipophorin in oocyte of the mosquito *Aedes aegypti*. Insect Biochem Mol Biol 31, 753-760.
20. Seo S-J, Cheon H-M, Sun J, Sappington TW & Raikhel AS (2003) Tissue- and stage-specific expression of two lipophorin receptor variants with seven and eight ligand-binding repeats in the adult mosquito. J Biol Chem 278, 41954-41962.
21. Lee CS, Han JH, Kim BS, Lee SM, Hwang JS, Kang SW, Lee BH & Kim HR (2003) Wax moth, *Galleria mellonella*, high density lipophorin receptor: alternative splicing, tissue-specific expression, and developmental regulation. Insect Biochem Mol Biol 33, 761-771.
22. Lee CS, Han JH, Lee SM, Hwang JS, Kang SW, Lee BH & Kim HR (2003) Wax moth, *Galleria mellonella* fat body receptor for high-density lipophorin (HDLp). Arch Insect Biochem Physiol 54, 14-24.
23. Gopalapillai R, Kadono-Okuda K, Tsuchida K, Yamamoto K, Nohata J, Ajimura M & Mita K (2006) Lipophorin receptor of *Bombyx mori*: cDNA cloning, genomic structure, alternative splicing, and isolation of a new isoform. J Lipid Res 47, 1005-1013.
24. Ciudad L, Belles X & Piulachs MD (2007) Structural and RNAi characterization of the German cockroach lipophorin receptor, and the evolutionary relationships of lipoprotein receptors. BMC Mol Biol 8, 53.
25. Herz J (2001) Deconstructing the LDL receptor--a rhapsody in pieces. Nat Struct Biol 8, 476-478.
26. Hobbs HH, Brown MS & Goldstein JL (1992) Molecular genetics of the LDL receptor gene in familial hypercholesterolemia. Hum Mutat 1, 445-466.
27. Maxfield FR & McGraw TE (2004) Endocytic recycling. Nat Rev Mol Cell Biol 5, 121-132.
28. Rudenko G, Henry L, Henderson K, Ichtchenko K, Brown MS, Goldstein JL & Deisenhofer J (2002) Structure of the LDL receptor extracellular domain at endosomal pH. Science 298, 2353-2358.
29. Beglova N, Jeon H, Fisher C & Blacklow SC (2004) Cooperation between fixed and low pH-inducible interfaces controls lipoprotein release by the LDL receptor. Mol Cell 16, 281-292.
30. Beglova N, Jeon H, Fisher C & Blacklow SC (2004) Structural features of the low-density lipoprotein receptor facilitating ligand binding and release. Biochem Soc Trans 32, 721-723.
31. Innerarity TL (2002) LDL Receptor's beta-propeller displaces LDL. Science 298, 2337-2339.
32. Gerasimenko JV, Tepikin AV, Petersen OH & Gerasimenko OV (1998) Calcium uptake via endocytosis with rapid release from acidifying endosomes. Curr Biol 8, 1335-1338.
33. Rudenko G & Deisenhofer J (2003) The low-density lipoprotein receptor: ligands, debates and lore. Curr Opin Struct Biol 13, 683-689.
34. Simonovic M, Dolmer K, Huang W, Strickland DK, Volz K & Gettins PG (2001) Calcium coordination and pH dependence of the calcium affinity of ligand-binding repeat CR7 from the LRP. Comparison with related domains from the LRP and the LDL receptor. Biochemistry 40, 15127-15134.

35. Malby S, Pickering R, Saha S, Smallridge R, Linse S & Downing AK (2001) The first epidermal growth factor-like domain of the low-density lipoprotein receptor contains a noncanonical calcium binding site. Biochemistry 40, 2555-2563.
36. Kurniawan ND, Atkins AR, Bieri S, Brown CJ, Brereton IM, Kroon PA & Smith R (2000) NMR structure of a concatemer of the first and second ligand-binding modules of the human low-density lipoprotein receptor. Protein Sci 9, 1282-1293.
37. North CL & Blacklow SC (2000) Solution structure of the sixth LDL-A module of the LDL receptor. Biochemistry 39, 2564-2571.
38. Fass D, Blacklow S, Kim PS & Berger JM (1997) Molecular basis of familial hypercholesterolaemia from structure of LDL receptor module. Nature 388, 691-693.
39. Huang W, Dolmer K & Gettins PGW (1999) NMR solution structure of complement-like repeat CR8 from the low density lipoprotein receptor-related protein. J Biol Chem 274, 14130-14136.
40. Schneider WJ, Beisiegel U, Goldstein JL & Brown MS (1982) Purification of the low density lipoprotein receptor, an acidic glycoprotein of 164,000 molecular weight. J Biol Chem 257, 2664-2673.
41. Goldstein JL, Brown MS, Anderson RG, Russell DW & Schneider WJ (1985) Receptor-mediated endocytosis: concepts emerging from the LDL receptor system. Annu Rev Cell Biol 1, 1-39.
42. Redgrave TG, Roberts DCK & West CE (1975) Separation of plasma lipoproteins by density-gradient ultracentrifugation. Anal Biochem 65, 42-49.
43. Kingsley DM & Krieger M (1984) Receptor-mediated endocytosis of low density lipoprotein: Somatic cell mutants define multiple genes required for expression of surface-receptor activity. Proc Natl Acad Sci USA 81, 5454-5458.
44. Beisiegel U, Schneider WJ, Goldstein JL, Anderson RG & Brown MS (1981) Monoclonal antibodies to the low density lipoprotein receptor as probes for study of receptor-mediated endocytosis and the genetics of familial hypercholesterolemia. J Biol Chem 256, 11923-11931.
45. Bauerfeind R & Komnick H (1992) Immunocytochemical localization of lipophorin in the fat body of dragonfly larvae (*Aeshna cyanea*). J Insect Physiol 38, 185-195.
46. Jeon H & Blacklow SC (2005) Structure and physiologic function of the low-density lipoprotein receptor. Annu Rev Biochem 74, 535-562.
47. Andersen OM, Benhayon D, Curran T & Willnow TE (2003) Differential binding of ligands to the apolipoprotein E receptor 2. Biochemistry 42, 9355-9364.
48. Bu G (2001) The roles of receptor-associated protein (RAP) as a molecular chaperone for members of the LDL receptor family. Int Rev Cytol 209, 79-116.
49. Andersen OM, Schwarz FP, Eisenstein E, Jacobsen C, Moestrup SK, Etzerodt M & Thogersen HC (2001) Dominant thermodynamic role of the third independent receptor binding site in the receptor-associated protein RAP. Biochemistry 40, 15408-15417.
50. Jensen GA, Andersen OM, Bonvin AM, Bjerrum-Bohr I, Etzerodt M, Thogersen HC, O'Shea C, Poulsen FM & Kragelund BB (2006) Binding site structure of one LRP-RAP complex: implications for a common ligand-receptor binding motif. J Mol Biol 362, 700-716.
51. Fisher C, Beglova N & Blacklow SC (2006) Structure of an LDLR-RAP complex reveals a general mode for ligand recognition by lipoprotein receptors. Mol Cell 22, 277-283.

52. Russell DW, Brown MS & Goldstein JL (1989) Different combinations of cysteine-rich repeats mediate binding of low density lipoprotein receptor to two different proteins. J Biol Chem 264, 21682-21688.
53. Esser V, Limbird LE, Brown MS, Goldstein JL & Russell DW (1988) Mutational analysis of the ligand binding domain of the low density lipoprotein receptor. J Biol Chem 263, 13282-13290.
54. Nguyen AT, Hirama T, Chauhan V, Mackenzie R & Milne R (2006) Binding characteristics of a panel of monoclonal antibodies against the ligand binding domain of the human LDLr. J Lipid Res 47, 1399-1405.
55. Nagele H, Gebhardt A, Niendorf A, Kroschinski J & Zeller W (1997) LDL receptor activity in human leukocyte subtypes: regulation by insulin. Clin Biochem 30, 531-538.
56. Iwasaki T, Takahashi S, Ishihara M, Takahashi M, Ikeda U, Shimada K, Fujino T, Yamamoto TT, Hattori H & Emi M (2004) The important role for betaVLDLs binding at the fourth cysteine of first ligand-binding domain in the low-density lipoprotein receptor. J Hum Genet 49, 622-628.
57. Maczek C, Recheis H, Bock G, Stulnig T, Jurgens G & Wick G (1996) Comparison of low density lipoprotein uptake by different human lymphocyte subsets: a new method using double-fluorescence staining. J Lipid Res 37, 1363-1371.
58. Mazurov AV, Preobrazhensky SN, Leytin VL, Repin VS & Smirnov VN (1982) Study of low density lipoprotein interaction with platelets by flow cytofluorimetry. FEBS Lett 137, 319-322.
59. Raungaard B, Heath F, Brorholt-Petersen JU, Jensen HK & Faergeman O (1998) Flow cytometry with a monoclonal antibody to the low density lipoprotein receptor compared with gene mutation detection in diagnosis of heterozygous familial hypercholesterolemia. Clin Chem 44, 966-972.
60. Hattori H, Hirayama T, Nobe Y, Nagano M, Kujiraoka T, Egashira T, Ishii J, Tsuji M & Emi M (2002) Eight novel mutations and functional impairments of the LDL receptor in familial hypercholesterolemia in the north of Japan. J Hum Genet 47, 80-87.
61. Boswell EJ, Jeon H, Blacklow SC & Downing AK (2004) Global defects in the expression and function of the low density lipoprotein receptor (LDLR) associated with two familial hypercholesterolemia mutations resulting in misfolding of the LDLR epidermal growth factor-AB pair. J Biol Chem 279, 30611-30621.
62. Davis CG, Goldstein JL, Sudhof TC, Anderson RG, Russell DW & Brown MS (1987) Acid-dependent ligand dissociation and recycling of LDL receptor mediated by growth factor homology region. Nature 326, 760-765.
63. Yu X, Wang Q-Y, Guo Y, Dolmer K, Young JAT, Gettins PGW & Rong L (2003) Kinetic analysis of binding interaction between the Subgroup A Rous Sarcoma Virus Glycoprotein SU and its cognate receptor Tva: calcium is not required for ligand binding. J Virol 77, 7517-7526.
64. Contreras-Alcantara S, Godby JA & Delos SE (2006) The single ligand-binding repeat of Tva, a low density lipoprotein receptor-related protein, contains two ligand-binding surfaces. J Biol Chem 281, 22827-22838.
65. Andersen OM, Petersen HH, Jacobsen C, Moestrup SK, Etzerodt M, Andreasen PA & Thogersen HC (2001) Analysis of a two-domain binding site for the urokinase-type plasminogen activator-plasminogen activator inhibitor-1 complex in low-density-lipoprotein-receptor-related protein. Biochem J 357, 289-296.

66. Zhang DW, Lagace TA, Garuti R, Zhao Z, McDonald M, Horton JD, Cohen JC & Hobbs HH (2007) Binding of proprotein convertase subtilisin/kexin type 9 to epidermal growth factor-like repeat A of low density lipoprotein receptor decreases receptor recycling and increases degradation. J Biol Chem 282, 18602-18612.
67. Cunningham D, Danley DE, Geoghegan KF, Griffor MC, Hawkins JL, Subashi TA, Varghese AH, Ammirati MJ, Culp JS, Hoth LR, Mansour MN, McGrath KM, Seddon AP, Shenolikar S, Stutzman-Engwall KJ, Warren LC, Xia D & Qiu X (2007) Structural and biophysical studies of PCSK9 and its mutants linked to familial hypercholesterolemia. Nat Struct Mol Biol 14, 413-419.
68. Piper DE, Jackson S, Liu Q, Romanow WG, Shetterly S, Thibault ST, Shan B & Walker NPC (2007) The crystal structure of PCSK9: a regulator of plasma LDL-cholesterol. Structure 15, 545-552.
69. Horton JD, Cohen JC & Hobbs HH (2007) Molecular biology of PCSK9: its role in LDL metabolism. Trends Biochem Sci 32, 71-77.
70. McNutt MC, Lagace TA & Horton JD (2007) Catalytic activity is not required for secreted PCSK9 to reduce low density lipoprotein receptors in HepG2 cells. J Biol Chem 282, 20799-20803.
71. Li A, Sadasivam M & Ding JL (2003) Receptor-ligand interaction between vitellogenin receptor (VtgR) and vitellogenin (Vtg), implications on low density lipoprotein receptor and apolipoprotein B/E. The first three ligand-binding repeats of VtgR interact with the amino-terminal region of Vtg. J Biol Chem 278, 2799-2806.
72. Nielsen KL, Holtet TL, Etzerodt M, Moestrup SK, Gliemann J, Sottrup-Jensen L & Thogersen HC (1996) Identification of residues in alpha-macroglobulins important for binding to the alpha2-macroglobulin receptor/low density lipoprotein receptor-related protein. J Biol Chem 271, 12909-12912.
73. Smolenaars MM, Kasperaitis MA, Richardson PE, Rodenburg KW & Van der Horst DJ (2005) Biosynthesis and secretion of insect lipoprotein: involvement of furin in cleavage of the apoB homolog, apolipophorin-II/I. J Lipid Res 46, 412-421.
74. Pitas RE, Innerarity TL & Mahley RW (1980) Cell surface receptor binding of phospholipid-protein complexes containing different ratios of receptor-active and -inactive E apoprotein. J Biol Chem 255, 5454-5460.
75. Pitas RE, Innerarity TL, Arnold KS & Mahley RW (1979) Rate and equilibrium constants for binding of apo-E HDLc (a cholesterol-induced lipoprotein) and low density lipoproteins to human fibroblasts: evidence for multiple receptor binding of apo-E HDLc. Proc Natl Acad Sci USA 76, 2311-2315.
76. Andersen OM, Christensen LL, Christensen PA, Sorensen ES, Jacobsen C, Moestrup SK, Etzerodt M & Thogersen HC (2000) Identification of the minimal functional unit in the low density lipoprotein receptor-related protein for binding the receptor-associated protein (RAP). A conserved acidic residue in the complement-type repeats is important for recognition of RAP. J Biol Chem 275, 21017-21024.

3

Lipid unloading of lipophorin affects its binding to the insect LDL receptor homologue, LpR: implications for the role of LpR-mediated endocytosis

Sigrid D. Roosendaal[1], Jan M. Van Doorn[1], Karine M. Valentijn[2], Dick J. Van der Horst[1] and Kees W. Rodenburg[1]

[1]Division of Endocrinology and Metabolism, Department of Biology and Institute of Biomembranes, Utrecht University, The Netherlands; and [2]Department of Molecular Cell Biology, Section Electron Microscopy, Leiden University Medical Center, The Netherlands

Submitted for publication

Abstract

The insect LDL receptor (LDLR) homologue, LpR, is able to bind and endocytose the insect lipoprotein, high-density lipophorin (HDLp). However, the ligand is not lysosomally degraded, but recycled in a transferrin-like manner, leaving the function of HDLp endocytosis to be uncovered. Since a hallmark of HDLp is its ability to function as a reusable shuttle that selectively loads and unloads lipids at target tissues, circulatory HDLp exists in several forms with respect to lipid loading. To investigate whether lipid content affects binding and subsequent endocytosis by LpR, HDLp was partially delipidated *in vitro* by incubation with α-cyclodextrin, yielding a particle of a buoyant density of 1.17 g/ml (HDLp-1.17). Binding experiments demonstrated that LpR bound HDLp-1.17 with a substantially higher affinity than HDLp both in LpR-transfected Chinese hamster ovary (CHO) cells and isolated insect fat body tissue endogenously expressing LpR. Similar to HDLp, HDLp-1.17 was targeted to the endocytic recycling compartment (ERC) after endocytosis in CHO(LpR) cells. The complex of HDLp-1.17 and LpR appeared to be resistant to endosomal pH, as was recently demonstrated for the LpR-HDLp complex, corroborating that HDLp-1.17 is recycled similar to HDLp, a conclusion that was further supported by the observation of a significant decrease with time of HDLp-1.17-containing vesicles after endocytosis of HDLp-1.17 in LpR-expressing insect fat body tissue. Collectively, our results indicate that LpR favors the binding and subsequent endocytosis of HDLp-1.17, suggesting a physiological role for LpR in the selective endocytosis and recycling of relatively lipid-unloaded HDLp particles, while lipid reloading during their intracellular itinerary might result in decreased affinity for LpR.

Introduction

Lipoproteins transport lipids and other hydrophobic compounds in the aqueous circulation of vertebrates as well as invertebrates. Whereas mammals rely on an array of lipoproteins, insect blood (hemolymph) generally contains relatively large quantities of a single multifunctional lipoprotein particle, lipophorin. The lipid components of lipophorin typically comprise diacylglycerols (DAG) in addition to phospholipids (PL), sterols, carotenoids and hydrocarbons[1,2]. The structural apolipoprotein components of the lipophorin particle consist of single copies of apolipophorin I and apolipophorin II (apoLp-I and apoLp-II), which are derived from the post-translational cleavage of their common precursor, apoLp-II/I[3-5]. ApoLp-II/I was demonstrated to be a homologue of apolipoprotein B-100 (apoB-100)[6,7], the structural protein component of mammalian lipoproteins such as low-density lipoprotein (LDL) and very-low-density lipoprotein (VLDL)[8,9]. Lipophorin is synthesized in the insect fat body, an organ combining the functions of mammalian liver and adipose tissue[10] which, similar to mammalian adipose tissue, retains large intracellular depots of triacylglycerols (TAG) that provide fuel for energy-demanding tissues including the flight muscles. In the resting situation, most particles fall within the density limits 1.21 and 1.07 g/ml and are defined as high-density lipophorin (HDLp)[2]. Circulatory HDLp is able to selectively load and unload lipids at different target tissues without being endocytosed or degraded[2,11]. This concept of lipophorin as a reusable lipid shuttle implies that, depending on physiological or developmental needs for lipid distribution, lipophorin in the hemolymph may exist in several forms with respect to relative lipid content, leading to differences in size and density of the particle.

In the face of this mechanism of lipid transport accomplished by HDLp as a reusable lipid shuttle, the identification of an HDLp receptor (LpR) in the fat body of young locusts that is able to endocytose HDLp[12] suggested that receptor-mediated uptake of HDLp may provide an additional mechanism implicated in lipid delivery during developmental periods. Sequence analysis demonstrated LpR to be a homologue of the LDL receptor (LDLR) and to consist of all the typical domains of a classical LDLR family member[12]. Generally, after internalization of an LDLR family member-ligand complex, receptor and ligand dissociate upon exposure to the slightly acidic pH of the endosomal environment, finally leading to recycling of the receptor back to the cell surface, while the ligand is degraded in lysosomes[13,14]. However, earlier studies from our group showed that HDLp follows a different pathway since the complex of LpR and HDLp is targeted to the endocytic recycling compartment (ERC)[15,16] from which the lipophorin is resecreted[17,18] in a manner similar to that of transferrin[15,17]. The function of this recycling of HDLp is however unknown. Since LpR is only expressed during developmental stages of larval and young adult locusts or re-induced after starvation, it was hypothesized that endocytosis of HDLp by LpR might be important to rapidly replenish the depleted fat body reserves once lipids

from dietary intake are available[18,19]. These findings are suggestive of a mechanism in which endocytosed HDLp unloads (part of) its lipid cargo in fat body cells prior to being recycled into the circulation, highlighting once more the function of HDLp as a reusable particle that is iteratively present in a relatively lipid-loaded and a lipid-unloaded form. To obtain more insight into the rationale of LpR-mediated HDLp endocytosis, partially delipidated HDLp of a buoyant density of 1.17 g/ml (HDLp-1.17) was produced *in vitro* by incubation of (native) HDLp (buoyant density 1.11 g/ml) with α-cyclodextrin, whereafter the binding characteristics of the interaction between HDLp and LpR or partially delipidated HDLp and LpR were compared. The results provide the unexpected new finding that after partial lipid extraction, HDLp bound to LpR with a higher affinity. However, neither the stability of the complex of HDLp-1.17 and LpR at endosomal pH, nor the localization and the fate of the lipoprotein in insect tissue as well as in LpR-transfected Chinese hamster ovary (CHO) cells appeared to be affected in comparison to the LpR-HDLp complex, suggesting that lipid-depleted HDLp is equally recycled. These findings propose that LpR favors the endocytosis of HDLp particles of relatively low lipid content. This specificity of LpR sheds new light upon the function of LpR and the mechanism of HDLp recycling.

Materials and Methods

Reagents and proteins

α-Cyclodextrin (Sigma) and SIGMAFAST™ OPD (o-Phenylenediamine dihydrochloride) (Sigma) were commercially obtained. Locust (*Locusta migratoria*) HDLp was isolated as described previously[15]. In brief, HDLp was isolated by subjecting collected hemolymph of adult animals (12 to 15 days after imaginal ecdysis) to density gradient ultracentrifugation. Tetra-methyl rhodamine-labeled transferrin (TMR-Tf) was purchased from Molecular Probes. Antibodies were raised against synthetic peptides representing the very N- and C-terminal 20 amino acids of apoLp-I and the C-terminus of apoLp-II, i.e. anti-IIC against a.a. 702-720, anti-IN against a.a. 721-739 and anti-IC against a.a. 3362-3380 of apoLp-II/I (GenBank accession CAB51918.1). Antibodies were purified from rabbit sera using CNBr-activated Sepharose 4 Fast Flow (Amersham Pharmacia Biotech) according to manufacturer's instructions.

Partial delipidation of HDLp

Incubation of HDLp with α-cyclodextrin was performed as described by Jouni *et al.*[20]. Shortly, HDLp was incubated in 40 mM of α-cyclodextrin in PBS for 15 min on

a head over head rotator (80 rpm) at room temperature. Subsequently, the turbid solution was centrifuged at 10,000 rpm for 10 min. The supernatant was subjected to density gradient ultracentrifugation on a KBr gradient (1.25 to 1.05 g/ml). The fractions containing protein were pooled, concentrated and used for analysis. The partially delipidated HDLp fraction was recovered at a density of 1.17 g/ml and designated HDLp-1.17.

Estimation of HDLp-1.17 molecular weight by HPLC analysis

Samples of HDLp or HDLp-1.17 (200-400 µg) were applied to a Superose-12 column in buffer containing 130 mM NaCl, 5 mM KCl, 1.7 mM K_2HPO_4, 1.9 mM NaH_2PO_4 and 5 mM EDTA, pH 7.4. Samples were eluted in the same buffer and the protein content (280 nm) of the fractions was measured using an ÄKTA Explorer chromatography system (Pharmacia). Based on the difference in elution time between HDLp-1.17 and HDLp, the molecular weight (MW) of HDLp-1.17 was estimated to be approximately 400 kDa.

Determination of lipid classes

The lipids of 4 mg HDLp or HDLp-1.17 were extracted with chloroform-methanol according to the method of Bligh and Dyer[21]. Lipid classes were separated by thin layer chromatography (TLC) on silica gel plates using the method of Freeman and West[22]. Individual lipid classes were visualized by spraying the plates with 3% cupric(II) acetate in 8% H_3PO_4 and heating at 180°C for 15 min, according to the method of Fewster and co-workers[23]. DAG and PL were quantified by densitometric analysis of images of TLC plates from at least three independent experiments using Quantity One 4.6.3 Basic software (BioRad; available on the Internet at www.bio-rad.com).

Electron microscopy

HDLp-1.17 was diluted to a concentration of 20 µg/ml in buffer (130 mM NaCl, 5 mM KCl, 1.7 mM K_2HPO_4, 1.9 mM NaH_2PO_4, 5 mM EDTA, pH 7.4) and immediately adsorbed to glow-discharged carbon-coated copper grids. Grids were stained with a drop of freshly prepared 2% phospho-tungsten acid. The specimen was inspected with a FEI Tecnai 12 electron microscope operated at 120 kV. Images were recorded at a magnification of 68,000 x on a FEI Eagle CCD 4K x 4K camera, with a specimen pixel size of 1.65 Å at specimen level. Using these images, the length and width of the particles (pixels) was determined and converted to Å using Adobe Photoshop professional.

Cell culture

LDLR-deficient CHO(*ldlA*) cells[24] were cultured in 25 cm^2 polystyrene culture flasks in growth medium (Ham F-10 nutrient mixture (GibcoBRL) supplemented medium, containing 5% heat-inactivated fetal bovine serum (FBS, GibcoBRL) and 100 U/ml penicillin G sodium and 100 µg/ml streptomycin sulfate in 85% saline (GibcoBRL)). The cells were maintained at 37°C and 5% CO_2.

Transfections

LDLR-deficient CHO(*ldlA*) cells[24] were grown until 40% confluency in 12-well multi-dishes (Costar). After washing the cells once, the growth medium was replaced with 500 µl of fresh growth medium. Subsequently, 4 µg DNA and 4 µg polyethylenimine in 50 µl serum-free medium (Ham F-10 nutrient mixture supplemented medium with 100 U/ml penicillin G sodium and 100 µg/ml streptomycin sulfate in 85% saline) was administered to the cells. After 4 h, 500 µl growth medium was added and cells were cultured overnight. The next day, cells were detached from dishes and cultured in 25 cm^2 culture flasks in growth medium supplemented with 400 µg/ml geneticin (GibcoBRL). Ten days after transfection cells were used for experiments.

Fluorescence labeling

HDLp and HDLp-1.17 were covalently labeled with Oregon green (OG) 488 carboxylic acid (Molecular Probes) as described previously[15].

Binding experiments using flow cytometry

Binding experiments were performed as described earlier[16]. In short, LpR-transfected CHO(*ldlA*) cells (CHO(LpR) cells) were washed with ice-cold binding buffer (50 mM Tris-HCl, 2 mM $CaCl_2$, 150 mM NaCl, pH 7.4) and subsequently incubated on ice with OG-HDLp or OG-HDLp-1.17 (25 µg/ml) in binding buffer for 30 min. After binding, cells were washed and incubated with binding buffer or low-pH buffer (25 mM Tris, 25 mM sodium succinate, 2 mM $CaCl_2$, 150 mM NaCl, pH 5.4, 4°C) for 30 min on ice. Subsequently, the cells were incubated with serum-free medium for 5 min at 37°C, to allow the bound ligand to be endocytosed. After endocytosis, the cells were detached from dishes by trypsin treatment and resuspended in growth medium. Resuspended cells were fixed in 0.5% paraformaldehyde (PFA) in PBS at 4°C for at least 30 min to overnight. Samples were measured using a fluorescence-activated cell sorter (FACS, Becton Dickinson FACS Calibur). Flow cytometry data were collected using Cell Quest (Becton Dickinson) and downloaded into the program WinMDI (TSRI FACS Core Facility, La Jolla, CA) for analysis.

Competition binding experiments

Competition binding experiments were performed similarly to the binding experiments. However, during binding of OG-HDLp or OG-HDLp-1.17 equimolar concentrations or a five-fold excess of unlabeled HDLp or HDLp-1.17 were added. The degree of binding was compared to the degree of binding without addition of unlabeled HDLp or HDLp-1.17.

Flow cytometry data analysis

Flow cytometry data were quantified as descried earlier[16]. In brief, for each sample (~ 100,000 cells) the fluorescence was plotted against the forward scatter (FSC). For each series of experiments, the region containing cells that bound and endocytosed OG-ligand (Region 1, R1) was defined in the plot based on a similar experiment performed using untransfected cells. Then the number of cells and the mean fluorescence (y-mean) in R1 were determined. For each cell line, the number of cells in R1 after different treatments was compared by a t-test for paired samples performed on the logarithms of the number of cells. In case of a significant ($p \leq 0.05$) difference in sample size due to the different treatments, the y-mean was corrected by using random values of the missing number of cells from the population of which the fluorescence did not exceed that of untransfected cells (outside R1). To test whether samples were significantly different from control samples, a t-test for paired samples was performed on the logarithms of the y-means. As negative control, for each sample the y-mean outside R1, i.e. of cells of which the fluorescence intensity did not exceed that of untransfected cells, was determined and compared between different treatments. For each sample the relative amount of fluorescence as compared to control samples was determined. Data presented as means of these relative values ± s.e.m. were obtained from at least three independent experiments.

Pulse-chase of OG-HDLp-1.17 in CHO(LpR) cells

Pulse-chase experiments were performed as described[15,17]. In short, CHO(LpR) cells were incubated with OG-HDLp-1.17 (25 µg/ml) and TMR-Tf (25 µg/ml) in hepes buffer (10 mM HEPES, 50 mM NaCl, 10 mM KCl, 5mM $CaCl_2$, 2 mM $MgSO_4$, pH 7.4) for 15 min at 37°C. Subsequently, cells were chased in serum-free medium for indicated time periods. After rinsing, cells were fixed in 4% PFA and examined by confocal fluorescence microscopy.

In vitro incubation of fat body tissue with fluorescently labeled ligands

Fat body tissue was excised from adult locusts two days after ecdysis. After rinsing the fat body tissue in hepes buffer (10 mM HEPES, 50 mM NaCl, 10 mM KCl, 5 mM $CaCl_2$, 2 mM $MgSO_4$, pH 7.4), tissue was incubated with OG-HDLp or OG-HDLp-1.17 (25 µg/ml) in hepes buffer for 30 min at 27°C. During competition binding experiments equimolar concentrations or a ten-fold excess of unlabeled HDLp or HDLp-1.17 was added. After incubation, the tissue was rinsed in PBS and immediately fixed in 4% PFA in PBS for 30 min at room temperature. Alternatively, after incubation in the presence of OG-ligand, the tissue was rinsed and incubated in insect-Xpress medium (Cambrex) for indicated time periods. After fixation the tissue was mounted in mowiol and examined on a fluorescence Axioscope microscope (Zeiss).

Immunoreactivity of HDLp

The immunoreactivity of HDLp and HDLp-1.17 with different antibodies was tested using an adapted protocol of the assay described by Chauhan *et al.*[25]. High-binding microplates (Costar) were coated with 200 µl of HDLp solution (30 µg/ml, PBS, pH 7.4) overnight at 4°C and subsequently the coating was saturated by incubations with 1% bovine serum albumin (BSA) in PBS for two hours at room temperature. Serial dilutions of HDLp or HDLp-1.17 were prepared and mixed with antibody appropriately diluted in PBS containing 1% BSA. The mixtures were incubated overnight at 4°C. Aliquots of the lipophorin-antibody mixture were transferred to the microplates and incubated for 1h at room temperature. Subsequently, the plates were washed with PBS containing 0.1% Tween-20 and incubated with a peroxidase-labeled secondary goat-anti-rabbit antibody for 30 min in PBS containing 0.1% BSA and 0.1% Tween-20. After washing with PBS containing 0.1% Tween-20 the bound secondary antibody was detected using SIGMAFAST™ OPD according to manufacturer's protocol. The amount of antibody binding in the absence of lipophorin in solution was set to 1. Relative values were calculated for each experiment. A (dose-response) model was fitted to the relative values and the statistical analysis was performed using the PROAST software running in S-Plus[26]. Statistically significant differences between HDLp and HDLp-1.17 were determined according to the likelihood ratio test ($p \leq 0.05$).

Results

Incubation of HDLp with α-cyclodextrin

To obtain lipophorin particles of which the lipid content was experimentally decreased, isolated HDLp was incubated with α-cyclodextrin[20]. α-Cyclodextrin-treated HDLp was subsequently isolated by re-subjection to density gradient ultracentrifugation. Both untreated HDLp and α-cyclodextrin-treated HDLp were recovered as sharp, yellow colored bands (Figure 1). Density measurements revealed a buoyant density of 1.172 ± 0.004 g/ml for the peak fraction of α-cyclodextrin-treated HDLp, whereas untreated HDLp was recovered at its normal density of approximately 1.11 g/ml[27-29]. Based on its buoyant density, α-cyclodextrin-treated HDLp was designated HDLp-1.17. Protein analysis by SDS-PAGE revealed an identical apolipoprotein profile (i.e. ~ 220 kDa apoLp-I and ~ 75 kDa apoLp-II) for HDLp-1.17 and HDLp (data not shown). Comparison of the lipid composition of HDLp-1.17 with that of HDLp revealed that particularly DAG and PL were extracted from HDLp by α-cyclodextrin, while the amount of other lipids did not significantly change (Figure 2), which is in line with other studies using α-cyclodextrin for lipid extraction[30]. Based on densitometric analysis, HDLp-1.17 comprised 53.1 ± 9.6% less DAG and 79.9 ± 2.9% less PL per µg protein than untreated HDLp, which would result in a 53.6% decrease in total lipid content, according to the lipid composition of HDLp[31]. Using gel filtration analysis, HDLp-1.17 appeared to elute as a single peak with an approximate MW of 400 kDa (data not shown), implying a decrease of ~ 20 % in MW compared to that of HDLp (MW ~ 500 kDa). Measurements of electron microscopy images of HDLp-1.17 (Figure 3) indicated a particle size of 13 ± 2 nm by 9 ± 2 nm (n = 100), which is smaller than untreated HDLp, that has been reported as an oval-shaped particle of ca. 19 ± 2 nm by 15 ± 2 nm[32] while in earlier studies by our laboratory, HDLp had emerged as a spherical particle with a diameter of approximately 17 nm[33]. In addition to its size, the morphology of HDLp-1.17 appears to differ from that of HDLp, since the oval shape of HDLp-1.17 particles is more irregular and sometimes bended, resulting in a crescent-shape (Figure 3).

Binding of OG-HDLp-1.17 to LpR

To characterize binding and endocytosis of HDLp-1.17 by LpR quantitatively, HDLp and HDLp-1.17 were labeled with Oregon green (OG). Since the decreased lipid content of HDLp-1.17 might lead to additional exposure of protein and OG is known to covalently modify mainly lysine residues[15], per lipophorin particle more lysine residues might be labeled in HDLp-1.17 than in HDLp. However, quantitative fluorescence measurements of OG-HDLp and OG-HDLp-1.17 performed using a fluorescence microplate reader indicated that OG-HDLp and OG-HDLp-1.17 contained equal amounts of fluorescence per µg protein, suggesting that both

Figure 1. Incubation of HDLp with α-cyclodextrin. Banding pattern after buoyant density gradient ultracentrifugation of α-cyclodextrin treated (+) and untreated (-) HDLp. On the left the buoyant densities are indicated.

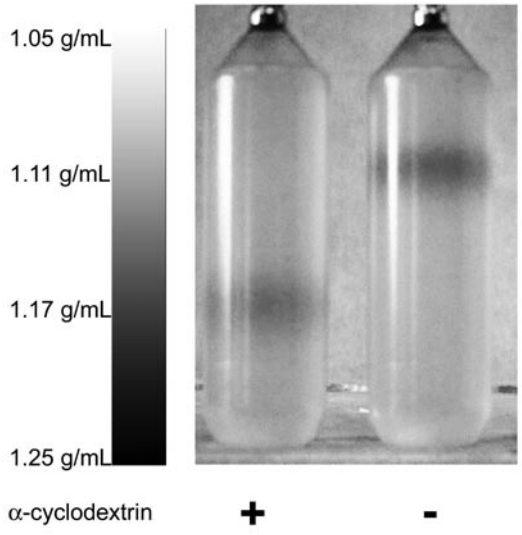

Figure 2. Lipid composition of HDLp and HDLp-1.17. Separation of total lipids extracted from equal amounts of lipoprotein samples (based on protein content) on silica gel TLC, showing the lipid classes of HDLp (left) and HDLp-1.17 (right). The different lipid classes are indicated on the left, abbreviations used are: TAG, triacylglycerol; DAG, diacylglycerol; FFA, free fatty acids; PL, phospholipids. FFA are recovered on the silica gel at the front (visible as a thin band) of the acidic acid present in the first solvent system.

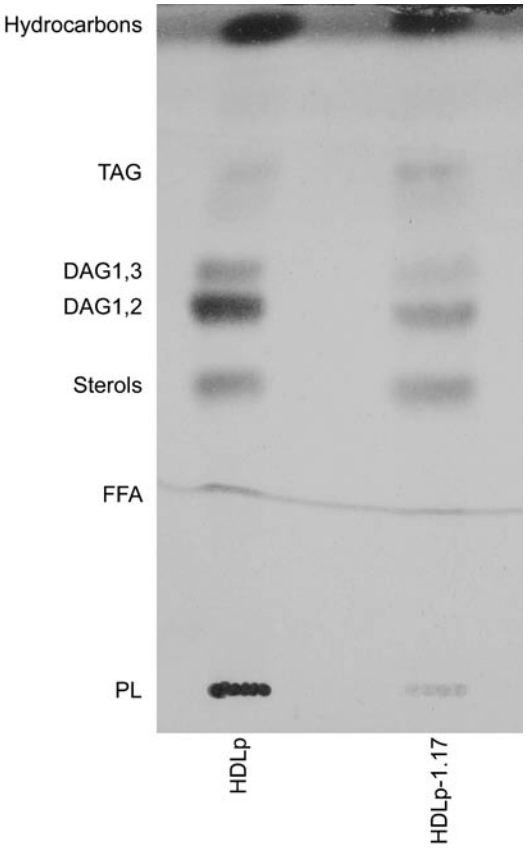

lipophorin particles were labeled to the same degree (data not shown). The results of experiments determining the binding and subsequent endocytosis of OG-HDLp and OG-HDLp-1.17 by LpR could therefore be directly compared quantitatively. To this end, LpR(CHO) cells were incubated with equimolar amounts of either of the labeled lipophorins. After binding of ligand at 4°C, the LpR-lipophorin complex was endocytosed by incubation of the cells at 37°C and the fluorescence of the cells was analyzed by flow cytometry. Since polyclonal cell lines were used, this resulted in a dotplot displaying at least two populations of cells with different fluorescence intensities (Figure 4A): the population in R1 consists of LpR-transfected cells that bound and endocytosed OG-ligand, while the population below R1 contains LpR-transfected cells of which the fluorescence does not exceed that of untransfected cells and therefore was used as an internal negative control[16]. The mean fluorescence of the cells in R1 appeared lower for endocytosed OG-HDLp (Figure 4A) than for OG-HDLp-1.17 (Figure 4B). Quantification of the mean fluorescence (y-mean) in R1 (Figures 4A, B) showed that the y-mean of cells that bound OG-HDLp-1.17 was three-fold higher than that of cells that had bound HDLp. However, also the mean fluorescence of the population of cells of which the fluorescence did not exceed that of untransfected cells appeared slightly higher in the plot after binding of OG-HDLp-1.17 as compared to that of OG-HDLp (Figures 4A, B). As similar experiments using untransfected cells also resulted in a higher fluorescence after incubation with OG-HDLp-1.17 than after incubation of OG-HDLp (data not shown), this latter effect indicates a higher nonspecific binding of OG-HDLp-1.17 to the cells. After correction for the difference in nonspecific binding of OG-HDLp-1.17 and OG-HDLp, the y-mean of cells that bound OG-HDLp-1.17 was 2.4-fold higher than the y-mean of cells that bound OG-HDLp. Congruent experiments using unlabeled HDLp or HDLp-1.17 that were immunodetected by a polyclonal antibody against HDLp and a fluorescently-labeled secondary antibody, confirmed the increased affinity of LpR for HDLp-1.17 (data not shown).

To corroborate that LpR had a higher affinity for HDLp-1.17 than for HDLp, we performed competition binding experiments using a similar experimental approach. CHO(LpR) cells were incubated with OG-HDLp or OG-HDLp-1.17 in the presence of either equimolar amounts or an excess of unlabeled HDLp or HDLp-1.17. The presence of an equimolar amount of unlabeled HDLp-1.17 during the binding of OG-HDLp prevented completely the binding of OG-HDLp, as indicated by the low number of cells in R1 (Figure 4C). In contrast, the fluorescence of cells that bound OG-HDLp-1.17 did not significantly decrease in the presence of an equimolar amount of unlabeled HDLp (Figure 4D). A five-fold excess of unlabeled HDLp was able to partially compete with OG-HDLp-1.17 (data not shown). Together, these results indicate that LpR binds HDLp-1.17 with a higher affinity than HDLp and suggest that the two lipophorin species most likely bind LpR using the same site of the receptor.

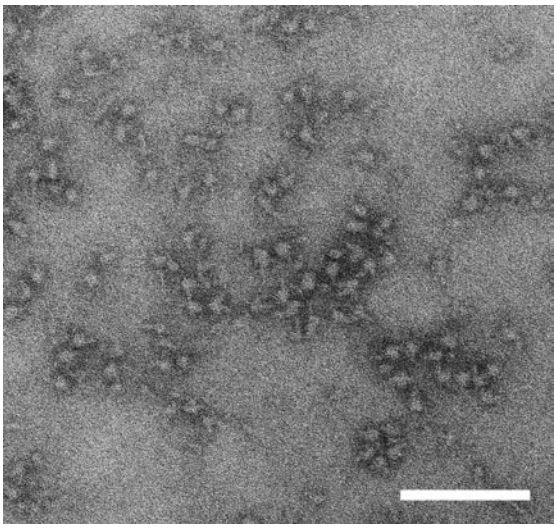

Figure 3. Negative staining electronmicrograph of HDLp-1.17. Representative HDLp-1.17 particles stained with 2% phosphotungsten acid. White bar represents 100 nm.

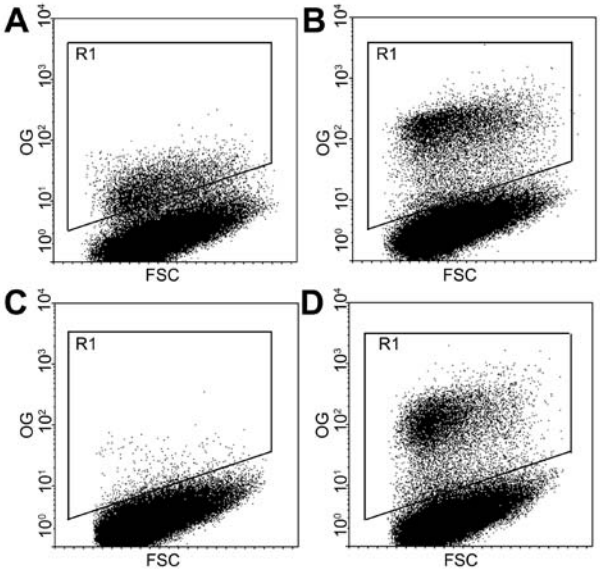

Figure 4. Binding and endocytosis of OG-HDLp and OG-HDLp-1.17 by CHO(LpR) cells. CHO(LpR) cells were incubated with either OG-HDLp (A), or OG-HDLp in the presence of an equimolar amount of HDLp-1.17 (C). Plots B and D were obtained from the reciprocal experiment; cells were incubated with either OG-HDLp-1.17 alone (B), or OG-HDLp-1.17 in the presence of an equimolar amount of HDLp (D). The amount of fluorescence is plotted on the y-axis (OG, relative values), and the forward scatter (FSC, relative values) on the x-axis. Cells in R1 are LpR-expressing cells that display a higher fluorescence intensity than the cells in the population below R1 used as negative control. The plots are representative of three independent experiments, performed on different cell lines. R1 indicates the region used for quantification.

Endocytosis of OG-HDLp-1.17 by insect fat body tissue

The LpR-mediated endocytic properties of HDLp-1.17 were analyzed *in vivo* by incubating fat body tissue of young adult locusts that endogenously expressed LpR[19] with OG-HDLp-1.17. After endocytic uptake of OG-HDLp-1.17, a similar punctate staining pattern as for OG-HDLp was apparent (Figures 5A, D). When fat body tissue of older adult animals (i.e. 12 days after imaginal ecdysis), that does not express LpR[19], was incubated with OG-HDLp-1.17, such a punctate staining pattern was absent (data not shown). These results are indicative of LpR-mediated endocytosis of HDLp-1.17, as was described for HDLp[19]. In accordance with the results for CHO(LpR) cells, an equimolar amount of unlabeled HDLp failed to substantially inhibit the endocytosis of OG-HDLp-1.17 (Figure 5B). Moreover, the punctate staining pattern was also observed in the presence of a ten-fold excess of unlabeled HDLp, indicating that endocytosis of OG-HDLp-1.17 by fat body cells was not inhibited completely (Figure 5C). By contrast, in the presence of an equimolar amount or a ten-fold excess of unlabeled HDLp-1.17, endocytosis of OG-HDLp was completely abolished (Figures 5E, F). Collectively, these results indicate that, consistent with the data for CHO(LpR) cells established in this investigation, endogenously expressed LpR displays a higher affinity for delipidated HDLp, proposing that in the insect fat body, LpR favors the endocytosis of lipid-unloaded forms of HDLp.

Stability of the HDLp-1.17-LpR complex at endosomal pH

The complex of OG-HDLp and LpR was shown to be stable at low pH, which may provide a key determinant for ligand recycling[16]. To analyze whether delipidation of HDLp affects the stability of the LpR-HDLp-1.17 complex at endosomal pH, CHO(LpR) cells were incubated with OG-HDLp-1.17, washed with buffer of pH 5.4 and subsequently analyzed by flow cytometry. Quantification of the mean fluorescence (y-mean) of the cells after washing with a buffer of pH 5.4 revealed no significant change as compared to that washed with a buffer of pH 7.4 (Figure 6), indicating that the complex of OG-HDLp-1.17 and LpR is stable at endosomal pH.

Endocytic recycling of HDLp-1.17

To investigate whether HDLp-1.17 is also recycled by LpR, the intracellular localization of HDLp-1.17 was examined in both CHO(LpR) cells and insect fat body tissue. To this end, CHO(LpR) cells were pre-incubated with OG-HDLp-1.17 and subsequently chased in serum-free medium for different periods of time. After a 10-min chase, OG-HDLp-1.17 appeared to localize predominantly in the juxtanuclear area (Figure 7A) that, by colocalization with TMR-Tf, was identified as the ERC (Figures 7B, C)[15]. After a 30-min chase, OG-HDLp-1.17 had disappeared from the cells

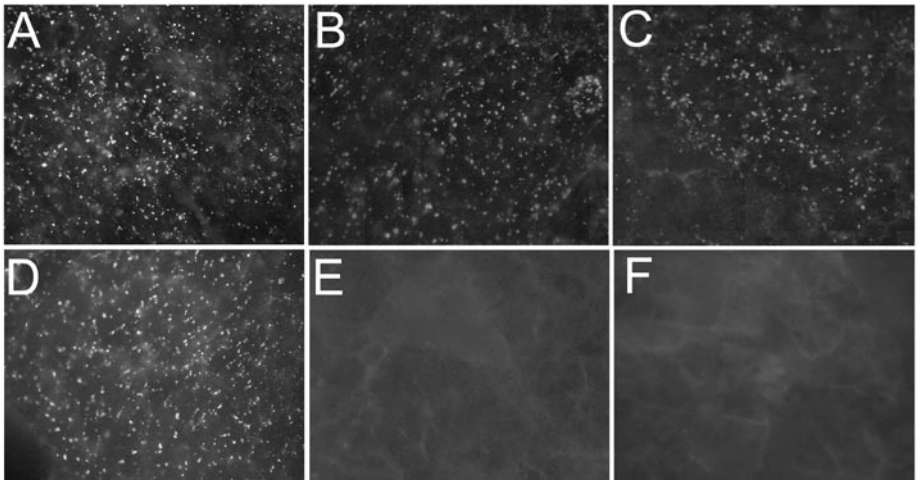

Figure 5. Endocytosis of HDLp-1.17 by LpR endogenously expressed by locust fat body tissue. Fluorescence microscopy images of fat body tissue incubated with OG-HDLp-1.17 (A-C) or OG-HDLp (D-F). Tissue from young adult animals (two days after ecdysis) was incubated with OG-HDLp-1.17 (A), OG-HDLp-1.17 in the presence of an equimolar amount of HDLp (B), or in the presence of a 10-fold excess of HDLp (C). Panels D-F show the reciprocal experiment, in which tissue was incubated with OG-HDLp (D), OG-HDLp in the presence of an equimolar amount of HDLp-1.17 (E) or OG-HDLp in the presence of a 10-fold excess of HDLp-1.17 (F). For a colored version of this figure see page 165.

Figure 6. Stability of the complex of HDLp-1.17 and LpR at endosomal pH. Bar representation of the results of binding experiments (n = 4) in which CHO(LpR) cells were incubated with OG-HDLp (dark grey bars) or OG-HDLp-1.17 (light grey bars), followed by extensive washing of the cells with a buffer of pH 7.4 or pH 5.4 as indicated below the bars. The fluorescence of the cells was measured by flow cytometry. The y-mean in region 1 (R1) was determined for each sample. Bars depict the relative y-mean compared to the y-mean for pH 7.4, which was set at 1. Error bars indicate the s.e.m.

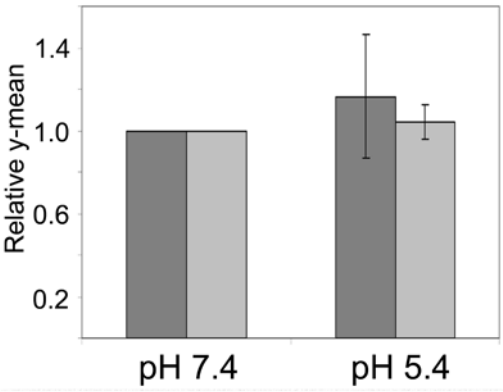

(data not shown), suggesting that in CHO(LpR) cells, HDLp-1.17 is recycled by LpR as was described previously for the complex of HDLp and LpR[15,16].

To determine whether HDLp-1.17 is also recycled by LpR *in vivo*, young adult fat body tissue was preincubated with OG-HDLp-1.17 and subjected to a chase in insect growth medium. After a chase time of 1 h, some endocytic vesicle structures were still visible in

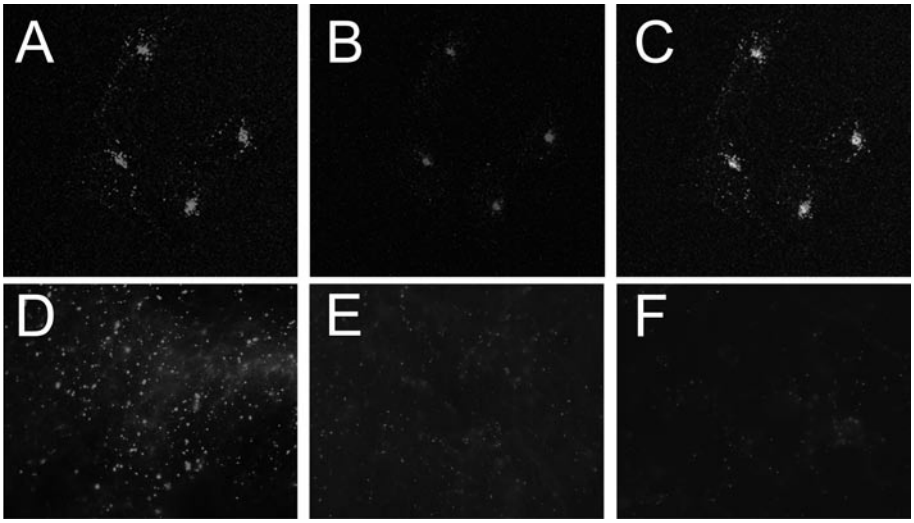

Figure 7. LpR-mediated recycling of HDLp-1.17 in CHO(LpR) cells and locust fat body tissue. Fluorescence microscopy images of CHO(LpR) cells used in a pulse-chase experiment with OG-HDLp-1.17 (A) and TMR-Tf (B). Endocytosis (the pulse) was followed by a 10-min chase in serum-free medium. Colocalization was visualized by merging the two images (C). Insect fat body of young adult animals (2 days after ecdysis) endogenously expressing LpR was either only pulsed with OG-HDLp-1.17 (D), or subsequently chased in insect growth medium for 1 h (E) or 2 h (F). For a colored version of this figure see page 165.

the fat body cells; however, after a 2 h chase the fat body tissue appeared depleted of OG-HDLp-1.17 (Figures 7D, E, F), as was shown to occur similarly for OG-HDLp (data not shown), and consistent with earlier studies from our laboratory[17]. This indicates that OG-HDLp-1.17 is recycled by LpR in the insect fat body to a similar extent as HDLp.

Immunoreactivity of antibodies with HDLp-1.17

Since the above binding experiments using flow cytometry indicated an increased affinity for the binding of HDLp-1.17 to LpR, it was considered whether an explanation for this phenomenon could be that the conformation of the protein moiety of HDLp-1.17 is affected by the decreased lipid content of the particle. To provide indications for potential differences in the conformation of apoLp-I and -II, the immunoreactivity of several antibodies for HDLp-1.17 and HDLp was assayed using a competitive solid-phase binding assay[25] in which the amount of binding of antibody to coated, reference HDLp in the presence of a range of excess HDLp or HDLp-1.17 was measured. Relative values compared to the binding of the anti-HDLp antibodies in the absence of excess HDLp were determined and a (dose-response) model was fitted to these values[26]. The experiments were performed using antibodies raised against peptides representing the N- and C-termini of apoLp-I (respectively anti-IN

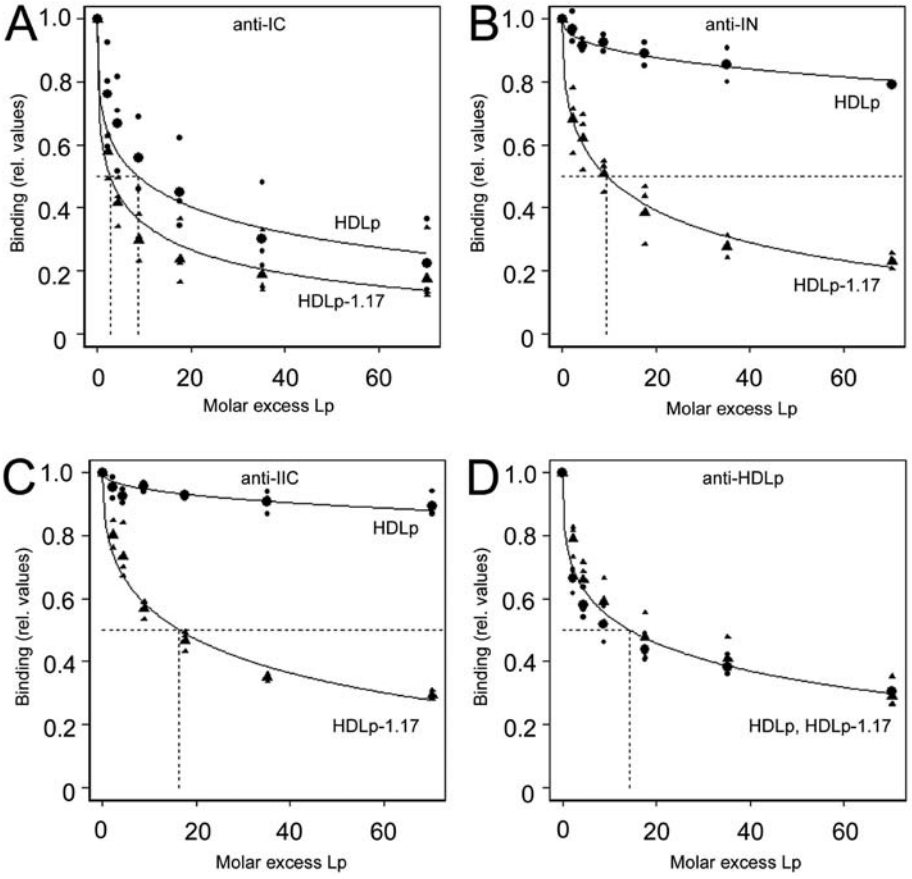

Figure 8. Immunoreactivity of HDLp and HDLp-1.17. Determination of the amount of excess HDLp or HDLp-1.17 required for competing with the binding of different antibodies to coated HDLp. A: antibody anti-IC raised against the C-terminus of apoLp-I; B: antibody anti-IN raised against the N-terminus of apoLp-I; C: antibody anti-IIC raised against the C-terminus of apoLp-II and D: antibody anti-HDLp raised against HDLp. On the y-axis the relative amount of binding of antibody to coated HDLp is indicated. On the x-axis the molar excess of lipophorin (Lp), either HDLp (filled circles) or HDLp-1.17 (filled triangles), is indicated. Large symbols represent the average values, small symbols are the calculated, relative values of separate experiments (n = 3). For anti-HDLp (D), the molar excess could not be determined due to the unknown concentration of antibodies in the serum. However, the same concentrations of HDLp and HDLp-1.17 were used as for the other experiments. A (dose-response) model was fitted to the relative values (curves). Dotted lines indicate the molar excess of HDLp and HDLp-1.17 that resulted in 50% inhibition of the binding of antibody to reference HDLp. Note that in B and C the IC_{50} could not be determined for the binding of anti-IN and anti-IIC to HDLp because 50% inhibition of the signal was not reached using these concentrations of HDLp as indicated by the dotted line.

and anti-IC) and the C-terminus of apoLp-II (anti-IIC). Only the binding of anti-IC to coated HDLp appeared to be effectively blocked by HDLp in solution (Figures 8A, B, C), suggesting that only the IC epitope, the C-terminus of apoLp-I, is exposed on the surface of native HDLp for antibody recognition. Approximately a nine-fold molar excess (calculated value 8.60) of HDLp was able to inhibit 50% of the antibody binding to coated HDLp. For anti-IN and anti-IIC 50% inhibition was not reached, even in the presence of a 70-fold molar excess of HDLp (Figures 8B, C). In contrast, HDLp-1.17 efficiently competed with the binding of anti-IN and anti-IIC to coated HDLp (Figures 8B, C). Additionally, the concentration of HDLp-1.17 to inhibit 50% of the binding of anti-IC to coated HDLp was three-fold lower (Figure 8A). These results are suggestive of a conformational change of apoLp-I and -II. However, there was no statistically significant different response between binding of a polyclonal anti-HDLp antibody[34] to coated HDLp in the presence of an excess of HDLp or HDLp-1.17 (Figure 8D), suggesting that the conformation of the epitopes recognized by this antibody is not altered upon delipidation. Together these data imply that the global conformation of apoLp-I and -II was not altered by delipidation of the particle; however, the decrease in lipid content leads to additional protein exposure, as illustrated by the higher affinity of antibodies for the N-terminus of apoLp-I and the C-terminus of apoLp-I and -II for HDLp-1.17 as compared to that for HDLp.

Discussion

In larval and adult insects, circulatory HDLp functions as a reusable shuttle. Consequently, lipid transport and delivery are efficiently mediated without endocytosis and lysosomal degradation of the lipoprotein particle[11,35]. Nevertheless, as was discovered in the locust, the endocytic HDLp receptor LpR is expressed during a few days after the energy-demanding process of ecdysis, as well as after experimental starvation[18,19]; the ligand, however, is not intracellularly degraded but recycled[15,17,35,36]. This led to the hypothesis that LpR-mediated endocytosis and subsequent recycling of HDLp might function to rapidly replenish the depleted fat body reserves once lipids from dietary intake are available[19]. As this would imply a mechanism in which endocytosed HDLp unloads (part of) its lipid cargo intracellularly, LpR was expected to display a preference for a relatively lipid-loaded form of HDLp. To this end, the present investigation compares the interaction of LpR with HDLp that displays its normal density of 1.11 g/ml and with a partially delipidated HDLp particle with a density of 1.17 g/ml, HDLp-1.17, produced by incubation of HDLp with α-cyclodextrin. Contrary to our expectations, however, the results indicate that LpR binds

HDLp-1.17 with a substantially higher affinity than HDLp. After endocytosis, HDLp-1.17 appears to be recycled by LpR, both in CHO(LpR) cells and in insect fat body tissue endogenously expressing LpR, similar to the fate previously described for HDLp[15,17]. Apparently, LpR displays a binding preference for (partially) lipid-depleted HDLp forms that, upon endocytosis, are being recycled and resecreted into the medium.

Using enzymatic methods, it has been shown before that the DAG and PL content of insect HDLp can be manipulated without disrupting the stability of the lipoprotein particle[37-40]. Incubation of HDLp with α-cyclodextrin was shown to efficiently modulate the DAG content of HDLp from *Manduca sexta* and *Bombyx mori*[20]. In this study, we show that additionally to DAG, also PL is extracted from *L. migratoria* HDLp, which is consistent with the observation that α-cyclodextrin, in addition to binding of DAG, is able to interact with PL[30]. Using gel filtration and electron microscopy, HDLp-1.17 was shown to behave as a single particle. In agreement with the decrease in MW found by gel filtration, measurements of particle size using electron microscopy revealed that HDLp-1.17 is substantially smaller than HDLp (13 ± 2 nm by 9 ± 2 nm vs. 19 ± 2 nm by 15 ± 2 nm). In addition to the differences in density and size, the irregular, crescent-like shape of HDLp-1.17 differs from the oval shape of untreated HDLp. Such a shape was also found for HDLps of a similar density from other insect species[38,41]. It has been proposed earlier that delipidation of insect lipoprotein might result in exposure of a cryptic receptor-binding site[33,41,42]. The explanation of exposure of an additional binding site in the lipoprotein may be relevant with respect to the 2.4-fold higher affinity of HDLp-1.17 for LpR as compared to that of HDLp, which compares well to the differential affinity range (2.2-fold) of different physiological density forms of LDL for LDLR[43]. The difference in affinity of LDLR for the latter LDL forms was proposed to be related to the number of molecules of apoE associated with the lipoprotein, that potentially generate additional binding sites in the lipoprotein for the receptor[43]. Since our data indicate that experimental lipid decrease of HDLp leads to additional exposure of the N-terminus of apoLp-I and the C-terminus of apoLp-II, it may be possible that this concurs with the exposure of additional receptor-binding sites. The affinity of LDLR for enzymatically modified LDL was shown to be increased upon decreasing lipid content[44-46], caused by conformational changes in specific regions of apoB-100[25,45,46] resulting in changes in the arrangement of lysine residues that mediate the binding to LDLR[46]. Whether such a mechanism also occurs during unloading of HDLp is not known. However, since immunoreactivity of a polyclonal antibody against HDLp did not change upon delipidation, this suggests that delipidation does not lead to a global conformational change of apoLp-I and -II since this would have resulted in a decrease in available epitopes for this antibody. Therefore, it seems more likely that the higher affinity is caused by local changes in the exposure of the apolipoproteins, which may coincide

with the exposure of one or more additional receptor-binding sites. Alternatively, we cannot exclude that the affinity of LpR for the particle is affected by the net change in charge of HDLp that likely occurred due to the selective α-cyclodextrin extraction of PL from the particle[30,47].

Consistent with the data on CHO(LpR) cells presented in this study, insect fat body tissue was also shown to endocytose experimentally delipidated HDLp. Competition binding studies revealed that endogenously expressed LpR also binds HDLp-1.17 with a higher affinity than HDLp. This suggests that LpR favors the binding of lipid-unloaded HDLp also *in vivo*. Since LpR expression in fat body tissue was shown to occur only after the energy-consuming process of ecdysis or a period of experimental starvation[19], a function of LpR in a rapid replenishment of the fat body with lipids by the uptake of HDLp particles has been proposed. Alternatively, receptor-mediated endocytosis of the HDLp particle has been suggested to provide a mechanism to efficiently internalize specific hydrophobic components, e.g. hydrocarbons[18,19], that are required after such a period of exhaustion, but are difficultly internalized by diffusion through the cell membrane. However, our new finding of increased binding of HDLp-1.17 to LpR, suggesting a preferential uptake of partially unloaded HDLp by LpR, renders both these hypotheses unlikely. Rather, the preference of LpR for delipidated HDLp combined with the expression pattern of the receptor is suggestive of a function for LpR to sense the lipid content of lipoprotein in the circulation, leading to down-regulation of LpR when circulating HDLp is fully lipidated. In this respect, it is important to note that the complex of HDLp-1.17 and LpR, similarly to the complex of HDLp and LpR[15-17], is not dissociated at endosomal pH and is targeted to the ERC, after which it disappears from the cell, indicative of resecretion of the particle. Therefore, we propose the delipidated HDLp that is internalized by LpR to be reloaded during its intracellular route, resulting in a decreased affinity of the particle for LpR that ultimately leads to release of the particle upon exocytosis. In this manner, LpR-mediated endocytosis of lipid-poor HDLp could function as a mechanism that allows for the uptake of lipids from the strongly diminished reserves in the fat body and their release into the circulation. This additional mechanism might be necessary to provide other vital organs (such as the eyes and the nervous system) with sufficient lipids or other hydrophobic components during periods of scarcity. However, it remains to be demonstrated that, coherent with the physiological periods in which the receptor is expressed, HDLp of a higher density is present in the circulation. For *L. migratoria*, analysis of hemolyph during early development of the insect failed to reveal the presence of HDLp of a higher density[27]. However, by experimental alternation of starvation for relative short periods (12-15 hours) and feeding of young adult locusts (2-4 days after imaginal ecdysis), HDLp subspecies with slightly higher densities were identified (Van Doorn J. M., Gracanin, A.,Van der Horst, D. J., Roosendaal, S. D., and Rodenburg K. W., unpublished

results). Although the lipid content of these particles was higher than that obtained by incubation of HDLp with α-cyclodextrin, this implies that young adult locusts are able to produce distinct HDLps with different densities, which normally might be rapidly metabolized. Conclusively, our results show that changes in lipid composition of HDLp affect the binding of the particle to its receptor, and suggest that the function of LpR may specifically relate to the differential endocytic uptake and recycling of lipophorins of decreased lipid content that result from (developmental) periods of metabolic exhaustion.

Acknowledgements

We thank Masja van Oort and Marcel Smolenaars for useful discussions, Montserrat Barcena-Martin and Ronald Limpens for their help with the electron microscopy to create Figure 3 and Bas Bokkers for the statistical analysis on the results of the solid phase binding assay. Yvonne Derks is thanked for the purification of the antibodies anti-IN, anti-IC and anti-IIC and Ana Gracanin for her contribution on the identification of lipophorins of differential densities in animal hemolymph.
Karine M. Valentijn and Yvonne Derks were financially supported by the Physical Biology Research programme II, project 01FB22 of the "Stichting voor Fundamenteel Onderzoek der Materie" and "Aard en Levenswetenschappen" (FOM/ALW), which is a part of the "Nederlandse Organisatie voor Wetenschappelijk Onderzoek" (NWO).

References

1. Chino H & Kitazawa K (1981) Diacylglycerol-carrying lipoprotein of hemolymph of the locust and some insects. J Lipid Res 22, 1042-1052.
2. Van der Horst DJ & Ryan RO (2005) Lipid transport. In Comprehensive molecular insect science (Gilbert LI, Iatrou K & Gill SS, editors), 4, pp. 225-246. Elsevier, New York, NY, USA.
3. Weers PM, Van Marrewijk WJ, Beenakkers AM & Van der Horst DJ (1993) Biosynthesis of locust lipophorin. Apolipophorins I and II originate from a common precursor. J Biol Chem 268, 4300-4303.
4. Smolenaars MM, Kasperaitis MA, Richardson PE, Rodenburg KW & Van der Horst DJ (2005) Biosynthesis and secretion of insect lipoprotein: involvement of furin in cleavage of the apoB homolog, apolipophorin-II/I. J Lipid Res 46, 412-421.
5. Bogerd J, Babin PJ, Kooiman FP, Andre M, Ballagny C, Van Marrewijk WJ & Van der Horst DJ (2000) Molecular characterization and gene expression in the eye of the apolipophorin II/I precursor from *Locusta migratoria*. J Comp Neurol 427, 546-558.
6. Babin PJ, Bogerd J, Kooiman FP, Van Marrewijk WJ & Van der Horst DJ (1999) Apolipophorin II/I, apolipoprotein B, vitellogenin, and microsomal triglyceride transfer protein genes are derived from a common ancestor. J Mol Evol 49, 150-160.
7. Mann CJ, Anderson TA, Read J, Chester SA, Harrison GB, Kochl S, Ritchie PJ, Bradbury P, Hussain FS, Amey J, Vanloo B, Rosseneu M, Infante R, Hancock JM, Levitt DG, Banaszak LJ, Scott J & Shoulders CC (1999) The structure of vitellogenin provides a molecular model for the assembly and secretion of atherogenic lipoproteins. J Mol Biol 285, 391-408.
8. Mahley RW & Innerarity TL (1983) Lipoprotein receptors and cholesterol homeostasis. Biochim Biophys Acta 737, 197-222.
9. Davidson NO & Shelness GS (2000) Apolipoprotein B: mRNA editing, lipoprotein assembly, and presecretory degradation. Annu Rev Nutr 20, 169-193.
10. Locke M (1998) Microscopic anatomy of invertebrates. In Insecta (Locke M, editor), pp. 641-686. Wiley-Liss, New York, NY, USA.
11. Ryan RO & Van der Horst DJ (2000) Lipid transport biochemistry and its role in energy production. Annu Rev Entomol 45, 233-260.
12. Dantuma NP, Potters M, De Winther MP, Tensen CP, Kooiman FP, Bogerd J & Van der Horst DJ (1999) An insect homolog of the vertebrate very low density lipoprotein receptor mediates endocytosis of lipophorins. J Lipid Res 40, 973-978.
13. Goldstein JL, Brown MS, Anderson RG, Russell DW & Schneider WJ (1985) Receptor-mediated endocytosis: concepts emerging from the LDL receptor system. Annu Rev Cell Biol 1, 1-39.
14. Brown MS & Goldstein JL (1986) A receptor-mediated pathway for cholesterol homeostasis. Science 232, 34-47.
15. Van Hoof D, Rodenburg KW & Van der Horst DJ (2002) Insect lipoprotein follows a transferrin-like recycling pathway that is mediated by the insect LDL receptor homologue. J Cell Sci 115, 4001-4012.

16. Roosendaal SD, Kerver J, Schipper M, Rodenburg KW & Van der Horst DJ (2008) The complex of the insect LDL receptor homologue, lipophorin receptor, LpR, and its lipoprotein ligand does not dissociate under endosomal conditions. FEBS J 275, 1751-1766.
17. Van Hoof D, Rodenburg KW & Van der Horst DJ (2005) Receptor-mediated endocytosis and intracellular trafficking of lipoproteins and transferrin in insect cells. Insect Biochem Mol Biol 35, 117-128.
18. Dantuma NP, Pijnenburg MA, Diederen JH & Van der Horst DJ (1997) Developmental down-regulation of receptor-mediated endocytosis of an insect lipoprotein. J Lipid Res 38, 254-265.
19. Van Hoof D, Rodenburg KW & Van der Horst DJ (2003) Lipophorin receptor-mediated lipoprotein endocytosis in insect fat body cells. J Lipid Res 44, 1431-1440.
20. Jouni ZE, Zamora J, Snyder M, Montfort WR, Weichsel A & Wells MA (2000) alpha-Cyclodextrin extracts diacylglycerol from insect high density lipoproteins. J Lipid Res 41, 933-939.
21. Bligh EG & Dyer WJ (1959) A rapid method of total lipid extraction and purification. Can J Biochem Physiol 37, 911-917.
22. Freeman CP & West D (1966) Complete separation of lipid classes on a single thin-layer plate. J Lipid Res 7, 324-327.
23. Fewster ME, Burns BJ & Mead JF (1969) Quantitative densitometric thin-layer chromatography of lipids using copper acetate reagent. J Chromatogr 43, 120-126.
24. Kingsley DM & Krieger M (1984) Receptor-mediated endocytosis of low density lipoprotein: Somatic cell mutants define multiple genes required for expression of surface-receptor activity. Proc Natl Acad Sci USA 81, 5454-5458.
25. Chauhan V, Wang X, Ramsamy T, Milne RW & Sparks DL (1998) Evidence for lipid-dependent structural changes in specific domains of apolipoprotein B100. Biochemistry 37, 3735-3742.
26. Slob W (2002) Dose-response modeling of continuous endpoints. Toxicol Sci 66, 298-312.
27. Weers PM, Van der Horst DJ, Van Marrewijk WJ, Van den Eijnden M, Van Doorn JM & Beenakkers AM (1992) Biosynthesis and secretion of insect lipoprotein. J Lipid Res 33, 485-491.
28. Van der Horst DJ, Van Marrewijk WJ & Diederen JH (2001) Adipokinetic hormones of insect: release, signal transduction, and responses. Int Rev Cytol 211, 179-240.
29. Van der Horst DJ, Van Doorn JM, Voshol H, Kanost MR, Ziegler R & Beenakkers AM (1991) Different isoforms of an apoprotein (apolipophorin III) associate with lipoproteins in *Locusta migratoria*. Eur J Biochem 196, 509-517.
30. Ohtani Y, Irie T, Uekama K, Fukunaga K & Pitha J (1989) Differential effects of alpha-, beta- and gamma-cyclodextrins on human erythrocytes. Eur J Biochem 186, 17-22.
31. Soulages JL & Wells MA (1994) Lipophorin: the structure of an insect lipoprotein and its role in lipid transport in insects. Adv Protein Chem 45, 371-415.
32. Valentijn KM, Koning R, Derks Y, Van Doorn JM, Van der Krift TP, Schouten A, Koerten HK, Van der Horst DJ, Gros P, Koster AJ & Rodenburg KW (2004) Preliminary three-dimensional model of insect lipoprotein HDLp by using electron miscroscopy and X-ray cristallography. In Proc Microsc Microanal (Anderson IM, Price R, Hall E, Clark E & McKernan S, editors), pp. 1514-1515, Savannah, GA, USA.

33. Van Antwerpen R, Linnemans WA, Van der Horst DJ & Beenakkers AM (1988) Immuno-cyto-chemical localization of lipophorins in the flight muscles of the migratory locust (*Locusta migratoria*) at rest and during flight. Cell Tissue Res 252, 661-668.
34. Schulz TK, Van der Horst DJ, Amesz H, Voorma HO & Beenakkers AM (1987) Monoclonal antibodies specific for apoproteins of lipophorins from the migratory locust. Arch Insect Biochem 6, 97-107.
35. Van der Horst DJ, Van Hoof D, Van Marrewijk WJ & Rodenburg KW (2002) Alternative lipid mobilization: the insect shuttle system. Mol Cell Biochem 239, 113-119.
36. Van Hoof D, Rodenburg KW & Van der Horst DJ (2005) Intracellular fate of LDL receptor family members depends on the cooperation between their ligand-binding and EGF domains. J Cell Sci 118, 1309-1320.
37. Ryan RO, Wessler AN, Price HM, Ando S & Yokoyama S (1990) Insect lipid transfer particle catalyzes bidirectional vectorial transfer of diacylglycerol from lipophorin to human low density lipoprotein. J Biol Chem 265, 10551-10555.
38. Kawooya JK, Van der Horst DJ, Van Heusden MC, Brigot BL, Van Antwerpen R & Law JH (1991) Lipophorin structure analyzed by *in vitro* treatment with lipases. J Lipid Res 32, 1781-1788.
39. Rimoldi OJ, Garda HA & Brenner RR (1996) Effect of phospholipids on the structure of *Triatoma infestans* lipophorin studied by fluorescence methods. J Lipid Res 37, 2125-2135.
40. Maya-Monteiro C, Oliveira PL, Gondim KC, Masuda H & Ferreira ST (1997) Role of phospholipids in the protein stability of an insect lipoprotein, lipophorin from *Rhodnius prolixus*. Biochemistry 36, 11216-11222.
41. Ryan RO, Kay CM, Oikawa K, Liu H, Bradley R & Scraba DG (1992) Effect of particle lipid content on the structure of insect lipophorins. J Lipid Res 33, 55-63.
42. Tsuchida K & Wells MA (1990) Isolation and characterization of a lipoprotein receptor from the fat body of an insect, *Manduca sexta*. J Biol Chem 265, 5761-5767.
43. Campos H, Arnold KS, Balestra ME, Innerarity TL & Krauss RM (1996) Differences in receptor binding of LDL subfractions. Arterioscler Thromb Vasc Biol 16, 794-801.
44. Aviram M, Bierman EL & Chait A (1988) Modification of low density lipoprotein by lipoprotein lipase or hepatic lipase induces enhanced uptake and cholesterol accumulation in cells. J Biol Chem 263, 15416-15422.
45. Kinoshita M, Krul ES & Schonfeld G (1990) Modification of the core lipids of low density lipoproteins produces selective alterations in the expression of apoB-100 epitopes. J Lipid Res 31, 701-708.
46. Aviram M, Lund-Katz S, Phillips MC & Chait A (1988) The influence of the triglyceride content of low density lipoprotein on the interaction of apolipoprotein B-100 with cells. J Biol Chem 263, 16842-16848.
47. Debouzy JC, Fauvelle F, Crouzy S, Girault L, Chapron Y, Goschl M & Gadelle A (1998) Mechanism of alpha-cyclodextrin induced hemolysis. 2. A study of the factors controlling the association with serine-, ethanolamine-, and choline-phospholipids. J Pharm Sci 87, 59-66.

4

The cleavage site of apolipophorin II/I does not mediate the binding of lipophorin to its receptor, LpR

Sigrid D. Roosendaal, Yvonne Derks, Jan M. Van Doorn, Dick J. Van der Horst and Kees W. Rodenburg

Division of Endocrinology and Metabolism, Department of Biology and Institute of Biomembranes, Utrecht University, The Netherlands

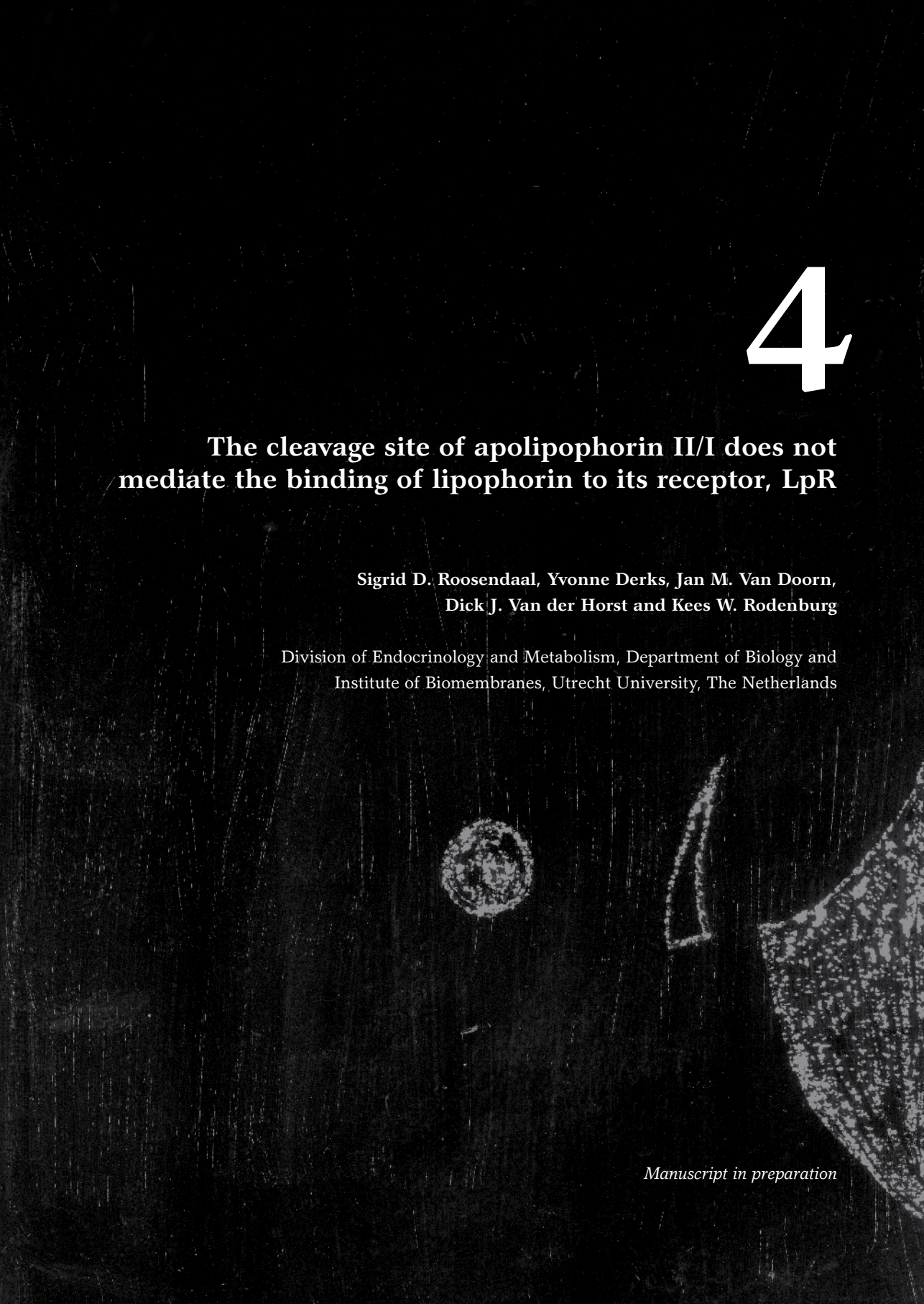

Manuscript in preparation

Abstract

The insect low-density lipoprotein receptor (LDLR) homologue, LpR, is able to bind and endocytose the major insect lipoprotein, high-density lipophorin (HDLp). HDLp is synthesized by co-translational lipidation of its apolipoprotein precursor protein, apolipophorin II/I, which is a homologue of mammalian apolipoprotein B-100 (apoB-100). In contrast to apoB-100, however, apoLp-II/I is cleaved by the serine endoprotease furin at a later stage of lipoprotein assembly, resulting in the recovery of two integral apolipoproteins (apoLp-I and -II) in the secreted particle. The function of apoLp-II/I cleavage is as yet unclear. Recently we showed that the cleavage site of the protein is not exposed at the surface of HDLp. On the other hand, in an experimentally produced stable form of HDLp that was partially delipidated (HDLp-1.17), this site appeared to be accessible. Additionally, the particle was shown to bind to LpR with a higher affinity than HDLp, suggesting a correlation between exposure of the cleavage site and high-affinity LpR binding. In this study, the putative correlation was studied using HDLp-1.17 as a tool. Competition binding studies show that antibodies against the two oligopeptides flanking the cleavage site were unable to prevent the binding of HDLp-1.17 to LpR. Moreover, binding studies revealed that the cleavage site is accessible for antibody binding when HDLp that exposes the cleavage site is bound to LpR. Together, these results indicate that in the binding of partly delipidated HDLp or wild-type HDLp to LpR, the cleavage site is not involved. Rather, similar to exposure of the cleavage site, delipidation may lead to (increased) exposure of other parts of the protein that may comprise a cryptic LpR-binding site. Sequence analysis of apoLp-I and -II suggests that such a site is most likely located in the amphipathic β-cluster of the protein, as was demonstrated for the LDLR-binding site in apoB-100.

Introduction

Circulatory transport of neutral lipids (fat) in animals relies on members of the large lipid transfer protein (LLTP) superfamily, including mammalian apolipoprotein B-100 (apoB-100) and insect apolipophorin II/I (apoLp-II/I)[1]. Comparative research has revealed the structural and functional adaptations in these lipid carriers[1,2]. For instance, in contrast to mammalian apoB-100, insect apoLp-II/I is post-translationally cleaved by a furin-like protease[3,4], resulting in the appearance of two structural proteins, apoLp-I and -II, in the single multifunctional insect lipoprotein, high-density lipophorin (HDLp). Although the precise function of apoLp-II/I cleavage remains to be established, it was demonstrated that cleavage is not essential for lipoprotein biogenesis, as uncleaved apoLp-II/I was also lipidated to form a lipoprotein of buoyant density identical to wild-type HDLp[4]. After biosynthesis in the insect fat body, HDLp is released into the insect blood (hemolymph) where it functions in taking up lipids released from cells of the fat body and other tissues and selectively unloading its lipid cargo at target tissues without endocytosis and lysosomal degradation[5,6]. In addition to this mechanism of lipid transport accomplished by HDLp as a reusable lipid shuttle, endocytic uptake of HDLp involving an insect homologue of the LDL receptor (LDLR) has been identified[7]. Sequence analysis indicated that this lipophorin receptor (LpR) consists of all the typical domains of a classical LDLR family member[7]. However, in spite of the high structural similarity of LpR to mammalian LDLR, in LpR-expressing Chinese hamster ovary (CHO) cells, endocytosed HDLp appeared not to be degraded in lysosomes, as is the case for mammalian LDL, but is resecreted in a manner similar to transferrin[8,9]. Additionally, HDLp internalized by fat body tissue endogenously expressing LpR also appeared to be resecreted[10,11]. The function of this recycling pathway is not yet clear.

LpR is expressed only in specific developmental stages (during a few days after ecdysis, both to the next larval stage as to the adult), indicative of additional uptake of HDLp by LpR in this developmental period[7]. Down-regulation of LpR in adult locusts appeared to be postponed by experimental starvation immediately after ecdysis, while by starving adult locusts after down-regulation of LpR, expression of the receptor was re-induced. These data suggest that LpR expression is regulated by the demand of fat body tissue for lipid components[12]. However, contrary to this suggestion, by using partially delipidated HDLp particles resulting from *in vitro* incubation with α-cyclodextrin (HDLp-1.17; buoyant density 1.17 g/ml) we recently showed that LpR appeared to prefer the binding of lipid-depleted HDLp over wild-type HDLp (buoyant density 1.11 g/ml)[13]. Since, similar to HDLp, HDLp-1.17 was found to be recycled by LpR-expressing CHO cells and insect fat body tissue, these data suggest that the expression and functioning of LpR may be related to the endocytic uptake and recycling of lipophorin particles of decreased lipid content[13]. Additionally to increased binding to LpR, experimental delipidation of HDLp was shown

to lead to exposure of the peptides flanking the cleavage site, that are not exposed at the surface of fully lipidated HDLp[13], suggesting a correlation between exposure of the cleavage site and high-affinity LpR binding. The sequence that comprises the cleavage site is rich in arginine (Arg) and lysine (Lys) residues, which were evidenced to mediate the binding of ligands to LDLR family members[14-18].

In this paper, HDLp-1.17 was used as a tool to investigate whether the cleavage site of the apolipoprotein precursor is involved in the increased binding of the HDLp particle to LpR. Competition binding studies demonstrated that antibodies against the two oligopeptides flanking the cleavage site were unable to prevent the binding of HDLp-1.17 to LpR. Moreover, these antibodies were able to bind to receptor-bound HDLp exposing these epitopes, suggesting that the cleavage site is not involved in the interaction interface of HDLp and LpR. These results indicate that the exposed cleavage site in HDLp-1.17 does not mediate its increased binding to LpR. Similar to the additional exposure of the cleavage site, delipidation may result in exposure of other parts of the protein that contribute to the high-affinity binding of HDLp-1.17 to LpR. Sequence analysis of apoLp-I and -II suggested possible receptor-binding sites to be most likely located in the amphipathic β-cluster of apoLp-I, which is comparable with that of the LDLR-binding site of apoB-100.

Materials and Methods

Materials

SIGMAFAST™ OPD (o-Phenylenediamine dihydrochloride) tablets (Sigma) and CNBr-activated Sepharose 4 Fast Flow (Amersham Pharmacia Biotech) were commercially obtained.

Proteins and antibodies

Locust (*Locusta migratoria*) HDLp was isolated as described previously[19]. Partly delipidated HDLp (HDLp-1.17) was prepared using α-cyclodextrin as described[13]. Antibodies were raised against synthetic peptides representing the very N- and C-terminal 20 amino acids of apoLp-I and apoLp-II, i.e. anti-IIN antibody against a.a. 28-47, anti-IIC antibody against a.a. 702-720, anti-IN antibody against a.a. 721-739 and anti-IC antibody against a.a. 3362-3380 of apoLp-II/I (GenBank accession CAB51918.1). Antibodies were purified from rabbit sera using CNBr-activated Sepharose 4 Fast Flow (Amersham Pharmacia Biotech) according to manufacturer's instructions.

Competitive solid phase binding assay

A competitive solid binding assay was performed as described[13]. The amount of antibody binding in the absence of competing HDLp in solution was set to 1. Relative values were calculated for each experiment. A (dose-response) model was fitted to the relative values and the statistical analysis was performed using the PROAST software running in S-Plus[20]. Statistically significant differences were determined according to the likelihood ratio test ($\alpha = 0.05$). Based on the fit, the IC_{50}, the concentration of ligand that inhibits 50% of the antibody binding was determined. The 90% confidence interval of the IC_{50} was determined by bootstrapping 500 times[21].

Solid phase binding assay

High-binding microplates (Costar) were coated with 200 µL of HDLp (30 µg/ml, PBS, pH 7.4) overnight at 4°C and subsequently saturated by incubations for 2 h with 1% bovine serum albumin (BSA) in PBS at room temperature. The plates were then incubated for 1 h with serial dilutions of the different antibodies in PBS containing 1% BSA. Subsequently, the plates were washed with PBS containing 0.1% Tween-20, and incubated with a peroxidase-labeled secondary goat anti-rabbit antibody for 30 min in PBS containing 0.1% BSA and 0.1% Tween-20. After washing with PBS containing 0.1% Tween-20, the bound secondary antibody was detected using SIGMAFAST™ OPD according to manufacturer's protocol. A (dose-response) model was fitted to the relative values and the statistical analysis was performed using the PROAST software running in S-Plus[20]. According to Michaelis-Menten kinetics, the K_d ($½B_{max}$) was determined based on the fit of the curve. The 90% confidence interval of the K_d was determined by bootstrapping 500 times[21].

Determination of the K_i

Using the IC_{50} and the K_d of the interaction of the antibodies with coated HDLp, the inhibition constant (K_i) was calculated according to the method of Cheng-Prusoff using the following formula: $K_i = IC_{50}/(1 + [Ab]/K_d)$, in which the IC_{50} is the concentration of excess HDLp necessary to block 50% of the antibody binding, [Ab] is the concentration of antibody used and the K_d is the dissociation constant of the binding of antibody to coated HDLp[22]. The variance in the IC_{50} and K_d (expressed by their confidence intervals) was propagated by Monte Carlo simulation. Here, values are randomly drawn from the IC_{50} and K_d distribution (by non-parametric sampling), and the K_i is calculated using these randomly drawn values. This action was repeated 500 times resulting in a K_i distribution. The (geometric) mean and the 90% confidence interval of this distribution are reported.

Cell culture

LDLR-deficient CHO(*ldlA*) cells[23] were cultured in 25 cm^2 polystyrene culture flasks in growth medium (Ham F-10 nutrient mixture (GibcoBRL) supplemented medium, containing 5% heat-inactivated fetal bovine serum (FBS, GibcoBRL) and 100 U/ml penicillin G sodium and 100 µg/ml streptomycin sulfate in 85% saline (GibcoBRL)). The cells were cultured at 37°C and 5% CO_2.

Transfections

CHO(*ldlA*) cells[23] were grown until 40% confluency in 12-well multidishes (Costar). After washing the cells once, the growth medium was replaced with 500 µl of fresh growth medium. Subsequently, 4 µg DNA and 4 µg polyethylenimine in 50 µl serum-free medium (Ham F-10 nutrient mixture supplemented medium with 100 U/ml penicillin G sodium and 100 µg/ml streptomycin sulfate in 85% saline) was administered to the cells. After 4 h, 500 µl growth medium was added and cells were cultured overnight. The next day, cells were detached from dishes and cultured in 25 cm^2 culture flasks in growth medium supplemented with 400 µg/ml geneticin (GibcoBRL). Ten days after transfection, cells were used for experiments.

Fluorescence labeling

HDLp and HDLp-1.17 were covalently labeled with Oregon green (OG) 488 carboxylic acid (Molecular Probes) as described previously[8].

Binding experiments using flow cytometry

Binding experiments were performed as described earlier[19]. In competition binding experiments OG-HDLp-1.17 (25 µg/ml) was preincubated in the absence or in the presence of a ten times molar excess of anti-IIC or anti-IN in binding buffer (50 mM Tris-HCl, 2 mM $CaCl_2$, 150 mM NaCl, pH 7.4) for 30 min at room temperature. LpR-transfected CHO cells were washed with binding buffer and incubated on ice with OG-HDLp-1.17-antibody mixtures. Subsequently, the cells were washed with binding buffer and incubated with serum-free medium for 5 min at 37°C, to allow the cells to endocytose bound ligand. After endocytosis, the cells were detached from dishes and resuspended in growth medium. Resuspended cells were fixed in 0.5% paraformaldehyde in PBS at 4°C for at least 30 min to overnight.

Binding experiments using unlabeled HDLp were largely performed as described above. The binding of HDLp and antibodies was performed on ice to prevent endocytosis. Briefly, LpR-transfected CHO cells were washed and incubated with unlabeled HDLp in binding buffer for 30 min. After binding, cells were washed

and incubated with the indicated primary antibodies in binding buffer for 30 min, followed by washing and incubation for 30 min with a fluorescein isothiocyanate (FITC)-labeled secondary anti-IgG antibody (Jackson ImmunoResearch Laboratories Inc). Then, the cells were allowed to endocytose the HDLp-antibody complex and cells were detached and fixed as described above.
The fluorescence intensity of the cells was measured using a fluorescence-activated cell sorter (FACS, Becton Dickinson FACS Calibur). Flow cytometry data were collected using Cell Quest (Becton Dickinson) and downloaded into the program WinMDI (TSRI FACS Core Facility, La Jolla, CA) for analysis.

Flow cytometry data analysis

Flow cytometry data were quantified as descried earlier[19]. In brief, for each sample (~ 100.000 cells) the fluorescence was plotted against the forward scatter (FSC). For each series of experiments, the region containing cells that bound and endocytosed OG-ligand (region 1; R1) was defined in the plot based on a similar experiment performed using untransfected cells to exclude the population of cells of which the fluorescence did not exceed that of untransfected cells from the analysis. Then the number of cells and the mean fluorescence (y-mean) in R1 were determined. For each cell line, the number of cells in R1 after different treatments was compared by a t-test for paired samples performed on the logarithms of the number of cells. In case of a significant ($p \leq 0.05$) difference in sample size due to the different treatments, the y-mean was corrected by using random values of the missing number of cells from the negative population. After correction, for each sample the relative amount of fluorescence as compared to control samples was determined. To test whether samples were significantly different from control samples, a t-test for paired samples was performed on the logarithms of the y-means. Data presented as means $\pm$ s.e.m. were obtained from at least three independent experiments.

Results

Immunoreactivity of the different antibodies with HDLp and HDLp-1.17

Antibodies were raised against peptides representing the N- and C-termini of apoLp-II and I (Figure 1A). However, of these peptides, only the C-terminus of apoLp-I appeared to be exposed at the surface of native HDLp, since only the binding of anti-IC to coated HDLp was significantly inhibited by an excess of HDLp (Figure 1B). By contrast, the binding of anti-IN and anti-IIC to coated HDLp was efficiently inhibited by HDLp-1.17 (Figures 1C, D). Thus, delipidation of the particle appears

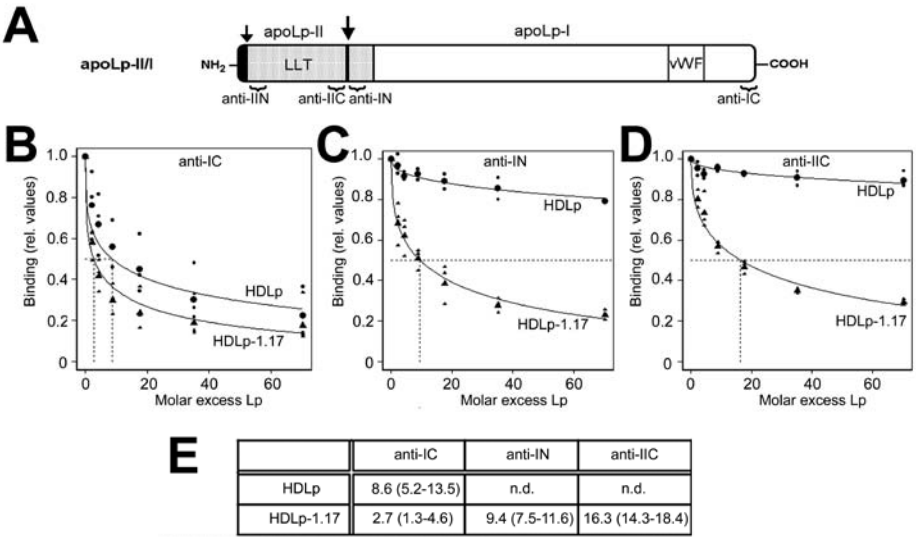

E

	anti-IC	anti-IN	anti-IIC
HDLp	8.6 (5.2-13.5)	n.d.	n.d.
HDLp-1.17	2.7 (1.3-4.6)	9.4 (7.5-11.6)	16.3 (14.3-18.4)

Figure 1. The binding of antibodies to HDLp and HDLp-1.17. A: Schematic representation of the *L. migratoria* apoLp-II/I construct. The small arrow indicates the predicted signal peptide cleavage site; the larger arrow indicates the cleavage site by furin; LLT: large lipid transfer module; Lp, lipophorin; vWF, von Willebrand factor D module. Positions of the antibody epitopes are indicated with braces. B-D: Immunoreactivity of HDLp and HDLp-1.17 with anti-IC (B), anti-IN (C) and anti-IIC (D). The relative amount of binding of the different antibodies is plotted against the molar excess of either HDLp (filled circles) or HDLp-1.17 (filled triangles) in solution. Large symbols represent the average values, small symbols are the calculated, relative values of individual experiments. A (dose-response) model was fitted to the relative values (curves) using PROAST software[20]. Dotted lines indicate the IC_{50}, the molar excess of HDLp and HDLp-1.17 that resulted in 50% inhibition of the binding of antibody to reference HDLp. Note that in B and C the IC_{50} could not be determined for the binding of anti-IN and anti-IIC to HDLp because 50% inhibition of the signal was not reached using these concentrations of HDLp as indicated by the dotted line. E: The IC_{50} for the different interactions. The confidence interval is indicated in brackets. n.d.: not determinable, since 50% inhibition was not reached.

Table 1. The inhibition constant (K_i) for the interactions between HDLp and antibodies. The K_i (nM) for the interaction between HDLp and the different antibodies is indicated, the confidence interval is indicated in brackets. Since the IC_{50} could not be determined for the binding of anti-IN and anti-IIC to HDLp (Figure 1), the K_i for these interactions could not be calculated.

	anti-IC	**anti-IN**	**anti-IIC**
HDLp	70.0 (41.5 - 112.5)	-	-
HDLp-1.17	21.1 (10.1 -37.2)	81.3 (63.8 - 99.5)	144.0 (115.5 -177.0)

to lead to exposure of the IN and IIC epitopes. Additionally, the concentration of HDLp-1.17 required for inhibition of 50% of the binding of anti-IC to coated HDLp was a significant three-fold lower than that of HDLp (Figures 1B, E), indicating that anti-IC displays a higher affinity for HDLp-1.17 than for HDLp. Anti-IIN did not bind HDLp or HDLp-1.17, either in solution or coated on a surface. However, analysis of HDLp by SDS-PAGE and subsequent immunoblotting using anti-IIN yielded a single band at ~ 75 kDa that migrated identically to the single band of apoLp-II identified by anti-IIC, indicating that the IIN epitope is present in the particle, but may be buried in the structure of (semi-) native HDLp (data not shown)[4].

The amount of inhibition can be expressed by the inhibition constant (K_i) which is the dissociation constant of the antibody-inhibitor complex, and described by the Cheng-Prusoff equation[22]. Since the K_i is corrected for differences in the antibody concentration and in affinities of the various antibodies for coated HDLp, the use of the K_i enables the comparison of the affinities of the different antibodies for HDLp. To determine the affinity of anti-IC, anti-IN and anti-IIC for coated HDLp, a solid phase binding assay was used. Determination of the K_ds of the interaction of the different antibodies with coated HDLp yielded similar results (Figure 2), indicating that the affinities of the antibodies for coated HDLp did not differ significantly. Since the K_ds of the different antibodies for coated HDLp were similar and the same concentration of the different antibodies was used in the competitive solid phase binding assay, the K_is are proportional to the IC_{50} of the interaction between the antibodies and HDLp in solution (Figure 1E and Table 1). The K_i of the interaction between HDLp-1.17 and anti-IC was the lowest (Table 1), suggesting that the IC epitope is most prominently exposed. The interaction between HDLp-1.17 and anti-IIC was characterized by the highest K_i, implying that the affinity of anti-IIC for HDLp-1.17 is lower than that of the other antibodies for HDLp-1.17, suggesting that this epitope is less exposed than the other ones. Since the IIN epitope is not exposed at the surface of HDLp, these results suggest that in both HDLp and HDLp-1.17, apoLp-I is more exposed at the surface. Additionally, it can be concluded that delipidation of HDLp leads to an increase in protein exposure of both apoLp-I and -II.

Involvement of the IN and IIC epitopes in binding to LpR

To investigate the involvement of the cleavage site in binding of HDLp-1.17 to LpR, it was tested whether the binding of HDLp-1.17 could be inhibited by anti-IN or anti-IIC. After preincubation of OG-HDLp-1.17 with anti-IN or anti-IIC, the binding of OG-HDLp-1.17 to LpR-transfected CHO cells was analyzed by flow cytometry[19], using untreated HDLp, which does not expose these epitopes, as a control.

As expected, the binding of untreated HDLp was not affected by the presence of the antibodies during the binding (data not shown). Additionally, the fluorescence of cells that bound HDLp-1.17 was not significantly affected by the presence of anti-IN or anti-IIC (Figure 3). This suggests that anti-IN and anti-IIC are not able to inhibit the binding of HDLp-1.17 to LpR, indicating that high-affinity binding of HDLp-1.17

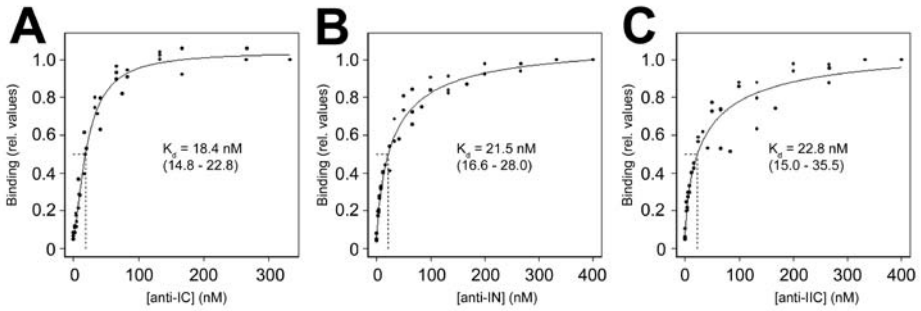

Figure 2. Affinities of anti-IC (A), anti-IN (B) and anti-IIC (C) for coated HDLp. HDLp was coated on a microtiterplate and incubated with different amounts of antibody, detected by a secondary peroxidase-labeled antibody. The relative amount of binding is plotted against the concentration of antibody used (nM). The measurements are indicated by filled circles, and were obtained in three independent experiments. Data were fitted using PROAST software[20]. Dotted lines indicate the $\frac{1}{2}B_{max}$. The K_d (= $\frac{1}{2}B_{max}$) of the interaction is indicated in the plots (the confidence interval in brackets).

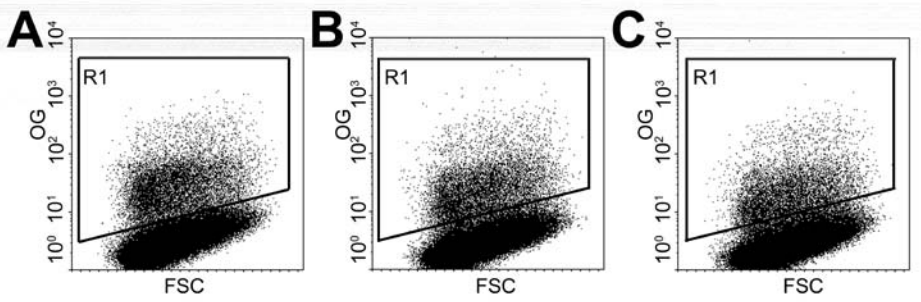

Figure 3. Competition binding studies of HDLp-1.17 to LpR-transfected CHO cells. CHO(LpR) cells were incubated with OG-HDLp-1.17 alone (A) or OG-HDLp-1.17 in the presence of a ten times excess of anti-IN (B) or anti-IIC (C). The fluorescence intensity of the cells was measured by flow cytometry. The amount of fluorescence is plotted on the y-axis (OG, relative values), and the forward scatter (FSC, relative values) on the x-axis. Based on control experiments using untransfected cells, region 1 (R1) was determined that contains LpR-expressing cells that bound and endocytosed OG-ligand. Plots are representative of three independent experiments, performed on cell lines created by different transfections.

to LpR is not mediated by these two epitopes. To further investigate the involvement of the cleavage site in high-affinity binding of HDLp to LpR, it was tested whether the antibodies were able to detect HDLp while the particle was bound to LpR. To this end, cleavage site-expressing HDLp bound to LpR-transfected CHO cells was assayed with anti-IN or anti-IIC. Bound antibodies were detected using a fluorescein-labeled secondary antibody, the fluorescence of which was measured by flow cytometry. Detection of ligand using anti-IN and anti-IIC yielded a similar amount of cells in region 1 (R1) as the positive control, HDLp detected by a polyclonal anti-HDLp antibody (Figure 4). The difference in intensity between cells in R1 incubated with HDLp and detected by anti-IN or anti-IIC (Figures 4A, B) and cells in R1 for which HDLp was detected using anti-HDLp (Figure 4C) is most likely caused by the difference in bound antibodies per particle. Since anti-HDLp is a polyclonal antibody raised against the entire particle, HDLp is expected to contain more binding epitopes for this antibody than for anti-IN and anti-IIC that are raised against a peptide of 20 amino acid residues. The latter results indicate that the IN and IIC epitopes are not hidden in the interface between HDLp and LpR. Together, this implies that the IN and IIC epitopes that comprise the cleavage site do not mediate the binding of HDLp to LpR.

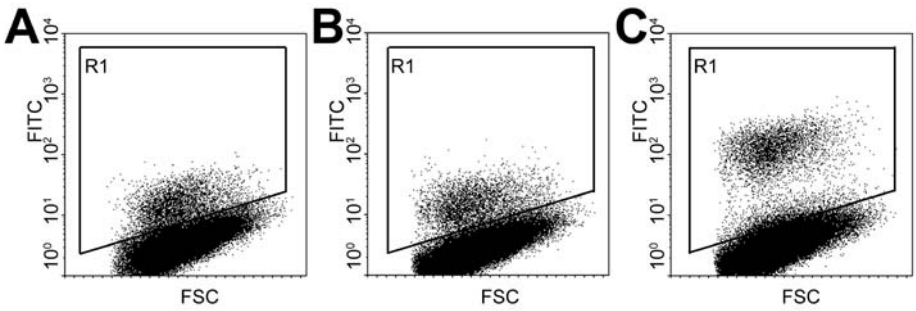

Figure 4. Antibody detection of HDLp bound to LpR-transfected CHO cells. CHO(LpR) cells were incubated on ice with HDLp particles that displayed the cleavage site. After washing, the cells were incubated with anti-IN (A), anti-IIC (B) or anti-HDLp (C). Primary antibodies were detected using a fluorescein-labeled secondary antibody. The fluorescence intensity of the cells was then measured by flow cytometry. The amount of fluorescence is plotted on the y-axis (FITC, relative values), and the forward scatter (FSC, relative values) on the x-axis. Based on control experiments using untransfected cells, region 1 (R1) was determined, containing cells that bound and endocytosed unlabeled HDLp, detected by the various antibodies. Plots are representative of three independent experiments, performed on cell lines created by different transfections.

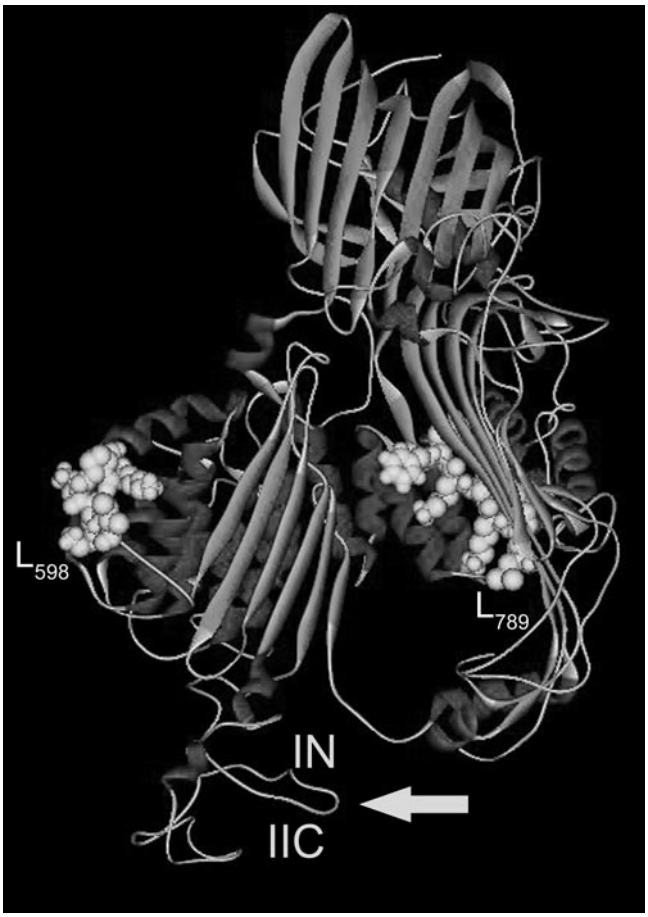

Figure 5. Model of *L. migratoria* apoLp-II/I. The model of locust apoLp-II/I includes amino acid residues 22-1,030 and was constructed based on the sequence homology with silver lamprey lipovitellin and human apoB-100[4]. The Cα backbone structure of apoLp-II/I is indicated by the ribbon colored by secondary structure, α-helices in dark grey, β-sheets in light grey. The consensus sequences L_{598}KPKKI$_{603}$ and L_{789}KKSKKF$_{795}$ are shown including their side chains as CPK model (white) and indicated by their first amino acid residue. The arrow indicates the cleavage site, which is flanked by the IIC and IN epitopes.

Discussion

Previously we have shown that partially delipidated HDLp, produced by incubation of isolated HDLp with α-cyclodextrin and recovered by density-gradient ultra-centri-fugation at a floating density of 1.17 g/ml (HDLp-1.17), binds to LpR with an approx. 2.5-fold higher affinity than native HDLp at its normal density in insect hemolymph of 1.11 g/ml[13]. Additionally, the decreased lipid content of the HDLp-1.17 particle was accompanied by an increase in immunoreactivity with antibodies against peptides flanking the cleavage site of apoLp-II/I[13]. Although these data may be taken to suggest that the increase in binding of HDLp-1.17 to LpR is mediated by the exposed cleavage site of apoLp-II/I, the results of our (competition) binding studies demonstrate that the cleavage site is not implicated in the binding of HDLp by LpR. Based on the K_is of the interaction between the various antibodies and

HDLp or HDLp-1.17, it appears that in both forms of HDLp apoLp-I is more exposed at the surface of the particle compared to apoLp-II, as was also found for the structures of HDLps from other species[24-28]. Since the immunoreactivities of anti-IIC, anti-IN and anti-IC were increased whereas the immunoreactivity of a polyclonal antibody raised against HDLp remained unchanged[13], it is apparent that partial delipidation of HDLp results in the additional exposure of apoLp-I and -II without affecting the conformation of already exposed protein. These results are in excellent agreement with studies of Ryan and colleagues who found an increase in protein exposure upon delipidation of HDLp from *Manduca sexta*[24] and suggested insect lipophorin to be composed of an apolipoprotein/phospholipid framework that encloses a central cavity to which lipid can be added or from which it can be removed. Additionally, delipidation might result in exposure of cryptic receptor-binding sites[24]. The shift in the affinity of LpR for HDLp-1.17 suggests that the high affinity of LpR for HDLp-1.17 may result from such an additional binding site.

Although the differential exposure of the cleavage site, which contains several Arg and Lys residues that are known to mediate the binding of ligands to LDLR family members[14,16,18], may suggest that the cleavage site comprises this binding site, our studies provide the new finding that antibodies against this region, e.g. anti-IN and anti-IIC, were not able to prevent the binding of HDLp or HDLp-1.17 to LpR. Additionally, both anti-IN and anti-IIC appeared to bind receptor-bound, cleavage site-expressing HDLp particles, indicating that the epitopes flanking the cleavage site are not buried in the LpR-HDLp interaction interface. Therefore, it seems more likely that the appearance of the IIC and IN epitopes at the surface of HDLp-1.17 marks the occurrence of additional protein exposure in general that might lead to the exposure of a cryptic LpR-binding site. For the binding site of ligands for LDLR family members, a consensus sequence was proposed involving two (basic) Lys residues separated by two to five residues, while both basic residues are N-terminally flanked by hydrophobic residues, preferentially leucine (Leu) or valine (Val)[16,18]. This consensus sequence is not completely satisfactory for the binding sites of all ligands, since for example in the binding site of apoB-100 for LDLR and in that of several other ligands for LDLR family members the N-terminal Leu is separated from the basic residue by a threonine (Thr) residue[16,29]. Additionally, also other clusters of Arg residues may be involved in the binding of ligand to receptor[15,30]. However, based on this consensus sequence, candidate sequences may be found. Sequence analysis of the apolipoprotein precursor apoLp-II/I revealed that this consensus sequence is numerously found in apoLp-I and once in apoLp-II. The latter, $L_{598}KPKKI_{603}$, is an interesting candidate for both the binding site involved in low-affinity binding of HDLp to LpR and the binding site involved in high-affinity binding of HDLp to LpR, since the three-dimensional model of apoLp-II/I reveals this motif to be situated at the end of an α-helix (Figure 5)[4], as is the case for the binding sites of the receptor-associated protein (RAP) and apoE for LDLR-related protein (LRP)[15,17].

Although apoLp-II is less exposed at the surface of HDLp (our data and[24-28]), the three-dimensional model suggests that the L_{598}KPKKI$_{603}$ sequence is located on the outside of the protein and therefore may be available to mediate the binding of HDLp to LpR. Additionally, L_{598}KPKKI$_{603}$ is located relatively close to the cleavage site; therefore, modulation of the exposure of this sequence may be possible. The consensus sequence is found seven times in the amphipathic β-cluster of apoLp-I, a region that was shown to be required for lipidation of the lipoprotein during biogenesis[2,31,32]. Interestingly, also the LDLR-binding site of apoB-100, the integral protein of LDL, is located in one of its amphipathic β-clusters[29,31]. Such a similar location of the receptor-binding sites in apoLp-I and apoB-100 may suggest that, in addition to the N-terminal LLT modules[1,2], also the C-terminal sequences of both LLTP family members may share a common evolutionary origin. For LDL, the amphiphatic β-strands were proposed to represent a nonflexible lipid-associating backbone displaying a high lipid affinity[2,32-34]. By contrast, delipidation of HDLp isolated from *M. sexta* resulted in a decrease in β-structures, suggestive of a certain degree of flexibility in this region[24]. One of identified sequences in this region, L_{789}KKSKKF$_{795}$, is located on the inside of the lipid-binding pocket close to the cleavage site (Figure 5), and therefore seems to be inaccessible when the particle is lipidated. Delipidation of HDLp might result in the exposure of this sequence, rendering this an interesting candidate for the LpR-binding site of partially delipidated HDLp. The consensus sequence is also present two times in the very C-terminal region of apoLp-I; however, since this region is also well exposed in wild-type HDLp, it seems unlikely that these sequences are involved in high-affinity binding of HDLp-1.17 to LpR. Additionally, since the antibody against this region (anti-IC) did not prevent binding of HDLp to LpR and the antibody was able to detect HDLp when bound to LpR (data not shown), this demonstrates that this region is equally not involved in the low-affinity binding of HDLp to LpR.
Conclusively, our results indicate that the cleavage site of apoLp-II/I is not involved in binding of HDLp to LpR. Our data additionally imply that the receptor-binding site of insect apoLp-II/I (and its resulting apoLp-I and –II in HDLp) may be in a similar position as that of apoB-100, i.e. located in the amphipathic β-cluster.

Acknowledgments

We thank Marcel Smolenaars for his help with sequence analysis of apoLp-II/I, Bas Bokkers for the statistical analysis on the results of the solid phase binding assay and Masja van Oort and Koert Burger for useful discussions. Yvonne Derks was financially supported by the Physical Biology Research programme II, project 01FB22 of the "Stichting voor Fundamenteel Onderzoek der Materie" and "Aard en Levenswetenschappen" (FOM/ALW), which is a part of the "Nederlandse Organisatie voor Wetenschappelijk Onderzoek" (NWO).

References

1. Babin PJ, Bogerd J, Kooiman FP, Van Marrewijk WJ & Van der Horst DJ (1999) Apolipophorin II/I, apolipoprotein B, vitellogenin, and microsomal triglyceride transfer protein genes are derived from a common ancestor. J Mol Evol 49, 150-160.
2. Smolenaars MM, Madsen O, Rodenburg KW & Van der Horst DJ (2007) Molecular diversity and evolution of the large lipid transfer protein superfamily. J Lipid Res 48, 489-502.
3. Weers PM, Van Marrewijk WJ, Beenakkers AM & Van der Horst DJ (1993) Biosynthesis of locust lipophorin. Apolipophorins I and II originate from a common precursor. J Biol Chem 268, 4300-4303.
4. Smolenaars MM, Kasperaitis MA, Richardson PE, Rodenburg KW & Van der Horst DJ (2005) Biosynthesis and secretion of insect lipoprotein: involvement of furin in cleavage of the apoB homolog, apolipophorin-II/I. J Lipid Res 46, 412-421.
5. Ryan RO & van der Horst DJ (2000) Lipid transport biochemistry and its role in energy production. Annu Rev Entomol 45, 233-260.
6. Van der Horst DJ & Ryan RO (2005) Lipid transport. In Comprehensive molecular insect science (Gilbert LI, Iatrou K & Gill SS, editors), 4, pp. 225-246. Elsevier, New York, NY, USA.
7. Dantuma NP, Potters M, De Winther MP, Tensen CP, Kooiman FP, Bogerd J & Van der Horst DJ (1999) An insect homolog of the vertebrate very low density lipoprotein receptor mediates endocytosis of lipophorins. J Lipid Res 40, 973-978.
8. Van Hoof D, Rodenburg KW & Van der Horst DJ (2002) Insect lipoprotein follows a transferrin-like recycling pathway that is mediated by the insect LDL receptor homologue. J Cell Sci 115, 4001-4012.
9. Van Hoof D, Rodenburg KW & Van der Horst DJ (2005) Intracellular fate of LDL receptor family members depends on the cooperation between their ligand-binding and EGF domains. J Cell Sci 118, 1309-1320.
10. Van Hoof D, Rodenburg KW & Van der Horst DJ (2005) Receptor-mediated endocytosis and intracellular trafficking of lipoproteins and transferrin in insect cells. Insect Biochem Mol Biol 35, 117-128.
11. Dantuma NP, Pijnenburg MA, Diederen JH & Van der Horst DJ (1997) Developmental down-regulation of receptor-mediated endocytosis of an insect lipoprotein. J Lipid Res 38, 254-265.
12. Van Hoof D, Rodenburg KW & Van der Horst DJ (2003) Lipophorin receptor-mediated lipoprotein endocytosis in insect fat body cells. J Lipid Res 44, 1431-1440.
13. Roosendaal SD, Van Doorn JM, Valentijn KM, Van der Horst DJ & Rodenburg KW (2008) Lipid unloading of lipophorin affects its binding to the insect LDL receptor homologue, LpR: implications for the role of LpR-mediated endocytosis. Submitted.
14. Roehrkasten A & Ferenz HJ (1992) Role of the lysine and arginine residues of vitellogenin in high affinity binding to vitellogenin receptors in locust oocyte membranes. Biochim Biophys Acta 1133, 160-166.
15. Jensen GA, Andersen OM, Bonvin AM, Bjerrum-Bohr I, Etzerodt M, Thogersen HC, O'Shea C, Poulsen FM & Kragelund BB (2006) Binding site structure of one LRP-RAP complex: implications for a common ligand-receptor binding motif. J Mol Biol 362, 700-716.

16. Li A, Sadasivam M & Ding JL (2003) Receptor-ligand interaction between vitellogenin receptor (VtgR) and vitellogenin (Vtg), implications on low density lipoprotein receptor and apolipoprotein B/E. The first three ligand-binding repeats of VtgR interact with the amino-terminal region of Vtg. J Biol Chem 278, 2799-2806.
17. Fisher C, Beglova N & Blacklow SC (2006) Structure of an LDLR-RAP complex reveals a general mode for ligand recognition by lipoprotein receptors. Mol Cell 22, 277-283.
18. Nielsen KL, Holtet TL, Etzerodt M, Moestrup SK, Gliemann J, Sottrup-Jensen L & Thogersen HC (1996) Identification of residues in alpha-macroglobulins important for binding to the alpha2-macroglobulin receptor/Low density lipoprotein receptor-related protein. J Biol Chem 271, 12909-12912.
19. Roosendaal SD, Kerver J, Schipper M, Rodenburg KW & Van der Horst DJ (2008) The complex of the insect LDL receptor homologue, lipophorin receptor, LpR, and its lipoprotein ligand does not dissociate under endosomal conditions. FEBS J 275, 1751-1766.
20. Slob W (2002) Dose-response modeling of continuous endpoints. Toxicol Sci 66, 298-312.
21. Moerbeek M, Piersma AH & Slob W (2004) A comparison of three methods for calculating confidence intervals for the benchmark dose. Risk Anal 24, 31-40.
22. Cheng Y & Prusoff WH (1973) Relationship between the inhibition constant (K1) and the concentration of inhibitor which causes 50 per cent inhibition (I50) of an enzymatic reaction. Biochem Pharmacol 22, 3099-3108.
23. Kingsley DM & Krieger M (1984) Receptor-mediated endocytosis of low density lipoprotein: Somatic cell mutants define multiple genes required for expression of surface-receptor activity. Proc Natl Acad Sci USA 81, 5454-5458.
24. Ryan RO, Kay CM, Oikawa K, Liu H, Bradley R & Scraba DG (1992) Effect of particle lipid content on the structure of insect lipophorins. J Lipid Res 33, 55-63.
25. Kashiwazaki Y & Ikai A (1985) Structure of apoproteins in insect lipophorin. Arch Biochem Biophys 237, 160-169.
26. Shapiro JP, Keim PS & Law JH (1984) Structural studies on lipophorin, an insect lipoprotein. J Biol Chem 259, 3680-3685.
27. Pattnaik NM, Mundall EC, Trambusti BG, Law JH & Kezdy FJ (1979) Isolation and characterization of a larval lipoprotein from the hemolymph of *Manduca sexta*. Comp Biochem Physiol B 63, 469-476.
28. Robbs SL, Ryan RO, Schmidt JO, Keim PS & Law JH (1985) Lipophorin of the larval honeybee, *Apis mellifera L.* J Lipid Res 26, 241-247.
29. Borén J, Lee I, Zhu W, Arnold K, Taylor S & Innerarity TL (1998) Identification of the low density lipoprotein receptor-binding site in apolipoprotein B100 and the modulation of its binding activity by the carboxyl terminus in familial defective apo-B100. J Clin Invest 101, 1084-1093.
30. Melman L, Cao ZF, Rennke S, Marzolo MP, Wardell MR & Bu G (2001) High affinity binding of receptor-associated protein to heparin and low density lipoprotein receptor-related protein requires similar basic amino acid sequence motifs. J Biol Chem 276, 29338-29346.
31. Smolenaars MM, De Morrée A, Kerver J, Van der Horst DJ & Rodenburg KW (2007) Insect lipoprotein biogenesis depends on an amphipathic beta cluster in apolipophorin II/I and is stimulated by microsomal triglyceride transfer protein. J Lipid Res 48, 1955-1965.

32. Segrest JP, Jones MK, De Loof H & Dashti N (2001) Structure of apolipoprotein B-100 in low density lipoproteins. J Lipid Res 42, 1346-1367.
33. Chauhan V, Wang X, Ramsamy T, Milne RW & Sparks DL (1998) Evidence for lipid-dependent structural changes in specific domains of apolipoprotein B100. Biochemistry 37, 3735-3742.
34. Wang L & Small DM (2004) Interfacial properties of amphipathic beta strand consensus peptides of apolipoprotein B at oil/water interfaces. J Lipid Res 45, 1704-1715.

5

Calcium is essential for folding and integrity of the ligand-binding site of the insect LDL-receptor homologue, LpR

Sigrid D. Roosendaal[1], Jürgen Gent[2], Santiago Cuesta-López[3], Dick J. Van der Horst[1], Ineke Braakman[2], Javier Sancho[4] and Kees W. Rodenburg[1]

From the [1]Division of Endocrinology and Metabolism, Department of Biology and Institute of Biomembranes, Utrecht University, The Netherlands; [2]Cellular Protein Chemistry, Department of Chemistry and Bijvoet Institute of Biomolecular Research, Utrecht University, The Netherlands; [3]Laboratoire de Physique, École Normale Supérieure de Lyon, France; and [4]Departamento de Bioquímica y Biología Molecular y Celular; Instituto de Biocomputación y Física de Sistemas Complejos, Universidad de Zaragoza, Spain.

Manuscript in preparation

Abstract

The insect low-density lipoprotein receptor (LDLR) homologue, LpR, mediates endocytosis of the insect lipoprotein, high-density lipophorin (HDLp). The ligand is, however, recycled and resecreted, whereas other LDLR family members target their ligands for lysosomal degradation. In line with the ligand-recycling capacity of LpR, we demonstrated the complex of LpR and HDLp to be resistant to endosomal pH and low Ca^{2+}-concentration as induced by EDTA treatment. Since Ca^{2+} is involved in the folding and functioning of LDLR family members, the resistance of the LpR-HDLp complex to EDTA treatment is remarkable. Therefore, we investigated the Ca^{2+}-dependence of LpR. Using an electrophoretic mobility assay in combination with metabolic labeling, we show that folding of LpR followed the same Ca^{2+}-dependent mechanism as disclosed for LDLR. Using a flow cytometric approach, treatment of cells with 5 mM EDTA prior to binding of HDLp to LpR was shown to abolish ligand binding, as observed for LDL binding to LDLR. The ligand-binding capacities of both LpR and LDLR were rescued by the addition of 2 mM Ca^{2+}, displaying the ability of their ligand-binding sites to reorganize to the native conformation in the presence of Ca^{2+}. After binding of HDLp to LpR, the complex appeared EDTA-resistant, in contrast to the LpR-RAP complex, suggesting this stability to be caused by a unique aspect of the interaction of insect lipoprotein with LpR. Molecular dynamics simulations of the ligand-binding (LA-) repeats involved in binding of lipoprotein predicted that although LA-repeats 4, 5 and 6 were stable in the presence of Ca^{2+}, they significantly unfolded on removal of Ca^{2+}. However, LA-6 seemed to display a higher stability in the absence of Ca^{2+} than LA-4 and -5. Together, these results indicate that the remarkable stability of the LpR-HDLp complex originates from the stabilizing properties of the interaction interface of LpR and its lipoprotein ligand, to which particularly LA-repeat 6 is proposed to contribute.

Introduction

Lipid transport in the circulatory system of animals is mediated by highly specialized lipoprotein complexes, the apolipoproteins of which stabilize the lipid components and mediate particle metabolism. The multifunctional insect lipoprotein, high-density lipophorin (HDLp), is synthesized in the insect fat body and secreted into the blood (hemolymph). In addition to lipid, the particle harbors two non-exchangeable apolipoproteins, apolipophorin I and apolipophorin II (apoLp-I and apoLp-II), which are derived from the post-translational cleavage of their common precursor, apoLp-II/I[1,2]. This precursor was demonstrated to be a homologue of apoB-100[3,4], the non-exchangeable apolipoprotein of mammalian lipoproteins such as very-low-density lipoprotein (VLDL) and low-density lipoprotein (LDL)[5,6]. Whereas in mammals, endocytic uptake of lipoprotein particles, mediated via members of the LDL receptor (LDLR) family, results in their degradation in lysosomes, insect HDLp was shown to act as a reusable shuttle which is capable of both lipid delivery and reloading. In apparent contrast to its functioning as a shuttle system, receptor-mediated endocytic uptake of HDLp was demonstrated in fat body tissue of larval and young adult locusts, which appeared to be mediated by an insect LDLR homologue, the lipophorin receptor, LpR[7-9]. The domain organization of LpR shows a high similarity to mammalian LDLR and VLDLR[8]. Notwithstanding the homology between LpR and LDLR, the O-linked glycosylation domain of LpR is half the size of that of LDLR, resulting in a lower number of serine (Ser) and threonine (Thr) residues in this domain[8,10], while the ligand-binding domain of LpR contains one additional cysteine-rich LDLR class A (LA-) repeat compared to the cluster of seven repeats in LDLR[8]. Moreover, in spite of the high structural similarity of LpR to mammalian LDLR, in a direct comparison of the functioning of both receptors in LpR-transfected Chinese hamster ovary (CHO) cells, endocytosed HDLp appeared not to be degraded in lysosomes, as is the case for mammalian LDL, but resecreted in a manner similar to transferrin[11-14]. Also in insect fat body tissue, endocytosed HDLp is most likely resecreted[15]. Although the physiological role of this pathway is not yet clear, binding and endocytosis studies using partially delipidated HDLp with a buoyant density of 1.17 g/ml (HDLp-1.17) indicate that LpR favors the binding of this partially delipidated HDLp over HDLp, suggesting that LpR-mediated recycling may function in intracellular loading of HDLp with lipids to be delivered to other tissues[16]. Binding studies propose that a crucial step in this recycling mechanism of LpR, both in LpR-transfected CHO cells and in the insect tissue, may result from the resistance of the LpR-HDLp complex to dissociation at endosomal conditions[17], such as low pH (pH 5 - 6.5) and a relatively low Ca^{2+} concentration[18,19]. Similar experiments using hybrid receptors composed of the ligand-binding domain of LpR and the other domains of LDLR showed that the resistance of the LpR-HDLp complex against EDTA-treatment is mediated by the interaction of HDLp and LA-2-7 of LpR[17].

LA-repeats of LDLR family members consist each of approximately 40 amino acid residues organized in a two-loop conformation stabilized by three disulfide bonds and a Ca^{2+} ion that is chelated by six amino acid residues, five of which are located in a conserved stretch of acidic residues (DCxDxSDE)[20-24]. During folding of LDLR family members, Ca^{2+} is essential for native disulfide bond formation in the LA-repeats[20,25,26]. After folding, when the native structure of the receptor is achieved, removal of the Ca^{2+} ion was shown to abolish ligand binding by LDLR[27]. Folding of LDLR has long been assumed to occur in a vectorial manner, i.e. domain by domain, starting with the most N-terminal LA-repeat. However, studies using an electrophoretic mobility assay in combination with metabolic labeling showed the newly synthesized LDLR polypeptide chain to fold rapidly into compact structures containing non-native disulfide bonds linking distant regions of the protein[28,29]. With time these non-native disulfide bonds are isomerized into native disulfide bonds between cysteines within individual LA-repeats[28,30,31]. The remarkably efficient folding of the LDLR may be caused by assistance of general chaperones, for example BiP[32]. Additionally, specific chaperones, such as the receptor-associated protein (RAP) and Boca/Mesd, contribute to the folding of LDLR family members[33-37]. Due to their high affinity for RAP, RAP is also used as a general ligand for LDLR family members[38-40] and was shown to efficiently compete with HDLp for binding to LpR[11,17].

Despite the EDTA resistance of the LpR-HDLp complex, sequence comparison of LpR with other LDLR family members revealed no unusual features that could suggest the absence of, or a significant difference in, Ca^{2+}-binding by the LA-repeats of LpR[17]. Therefore, in this study, we investigate the role of Ca^{2+} in LpR folding and ligand binding to LpR, as well as the remarkable stability of the LpR-HDLp complex in the absence of Ca^{2+} in addition to the stability of the LA-repeats involved in the interaction of HDLp and LpR in the absence and presence of Ca^{2+}. Together, our results suggest that the high stability of the LpR-lipoprotein complex at low Ca^{2+} concentration conditions seems to arise from the specific binding of HDLp to LpR, possibly stabilized by an increased intrinsic stability of LA-6.

Materials and Methods

Proteins and antibodies

HDLp was isolated from locust hemolymph by density gradient ultracentrifugation as described earlier[11]. Partially delipidated HDLp (HDLp-1.17) was prepared using α-cyclodextrin as described[16]. Human LDL was isolated from blood plasma as described (Plasma obtained from the Bloedbank Midden Nederland)[17]. Polyclonal rabbit-anti-LpR 2189/90 antibody was raised against a synthetic peptide representing the unique N-terminal 20 amino acids (34-53) of LpR[9]. The 121 rabbit polyclonal

antiserum was raised against amino-acids 59-343 of LDLR[11]. Mouse anti-LDLR antibody C7[41] and anti-HA antibody 12CA5[42] were obtained from hybridoma cells. Human his-tagged RAP (RAP-his) was a generous gift from Dr. Michael Etzerodt (IMSB, Aarhus University, Århus, Denmark).

DNA constructs

Constructs for expression of LpR and hybrid receptors were described before[11,12]. A short immunoreactive tag, the hemagglutinin epitope YPYDVPDYA (HA-tag) from the influenza virus A, was fused to the C-terminal end of LpR and LDLR to generate LpR-HA and LDLR-HA, respectively. Cloning of the expression vectors encoding the fusion proteins was performed according to standard molecular biological laboratory procedures and to protocols provided with endonucleases and kits. A PCR fragment was generated using PfuTurbo DNA polymerase (New England Biolabs) and synthetic oligonucleotide primers (Biolegio, Malden, The Netherlands). The nucleotide sequence encoding the HA-tag was inserted immediately downstream of the codon encoding the C-terminal residue of LpR or LDLR. To this end, for LpR a 1562 bp fragment was generated by PCR from pcDNA3-LpR (piLR-e;)[8] containing an *Xba*I site at the 5′ end and a *Kpn*21 site at the 3′ end, using the forward oligonucleotide primer 5′ggt acc aat gaa tgt gct gta aat aat gg 3′, and the reverse primer 5′gatc tct aga tca cac agc *gta gtc cgg gac gtc gta cgg gta* tac ata atc att tgt ccc agg 3′ (HA-tag encoding sequence indicated in italics). Subsequently, the obtained fragment was digested with *Xba*I (New England Biolabs) and *Kpn*21 (Fermentas) and the resulting 1190 bp fragment was cloned into pcDNA3-LpR digested with the same two endonucleases to replace the sequence at the 3′ end with that encoding the HA-tag. The pcDNA3-LDLR-HA construct was made similarly using the forward primer 5′ cct gtc cca gag aat gat cgc cag cac cca gct tga cag agc 3′ and the reverse oligonucleotide primer 5′ gatc ggt acc tca cac agc *gta gtc cgg gac gtc gta cgg gta* cgc cac gtc atc ctc cag act gac 3′ (HA-tag encoding sequence indicated in italics) and subsequent cloning using *Bgl*II and *Kpn*I.

Cell culture

LDLR-deficient Chinese hamster ovary cells, CHO(*ldlA*)[43] were cultured in Ham F-10 nutrient mixture (Invitrogen) supplemented with 5 % heat-inactivated fetal bovine serum (FBS, Invitrogen) and 100 U/ml penicillin G sodium and 100 µg/ml streptomycin sulfate in 85% saline (Invitrogen). Wt CHO cells were maintained in α-minimal essential medium (αMEM, Invitrogen) supplemented with 8 % fetal calf serum, 100 U/ml penicillin, 100 µg/ml streptomycin, and 2 mM Glutamax (Invitrogen). Human cervical carcinoma (HeLa) cells were cultured in minimal essential medium (MEM,

Invitrogen) supplemented with 10 % fetal calf serum, 100 units/ml penicillin, 100 µg/ml streptomycin, 2 mM Glutamax (Invitrogen), and non-essential amino acids (Invitrogen). All cell types were maintained at 37°C and 5 % CO_2.

Transfections

LDLR-deficient CHO(*ldlA*)[43] cells were cultured until 40% confluency in 12-well multidishes (Costar). After washing the cells once, the culture medium was replaced with 500 µl of fresh culture medium. Subsequently, 4 µg DNA and 4 µg 25 kDa linear polyethylenimine (PEI; Polysciences) in 50 µl serum-free medium (Ham F-10 nutrient mixture supplemented medium with 100 U/ml penicillin G sodium and 100 µg/ml streptomycin sulfate in 85% saline) was administered to the cells. After 4 h, 500 µl culture medium was added and cells were cultured overnight. The next day, cells were detached from dishes by trypsinization and cultured in 25 cm^2 culture flasks in growth medium supplemented with 400 µg/ml geneticin (GibcoBRL). Ten days after transfection, cells were used for experiments. For transient transfections, wt CHO or HeLa cells were transfected with DNA plasmids using PEI as described above and used for experiments 24 h post-transfection.

Electrophoretic mobility assay and metabolic labeling

Pulse-chase experiments were performed as described before[28,44]. Briefly, transiently transfected cells were incubated for 15-30 min in MEM deprived of methionine and cysteine (MP Biomedicals) and supplemented with 10 mM HEPES pH 7.4. Newly synthesized proteins were radiolabeled by incubating the cells for 5 min at 37°C with ^{35}S-labeled methionine and cysteine (RedivueTM PRO-MIX, Amersham Biosciences). Subsequently, radiolabeled proteins were chased for the times indicated by incubating cells with culture medium containing 5 mM of unlabeled cysteine and methionine, 5 % fetal calf serum, 10 mM HEPES pH 7.4 and 1 mM cycloheximide to terminate nascent chain elongation. At the end of the chase, cells were cooled to 4°C and free sulfhydryl groups were blocked with 20 mM alkylating agent N-ethylmaleimide (NEM, Sigma).

To study the effect of Ca^{2+}-depeletion on receptor folding, cells were pretreated for 30 min with thapsigargin (100 nM, ICN) or DMSO as control. Thapsigargin or DMSO was also present in the labeling and chase media.

Immunoprecipitation and SDS-PAGE

Cellular detergent lysates were prepared in lysis buffer (1 % Triton X-100, 10 mM HEPES pH 7.4, 200 mM NaCl, 2 mM $CaCl_2$, 2.5 mM $MgCl_2$, 2.2 % DMSO) supplemented with 1 mM phenylmethylsulfonyl fluoride (PMSF), 20 mM NEM, and

10 µg/ml each of chymostatin, leupeptin, antipain, pepstatin A (CLAP) for 10 min at 4°C. After incubation, cell remains were scraped and the lysate was centrifuged for 10 min at 16,000 x g and 4°C. Supernatants were subjected to immunoprecipitation using the anti-HA antibody 12CA5. Alternatively, $LpR_{1-342}LDLR_{293-839}$ and $LDLR_{1-292}LpR_{343-850}$ were precipitated using antibody 2189/90 or the 121 rabbit polyclonal antiserum respectively. Immune complexes were captured using Protein A-Sepharose beads (Amersham Biosciences) and washed twice with 50 mM Tris-HCl pH 8.6, 150 mM NaCl, 1 % Triton X-100, 0.5 % SDS. Immunoisolates were resuspended in 10 mM Tris-HCl pH 6.8, 1 mM EDTA and heated for 5 min at 95°C in sample buffer (200 mM Tris-HCl pH 6.8, 3 % SDS, 10 % glycerol, 1 mM EDTA and 0.004 % bromophenol blue). For reduction of disulfide bonds, samples were incubated in sample buffer containing 50 mM dithiotreitol (DTT) for 5 min at 95°C; after reduction, 100 mM NEM was added to block free sulfhydryl groups. The electrophoretic mobility of the proteins was analyzed by separation of the proteins by SDS-PAGE on a 6 % polyacrylamide gel. Subsequently, SDS-PAGE gels were dried and exposed to Kodak MR BioMax films.

Fluorescence labeling

HDLp and LDL were covalently labeled with Oregon green (OG) 488 carboxylic acid (Molecular Probes) as described before[11].

Binding experiments using flow cytometry

Binding experiments were performed as described earlier[17]. In short, CHO(*ldlA*) cells stably transfected with LpR or LDLR were washed with ice-cold binding buffer (50 mM Tris-HCl, 2 mM $CaCl_2$, 150 mM NaCl, pH 7.4) and subsequently incubated with OG-HDLp (25 µg/ml) or OG-LDL (35 µg/ml) in binding buffer for 30 min. Alternatively, cells were preincubated with EDTA-containing buffer (50 mM Tris, 150 mM NaCl, 5 mM EDTA, pH 7.4, 4°C) for 30 min, after which binding was performed in binding buffer or in binding buffer without Ca^{2+} (50 mM Tris-HCl, 150 mM NaCl, pH 7.4, 4°C). To determine the ligand-specificity of the EDTA resistance of the LpR-ligand complex, LpR-transfected CHO(*ldlA*) cells were incubated with OG-HDLp (25 µg/ml), OG-HDLp-1.17 (25 µg/ml) or RAP-his (3.6 µg/ml). After binding, cells were washed and incubated with EDTA-containing buffer. RAP-his was detected by subsequent washing and incubation of mouse-anti-his antibody (Amersham Biosciences) in binding buffer, followed by washing and incubation with a fluorescein isothiocyanate (FITC)-labeled secondary anti-IgG antibody (Jackson ImmunoResearch Laboratories Inc). The above described incubations were performed on ice to prevent endocytosis. After the binding, cells were washed once with binding buffer and once with serum-free medium, followed by incubation with serum-free

medium for 5 min at 37°C, to allow the bound ligand to be endocytosed. After endocytosis, cells were detached from dishes by trypsin treatment and resuspended in growth medium. Resuspended cells were fixed in 0.5 % paraformaldehyde in PBS at 4°C for at least 30 min to overnight. Samples were measured by flow cytometry using a fluorescence-activated cell sorter (FACS, Becton Dickinson FACS Calibur). Flow cytometry data were collected using Cell Quest (Becton Dickinson) and downloaded into the program WinMDI (TSRI FACS Core Facility, La Jolla, CA) for analysis.

Flow cytometry data analysis

Flow cytometry data were quantified as descried earlier[17]. In brief, of each sample (approximately 100,000 cells) the fluorescence was plotted against the forward scatter (FSC). For each series of experiments, the region containing cells that bound and endocytosed OG-ligand (Region 1, R1) was defined in the plot based on a similar experiment performed using untransfected cells. Then the number of cells and the mean fluorescence (y-mean) in R1 were determined. For each cell line, the number of cells in R1 after different treatments was compared by a t-test for paired samples performed on the logarithms of the number of cells. In case of a significant ($p \leq 0.05$) difference in sample size due to the different treatments, the y-mean was corrected by using random values of the missing number of cells from the population of which the fluorescence did not exceed that of untransfected cells. To test whether samples were significantly different from control samples, a t-test for paired samples was performed on the logarithms of the y-means. As negative control, the y-mean outside R1 was determined and compared between different treatments. For each sample the relative amount of fluorescence as compared to control samples was calculated. Data presented as means of these relative values $\pm$ s.e.m. were obtained from at least three independent experiments.

Molecular dynamics

The structures of LA-repeats 4, 5 and 6 of LpR were modeled in pairs using Modeller 8v2 using the structure of LA-repeats 3 and 4 of LDLR (PDB-bank 2FCW) as a template. The different models for the LA-repeats of LpR were initially refined in vacuo through a minimization schema that uses several cycles of Conjugate Gradient up to 20000 steps in total. Molecular dynamics (MD) simulations were performed using NAMD 2.6[45] with the CHARMM 27 force field[46]. Solvation of the systems was achieved by placing a pre-equilibrated rectangular box (55 Å x 55 Å x 60 Å) of approximately 5000 TIP3P water molecules[47] around the protein structures. Periodic boundary conditions were applied and rigid bonds (SHAKE algorithm)[48] were used to hold rigid the internal geometry of the water molecules (Jorgensen description).

Long-range electrostatic interactions were modeled with the particle-mesh Ewald method[49], using a cutoff of 14.0 Å and a grid space between 0.95-1.0 Å. To reach an appropriate neutralization, solvent environment setup was complemented with an equilibrated atmosphere of Na^+ and Cl^- counter ions. Diffusion of the counter ions and suppression of potential internal strains present in the solvation cage were achieved through 1 ns (300 K, 1 at) of CPT (constant pressure and temperature) dynamics, using the Nosé-Hoover Langevin Piston for pressure coupling[50,51] with a fixed solute. In the Ca^{2+}-removal simulations, additional steps of neutralization and equilibration of the solute environment were required and were performed following a similar protocol. System heating and equilibration phases proceeded as follows: after proper system solvation, neutralization and spatial organization, a slow progressive heating of 100 ps to the working temperature (300K) was done using Langevin dynamics, and a sufficiently long equilibration phase (500 ps) using CPT dynamics (250 ps) and Langevin dynamics (250 ps with a friction coefficient of 5 ps^{-1}) consecutively. Ulterior protein structure refinement was achieved using constrained molecular dynamics, imposing on the different protein residues harmonic constraints that decrease linearly (until full removal) as the simulation evolves. Finally, in the production phase, traditional Brownian dynamics gave rise to a set of production trajectories of up to 10 ns length each. In case of simulations in the presence of Ca^{2+} the initial structure subjected to a 10 ns simulation was the one obtained by modeling of the repeat. For simulations in the absence of Ca^{2+}, the minimized final structure after 10 ns simulation of the initial model was used as initial structure from which the Ca^{2+} ion was then removed so that a subsequent 10 ns simulation was run. In all cases, the friction coefficients in the Langevin equations were set to 60 ps^{-1} for the solvent molecules while a much lower one (0.5-1.0 ps^{-1}) was used for the atoms in the protein. Vibrational analysis and B factor prediction were performed with user-made subroutines in cooperation with the elastic network model implemented in the "El Nemo" server[52]. Molecular visual graphics were generated using the VMD package[53].

Results

Folding of LpR

To study the folding pattern of LpR in comparison with that of LDLR, radiolabeling pulse-chase experiments were used to monitor disulfide bond formation of newly synthesized receptors in CHO cells transiently transfected with either HA-epitope-tagged LpR (LpR-HA) or LDLR (LDLR-HA). Subsequently, the radiolabeled receptors were immunoisolated using an anti-HA antibody and the electrophoretic mobility of the receptors was analyzed by non-reducing (Figure 1A) and reducing (Figure 1B)

SDS-PAGE. Immediately after synthesis, under non-reducing conditions LpR ran as a smear (Figure 1A, 0 min chase), indicative of a heterogeneous pool of LpR folding intermediates. Upon reduction of the sample, the signal appeared as a single band (Figure 1B, 0 min chase), indicating that the difference between the LpR forms in the non-reducing gel was due to variability in number and/or organization of disulfide bonds. Similar to LDLR (Figure 1A)[28], the electrophoretic mobility of the non-reduced LpR molecules decreased with time, whereas that of the reduced samples remained similar (Figure 1), indicating that also in LpR initially formed non-native disulfide bonds isomerize into the native set. After a chase time of 30 min, an additional band migrating with a lower electrophoretic mobility appeared in both reducing and non-reducing conditions (Figure 1). Like for LDLR, this band most likely represents LpR molecules that are O-linked glycosylated in the Golgi-complex. For LpR, however, a smaller shift between the endoplasmic reticulum (ER) and Golgi-form was seen than for LDLR (Figure 1). This suggests LpR to be O-glycosylated less than LDLR, which is in agreement with its shorter O-glycosylation domain (Figure 2). As for untagged

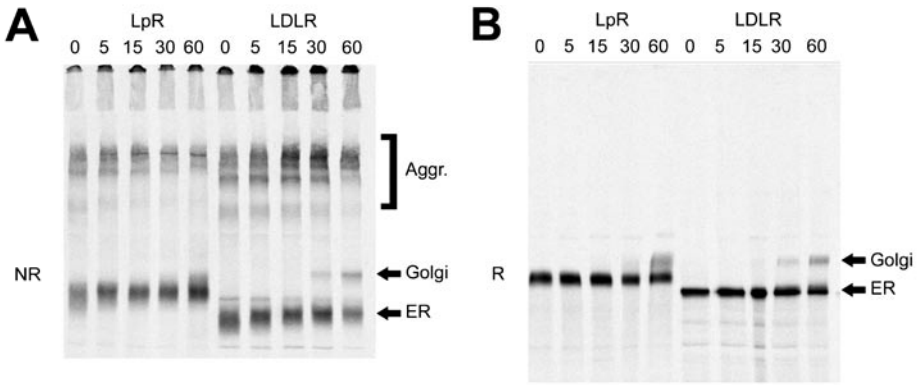

Figure 1: Folding of LpR and LDLR in transiently receptor-transfected CHO cells. Cells were radiolabeled by a 5 min pulse and subsequently chased for the times indicated (min). LpR-HA and LDLR-HA were immunoprecipitated from cell lysates using an anti-HA antibody. Samples were subjected to non-reducing (A) or reducing (B) SDS-PAGE. Aggregates (Aggr.), Golgi- and ER-forms are indicated. NR: non-reduced, R: reduced.

```
LpR    ----------AEAASPNESTTKLVAEPEAFP----------IEDADSGMV----------
LDLR   TQETSTVRLKVSSTAVRTQHTTTRPVPDTSRLPGATPGLTTVEIVTMSHQALGDVAGRGNEKKPSSVRA
```

Figure 2: Alignment of the amino acid sequences of the O-linked glycosylation domain of LpR and LDLR. The alignment was obtained using the on-line CLUSTAL W (1.82) multiple sequence alignment tool. Potential sites for O-linked glycosylation (Ser, S and Thr, T) are shaded in grey.

LDLR (F. Pena, J. Gent and I. Braakman, unpublished results), we found similar results for the folding of untagged LpR (data not shown). Together these results indicate that the folding pattern of LpR is similar to that of LDLR.

To investigate whether the observed folding pattern represents a general mechanism for folding of LDLR family members, we examined whether the ligand-binding domains of LDLR and LpR were exchangeable without affecting folding. For these experiments, HeLa cells were transiently transfected with cDNA encoding a hybrid receptor composed of domains from LpR and LDLR (Figure 3A). The folding pattern of LpR and LDLR was similar in HeLa and CHO cells (data not shown). Pulse-chase analysis of $LDLR_{1\text{-}292}LpR_{343\text{-}850}$, composed of the LDLR ligand-binding domain and the other domains from LpR (Figure 3A) showed a similar folding pattern as for LpR and LDLR (Figures 3B and 1A). The folding pattern of the reciprocal receptor, $LpR_{1\text{-}342}LDLR_{293\text{-}839}$ (Figure 3A) was also similar (Figures 3B and 1A). The observed difference in the amount of precipitated aggregates for the hybrid receptors as compared to that of LpR and LDLR (Figures 1A and 3A) may be caused by the use of antibody 2189/90 to precipitate $LpR_{1\text{-}342}LDLR_{293\text{-}839}$ and antiserum 121 to precipitate $LDLR_{1\text{-}292}LpR_{343\text{-}850}$ instead of the anti-HA antibody. Using antibody 2189/90 or 121 to precipitate LpR or LDLR, respectively, resulted in similar differences in the amount of precipitated aggregates, which were not observed when the anti-HA antibody was used (Figure 1; data not shown), indicating that the difference is due to a difference in specificity of the antibodies. Collectively, these results indicate that swapping of the ligand-binding domains of LpR and LDLR resulted in the formation of hybrid receptors that are able to fold properly and to reach the Golgi-system. This suggests that the observed folding pattern may be general for LDLR family members.

Involvement of Ca^{2+} in folding of LpR

The formation of native disulfide bonds during folding of the LA-repeats of LDLR is closely associated with Ca^{2+} binding by the repeats[20,26,28,54]. To examine the role of Ca^{2+} in folding of LpR, pulse-chase experiments were performed in the presence of thapsigargin, an inhibitor of the Ca^{2+}-ATPase pump, leading to depletion of Ca^{2+} from the ER[55,56]. For these experiments, CHO cells were transiently transfected with LpR-HA. In the presence of thapsigargin the electrophoretic mobility of the LpR-HA folding intermediates was higher than in DMSO-treated cells (Figure 4A). However, upon reduction no mobility differences were observed between LpR-HA molecules from thapsigargin- or DMSO-treated cells (Figure 4B). These results indicate that the difference in electrophoretic mobility in the presence of thapsigargin is due to a variation in number or position of the non-native disulfide bonds. After 2h, O-linked glycosylated receptors were observed (Figure 4), but the electrophoretic mobility under non-reducing conditions of these receptors folded in the presence of thapsigargin differed from that of receptors folded in control cells (Figure 4A).

Additionally, much more disulfide-linked LpR-HA aggregates were observed in the presence of thapsigargin. A similar effect of Ca^{2+} depletion was observed for the biosynthesis of HA-tagged LDLR (LDLR-HA) (Figure 4)[25]. These results suggest that depletion of Ca^{2+} from the ER disturbs the folding pattern of LpR in the same way as that of LDLR, indicating that Ca^{2+} is necessary for proper disulfide bond formation of LpR.

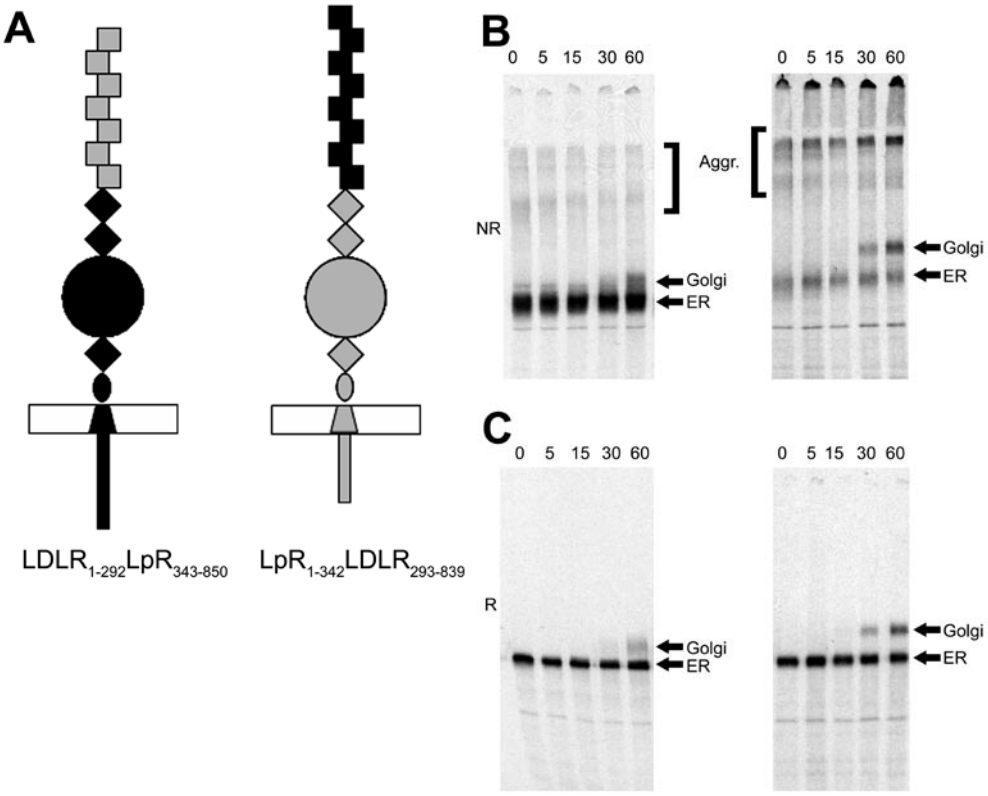

Figure 3: Folding of $LDLR_{1-292}LpR_{343-850}$, and $LpR_{1-342}LDLR_{293-839}$ in HeLa cells. A: Schematic representation of the hybrid receptors. LDLR domains are depicted in grey and LpR domains in black. Both receptors contain a ligand-binding domain composed of LA-repeats (squares), an EGF-precursor homology domain composed of two EGF-repeats (diamonds) that are separated from a third by a β-propeller containing YWTD-repeats (circle), an O-linked glycosylation domain (oval), a transmembrane domain (trapezoid) and an intracellular C-terminal domain (long rectangle). The wide and open rectangle represents the plasma membrane. The numbers indicate the amino acid residues of the mature proteins. B, C: Cells were radiolabeled by a 5 min pulse followed by a chase for the indicated times (min). Receptors were immunoprecipitated with antibody 121 ($LDLR_{1-292}LpR_{343-850}$, left panel) or 2189/90 ($LpR_{1-342}LDLR_{293-839}$, right panel). Samples were subjected to non-reducing (B) or reducing (C) SDS-PAGE. Aggregates (Aggr.), the Golgi- and ER-forms are indicated. NR: non-reduced, R: reduced.

Requirement of Ca^{2+} for the integrity of the ligand-binding site of LpR

Since Ca^{2+} appeared essential for proper disulfide bond formation of LpR, it became vital to determine whether Ca^{2+} is necessary to maintain the conformation of the ligand-binding site of LpR. After binding at 4°C of OG-labeled HDLp to LpR-transfected CHO(*ldlA*) cells, endocytosis of bound ligand was allowed by incubation at 37°C in serum-free medium, while subsequently the fluorescence of resuspended cells was analyzed by flow cytometry[17]. A preincubation of the LpR-transfected CHO(*ldlA*) cells with an EDTA-containing (5 mM) buffer, followed by binding of OG-HDLp in the absence of Ca^{2+}, abolished ligand binding (Figures 5A, B). Quantification of the fluorescence in region 1 (R1) containing cells which had bound and endocytosed OG-HDLp[17] revealed a decrease in the mean fluorescence (y-mean) of 80.2 ± 3.0% compared to the y-mean of cells from control experiments. Such a decrease was also apparent in a similar experiment using CHO(*ldlA*) cells stably transfected with LDLR and measuring binding of OG-LDL (Figures 5D, E). It should be noted that the endocytosis step was performed in the presence of Ca^{2+}, indicating that the decrease in fluorescence was not caused by the disability of the cells to endocytose ligand in the absence of Ca^{2+}. A similar experiment assaying the binding and endocytosis of anti-LDLR antibody 121 that is able to bind LDLR after Ca^{2+} depletion[11] resulted in endocytosis of this antibody (data not shown), confirming that after preincubation with EDTA, the cells retain their ability to endocytose ligand.

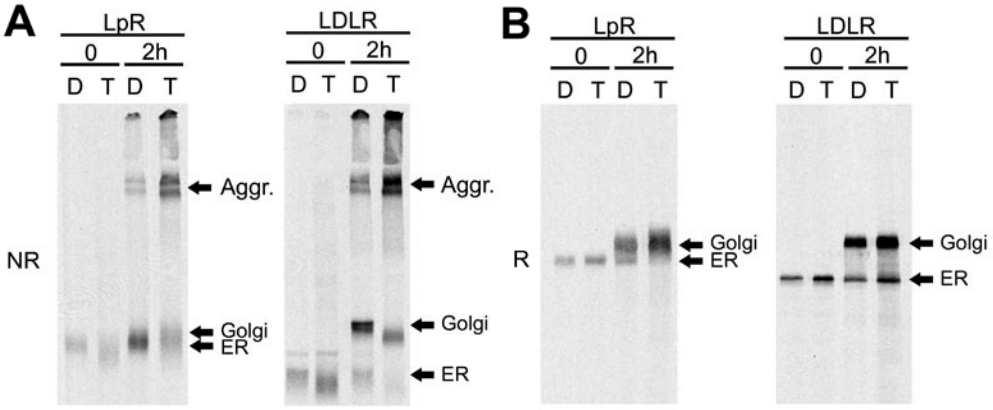

Figure 4: Effect of ER Ca^{2+} depletion on folding of LpR and LDLR. CHO-cells transfected with LpR-HA or LDLR-HA were pretreated for 30 min with 100 nM thapsigargin (T) or DMSO (D) as control. Subsequently, cells were radiolabeled by a 5 min pulse followed by a chase in the presence of thapsigargin or DMSO for the time points indicated. Receptors were immunoprecipitated with anti-HA antibody and subjected to non-reducing (A) or reducing (B) SDS-PAGE. Aggregates (Aggr.), Golgi- and ER-forms are indicated. NR: non-reduced, R: reduced.

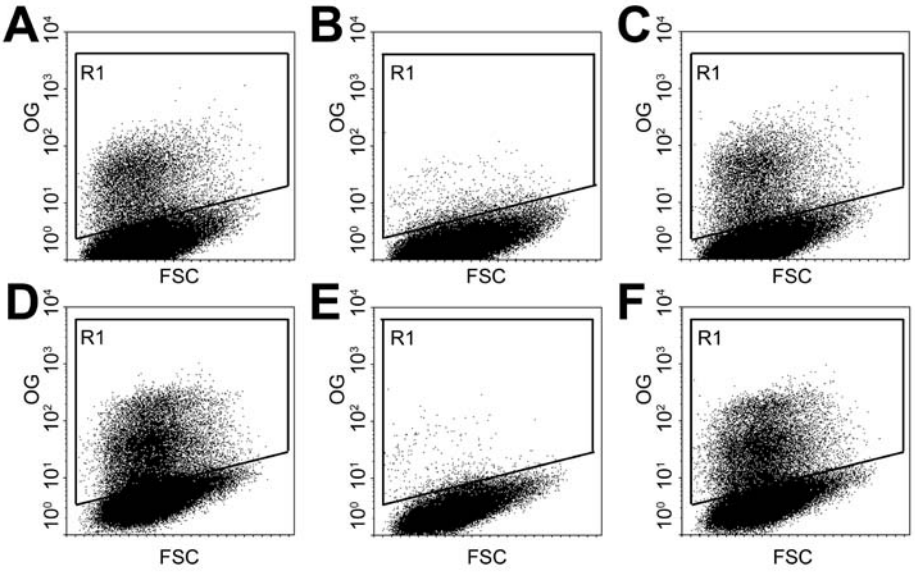

Figure 5: FACS analysis of Ca^{2+} dependence of ligand binding to LpR and LDLR. CHO(*ldlA*) cells stably transfected with LpR (A-C) or LDLR (D-F) were incubated with OG-HDLp (A-C) or OG-LDL (D-F). After binding and subsequent endocytosis of OG-ligand, the cells were trypsinized and analyzed by flow cytometry. The amount of fluorescence is plotted on the y-axis (relative values), and the forward scatter (FSC, relative values) on the x-axis. Cells in region 1 (R1) are transfected cells that bound en endocytosed OG-ligand. A, D: control experiments assaying the binding of OG-HDLp (A) or OG-LDL (D) in the presence of Ca^{2+}; B, E: cells were pre-treated with a buffer containing 5 mM EDTA, subsequently binding of OG-HDLp (B) or OG-LDL (E) was performed in the absence of Ca^{2+}; C, F: cells were pre-treated with a buffer containing 5 mM EDTA, whereafter binding of OG-HDLp (C) or OG-LDL (F) was performed in the presence of 2 mM Ca^{2+}. The data shown in the plots are representative of seven independent experiments.

This indicates that in the binding site of LpR, Ca^{2+} is indispensable for binding of the ligand, as was found for the binding site of LDLR for LDL (Figure 5)[23,27,57]. EDTA treatment of the cells followed by binding of OG-HDLp in the presence of Ca^{2+} completely restored the ability of LpR to bind HDLp (Figure 5C). Similar results were obtained for an equivalent experiment monitoring the binding of OG-LDL to CHO(*ldlA*) cells stably transfected with LDLR (Figure 5F). This indicates that the structural organization of the binding sites of LpR and LDLR for their respective lipoproteins after initial Ca^{2+} removal is efficiently restored in the presence of Ca^{2+}. For the binding of OG-HDLp to $LpR_{1\text{-}342}LDLR_{293\text{-}839}$ or OG-LDL to $LDLR_{1\text{-}292}LpR_{343\text{-}850}$ (Figure 3A), similar results were acquired (data not shown), suggesting that exchanging the ligand-binding domains of LDLR and LpR did not disrupt the ability of the LA-repeats to refold in the presence of Ca^{2+}. Therefore, it seems that for restoring the disrupted structural organization of the LA-repeats in the presence of Ca^{2+} the ligand-binding domein is sufficient.

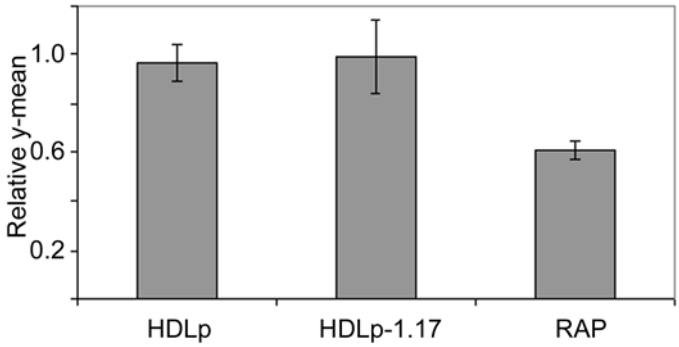

Figure 6: Stability of the complex of LpR with HDLp, HDLp-1.17 or RAP upon EDTA treatment. Bar representation of the results of binding experiments (n = 3) in which CHO(*ldlA*) cells stably transfected with LpR were incubated with OG-HDLp, OG-HDLp-1.17 or RAP followed by extensive washing of the cells with a buffer containing 5 mM EDTA. RAP-his binding was analyzed by subsequent binding of an anti-his-labeled antibody, which was detected by a fluorescently-labeled secondary antibody. After endocytosis of bound ligand, cells were trypsinized and the fluorescence of the cells was measured by flow cytometry. The y-mean in region 1 (R1) was determined for each sample. Bars depict the relative y-mean compared to the y-mean of control experiments assaying the binding of the respective ligands without subsequent EDTA treatment, which were set at 1. Error bars indicate the s.e.m.

Ligand specificity of the EDTA resistance of the LpR-ligand complex

Despite the Ca^{2+}-dependence of LpR for folding and ligand binding, the LpR-HDLp complex appeared EDTA-resistant, in contrast to the LDLR-LDL complex[17], suggesting that HDLp contributes to the stability of the complex in a unique manner. To investigate this specific interaction with HDLp in complex stabilization it was assayed whether the stabilizing properties are ligand-specific, using other LpR ligands such as RAP and partially delipidated HDLp (HDLp-1.17)[16]. The complex of LpR with HDLp-1.17 also appeared EDTA-resistant (Figure 6). However, in contrast to what was observed for the LpR-lipoprotein complexes, EDTA treatment disrupted the interaction between LpR and RAP (Figure 6). These results suggest that the stability of the complex is caused by the specific interaction between the insect lipoprotein and LpR.

Molecular dynamics simulations of LpR LA-4, 5 and 6 with or without bound Ca^{2+}

Earlier studies using hybrid receptors showed the EDTA resistance of the LpR-HDLp complex to be attributable to LA-2 to 7 of LpR[17]. Modeling these repeats using the structure of LA-3-4 of human LDLR as a template revealed that only LA-4, 5 and 6 contain both a central Trp and a negatively charged binding pocket coordinated by a

Ca^{2+} ion, which contribute to the interaction of LDLR family members with their ligands[58,59]. This suggests that LA-4-6 may be involved in the interaction with HDLp. For that reason, the stability of these repeats in the presence and absence of Ca^{2+} was assessed using MD simulations. Previous studies showed that, in agreement with experimental observations, the Ca^{2+}-containing LA-5 of LDLR remains stable during

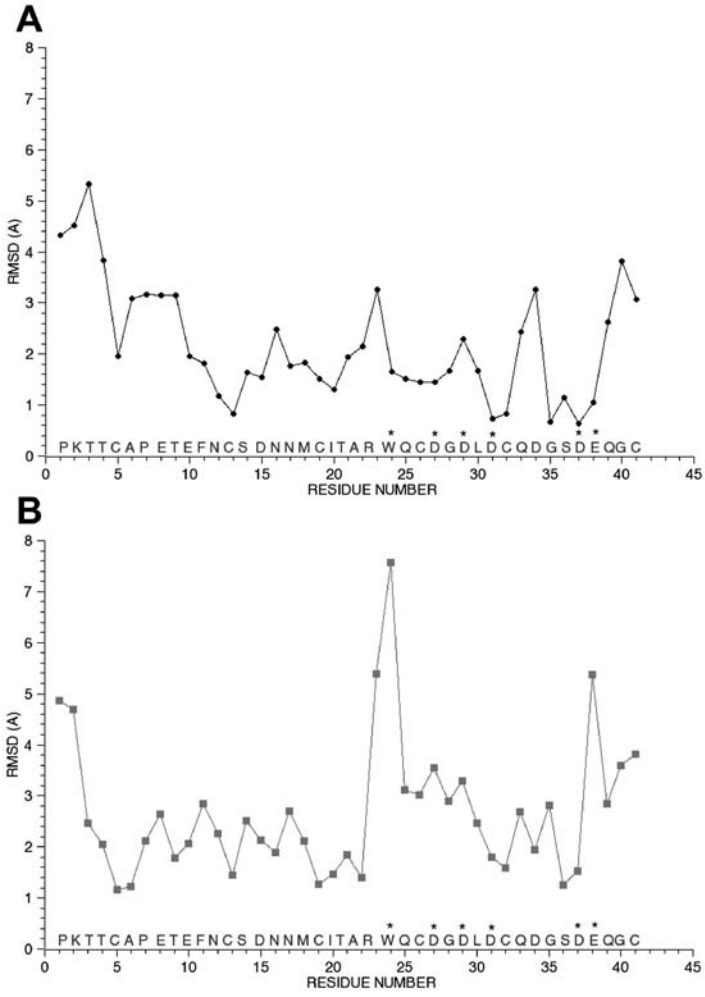

Figure 7: MD simulations of LA-5 of LpR. RMSD (Å) of the amino acid residues of LA-5 of LpR after MD simulation (10 ns) with bound Ca^{2+} (A) and after Ca^{2+} removal (B), relative to their initial structures (See Materials and Methods). B: A large departure from the Ca^{2+}-containing structure was observed, especially for the Ca^{2+}-coordinating residues, indicated by asterisks. The RMSD (Å) is plotted on the y-axis; on the x-axis the amino acid residues of LA-5 are indicated by one-letter code, numbering is based on the amino acid sequence of the individual repeat.

10 ns simulations but it unfolds when the Ca^{2+} ion is removed[60]. MD simulations can thus be used to predict whether Ca^{2+} removal by EDTA is compatible with the LpR repeats retaining their native fold. To this end, MD simulations were performed on the models of LA-4, LA-5 and LA-6 of LpR. The quality of the models and the stability of the repeats were tested by performing 10 ns MD simulations in explicit solvent. After the simulation, the root mean square deviation (RMSD), i.e. the measure of the average distance between the backbones of the Cα-atoms of the amino acid residues of the repeats at the end of the simulation relative to the initial structures, was determined. Except for the N-terminal tail of the repeats, the RMSD of the Cα-atoms of the amino acid residues of LA-4, 5 and 6 was low (0.6-3.5 Å for LA-5; Figure 7A). The average RMSD of the six Ca^{2+}-binding residues in LA-5 is 1.3 Å. Since different NMR structures of LA-6 of human LDLR already show an RMSD of 0.6 Å (data not shown), the obtained value of 1.3 Å seems to be comparable with the flexibility of other LA-repeats, indicating that the models built for LA-4, 5 and 6 are fairly accurate and stable. We noticed nevertheless that, compared to LA-4 and 5, the N-terminal lobe of

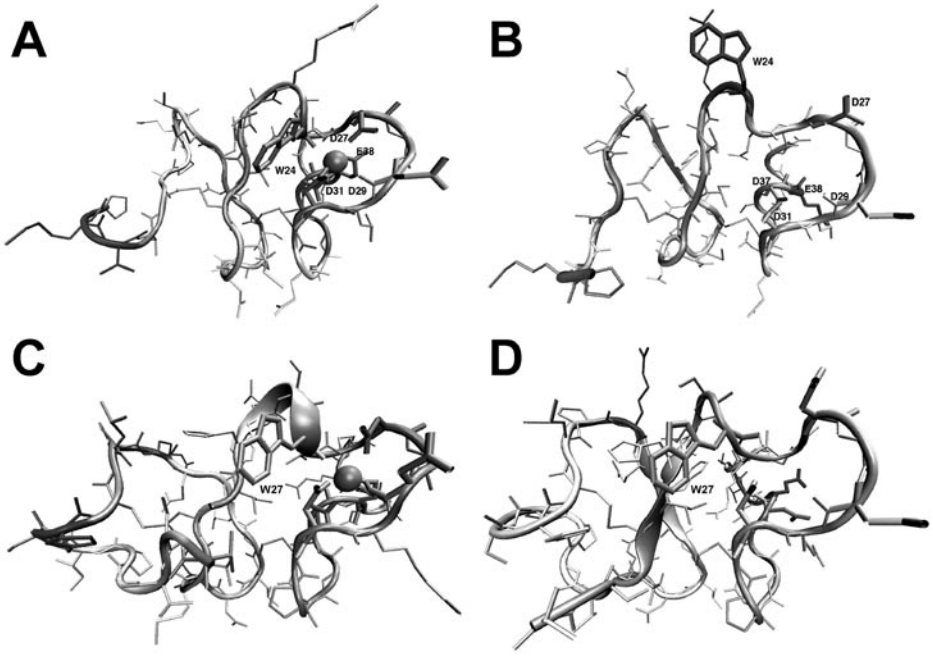

Figure 8: Three-dimensional models of LA-5 and LA-6 of LpR in the presence (A, C) and absence (B, D) of Ca^{2+}. Images show the last snapshot after 10 ns for LA-5 (A, B) and LA-6 (C, D). The models are colored according to the RMSD of the Cα of the amino acid residues, ranging from red (0 Å), via white (3 Å), to blue (6 Å). Important residues mentioned in the text are indicated by one-letter code, numbers are based on individual repeats. The Ca^{2+} ion is depicted as a green sphere. For a colored version of this figure see page 169.

LA-6 showed more flexibility, which could reflect the true structural flexibility; however, we cannot exclude that this could be indicative of a poor quality of this model in the N-terminal region. The flexibility observed in the C-terminal Ca^{2+}-containing lobe of LA-6 is nevertheless comparable to that of the other repeats. As previously observed for LA-5 of LDLR[60], the RMSD of the Ca^{2+}-binding residues form local minima (Figure 7A), indicating that they are strongly stabilized by interaction with the Ca^{2+} ion. Together, these results suggest that in terms of Ca^{2+}-binding features and stability according to MD simulations, the modeled LA-4, LA-5 and LA-6 modules of LpR behave, in the presence of bound Ca^{2+}, similarly to the LA-5 module of LDLR whose simulation, performed on the x-ray structure, was in agreement with experimental observations on the isolated repeat[60].

Subsequently we used MD simulations to investigate the dynamics of the LA-repeats in the absence of Ca^{2+}. As found for LA-5 of LDLR[60], removal of the Ca^{2+} ions from LA-4 and -5 of LpR led to a large increase in flexibility in the Ca^{2+}-coordinating region. The most striking feature is the large RMSD for the central Trp of LA-5 (around 7 Å, Figure 7B), reflecting the disorganization of the ligand-binding site. Additionally, the RMSD of the Ca^{2+}-coordinating residues (3.9 Å on average) no longer populated minima, but maxima along the sequence (Figure 7B). Ca^{2+} removal thus led to a drastic disordering of the Ca^{2+}-binding site and reorientation of the side chains of the amino acid residues involved, but did not lead to an entirely unfolded structure (Figures 8A, B). Compared to what is observed for LA-4 and 5, Ca^{2+} removal from LA-6 gave rise to a small RMSD for the coordinating Trp (1 Å, Figure 8D). This suggests that the orientation of its side chain is not significantly changed upon removal of Ca^{2+} (Figures 8C, D), at least in the same short time scale where significant disordering was observed in LA-4 and LA-5. Together, these results indicate that Ca^{2+} stabilizes the structures of LA-4 and 5 of LpR in a similar way as was observed for LA-5 of human LDLR and raises the possibility that LA-6 of LpR may be more stable upon Ca^{2+} removal than the other modules.

Discussion

Previous studies demonstrated that HDLp is recycled by LpR in a transferrin-like manner[7,11,12]. Key in this recycling mechanism is the stability of the LpR-HDLp complex at endosomal conditions, e.g. low pH, as well as low Ca^{2+} concentration resulting from EDTA treatment of the complex, as determined by an earlier study from our group[17]. The stability at low pH and the EDTA resistance of the LpR-HDLp complex is remarkable, since ligand binding to LDLR family members is known to depend on neutral pH and on Ca^{2+}[27,61]. In apparent contrast to the EDTA resistance of the LpR-HDLp complex, sequence comparison of the LA-repeats of LpR with those of other LDLR family members, as well as modeling studies, indicate that each

LA-repeat of LpR is most likely stabilized by a Ca^{2+} ion[17]. In the present study we show that the Ca^{2+} dependence of LpR during folding, ligand binding and for the structural integrity of the ligand-binding site does not differ from that of LDLR. Earlier studies using hybrid receptors indicated that the EDTA resistance of the LpR-HDLp complex is attributable to the binding site for HDLp, which is located in LA-2-7 of LpR[17]. The EDTA resistance appeared specific for the interaction between lipoprotein and LpR, and does not apply to the LpR-RAP complex, suggesting the stability to be due to the interaction interface between lipoprotein and LpR. Therefore, we used MD simulations to analyze the stability of LA-repeats 4, 5 and 6 of LpR, that are most likely involved in this interface, in the presence or absence of Ca^{2+}. The MD data indicates that depletion of Ca^{2+} from LA-4, 5 and 6 leads to unfolding of these repeats; however, LA-6 may be more stable upon Ca^{2+} removal than LA-4 and 5 of LpR and LA-5 of LDLR[60]. Due to the requirement of LpR for Ca^{2+} to maintain its structure prior to ligand binding, the remarkable stability of the LpR-HDLp complex must be inferred from the unique stabilizing properties of the interaction interface of LpR and lipoprotein, which may involve LA-repeat 6.

To localize the origin of the EDTA resistance of the LpR-HDLp complex, we first set out to study the involvement of Ca^{2+} during the folding of LpR in comparison with that of LDLR. The folding pathway of LDLR is characterized by non-native disulfide bond formation and subsequent isomerization of these bonds into native disulfide bonds[28,31]. A similar pattern was revealed for LpR, suggesting that, similarly to LDLR, first a compact folding intermediate is formed, containing non-native disulfide bonds linking distant regions of the protein. Subsequent reshuffling of these non-native bonds leads to formation of the native, less compact LpR structure. Not only folding of LpR, but also the folding pattern of two hybrid receptors, $LpR_{1\text{-}342}LDLR_{293\text{-}839}$ and $LDLR_{1\text{-}292}LpR_{343\text{-}850}$, appeared to be similar to that of LDLR, indicating that the ligand-binding domains of LpR and LDLR are interchangeable during folding, suggesting the folding pattern disclosed for LDLR[28] to be a general mechanism for folding of LDLR family members that is evolutionary conserved from insect to human. Previous studies showed that after reaching the Golgi system, the hybrid receptors also reach the plasma membrane and are able to bind and endocytose ligand. However, after endocytosis of ligand, alterations were seen in ligand release and/or intracellular targeting of the receptors[12,17].

For the formation of correct disulfide bonds in the ligand-binding domains of LDLR family members, Ca^{2+} incorporation is essential[24-26,54,57,62]. Folding of LpR in the absence of Ca^{2+} yielded more aggregation of LpR molecules and a difference in mobility of the folding intermediates, which is, in combination with similar results for LDLR, suggestive of aberrant disulfide bond formation. This data indicates that Ca^{2+} is indispensable for the formation of native disulfide bonds in LpR, in agreement with the Ca^{2+}-dependent folding of LA-repeats of other LDLR family members[24,26,54,57,62].

In line with the Ca^{2+}-dependent ligand binding of other LDLR family members[23,27,57], our binding studies show that Ca^{2+} is essential for the integrity of the functional binding site of LpR, since Ca^{2+} depletion by EDTA treatment prior to binding abolishes HDLp binding to the receptor. Several other studies have shown that the interaction between ligands and LDLR family members is mediated by docking of ligand on an LA-repeat, the interaction interface at each docking site of which is dominated by electrostatic interactions between conserved acidic residues of the LA-repeat and a Lys residue from the ligand, stabilized by the central Trp of the involved LA-repeat[58,59,63]. In agreement with the lack of binding after chelation of Ca^{2+} from LpR, MD simulation of LA-4, 5 and 6 of LpR, that are presumably part of the binding site of LpR for HDLp, predicted that chelation of Ca^{2+} from the structure promotes an increased flexibility and local disorganization of the Ca^{2+}-coordinating residues and the central Trp of LA-4 and 5, abolishing the structure of the docking sites of these repeats. Although the orientation of the Trp in LA-6 is less altered in the absence of Ca^{2+} and therefore may be in the right conformation to bind HDLp, one docking site only is apparently not sufficient for binding of HDLp to LpR. Addition of Ca^{2+} after EDTA treatment could easily rescue the binding capacity of the repeats, indicating that Ca^{2+}-depleted LA-repeats are able to efficiently restore their native conformation when Ca^{2+} is present. The latter is in accordance with the findings of Blacklow and colleagues, who showed with biochemical studies that when at least two cystine bonds are present, the conformational diversity of unliganded LA-5 of LDLR is restricted enough for the free energy of Ca^{2+} coordination to overcome the entropic cost of organizing the Ca^{2+}-binding site[54]. The efficient refolding after Ca^{2+} addition of the binding sites of hybrid receptors $LpR_{1\text{-}342}LDLR_{293\text{-}839}$ and $LDLR_{1\text{-}292}$ $LpR_{343\text{-}850}$ suggests that the refolding of the repeats is independent of other domains, in agreement with the ability of single repeats to refold[54]. Together, these data indicate that the Ca^{2+} dependence of LpR for folding and ligand-binding is similar to that of other LDLR family members, indicating that the remarkable stability of the LpR-HDLp[17] complex is acquired upon complex formation.

Analysis of the ligand specificity of the EDTA resistance of the LpR-ligand complex indicated that HDLp or partially delipidated HDLp are able to form an EDTA-resistant complex with LpR, in contrast to RAP. It would seem conceivable that the stability of the LpR-lipoprotein complex results either from shielding the Ca^{2+} ions from the chelating agent by the lipoprotein, or from the ability of lipoprotein to constrain the conformational diversity of the LA-repeats of LpR in the absence of Ca^{2+}. In view of the size of the lipoproteins, it would seem plausible that HDLp and HDLp-1.17 are able to shield the Ca^{2+} from EDTA, in contrast to a small protein like RAP. However, in spite of the size of LDL, the LDLR-LDL complex is EDTA-sensitive, suggesting that LDL is not able to shield the Ca^{2+} ions. This suggests that the potential for shielding of Ca^{2+} is not determined by the size of the ligand, but by specific interactions of the ligand with the LA-repeats involved in its binding. The binding site of LpR for

HDLp is composed of LA-2-7, while that of LDLR for LDL consists of LA-3-7 and EGF-A. Since the affinity of EGF-A for Ca^{2+} is much lower than that of the LA-repeats of LDLR[62], such a difference in binding site may contribute to the stability of the LpR-lipoprotein complex. However, it should be noted that also the binding of LDL to $LDLR_{1\text{-}292}LpR_{343\text{-}850}$ is EDTA-sensitive (data not shown), suggesting the EDTA-sensitive LDL binding not to be created exclusively by the binding interaction with EGF-A. The LpR-RAP complex is not EDTA-resistant, while RAP efficiently competes for the binding of HDLp to LpR[11,17], indicating that the difference in complex stability cannot be caused by the use of an entirely different binding site of LpR for HDLp. The stoichiometry of the binding of RAP to LDLR family members is most probably one RAP per two LA-repeats. Additionally, LA-repeats involved in RAP binding most likely contain a conserved acidic residue[39] and a conserved Trp[58]. Based on the presence of both the acidic residue and the Trp, for LpR it is most likely that the stoichiometry is one RAP molecule per LpR molecule, either binding to the pair of LA-4-5 or the pair of LA-5-6[17]. Since the binding of HDLp to LpR may involve more LA-repeats, this raises the possibility that the stability of the interaction between the lipoprotein and LpR may be caused by binding to LA-repeats not involved in RAP binding. Although mutational analysis is necessary to determine the precise binding sites of LpR for RAP and insect lipoprotein, binding of RAP to LA-4-5 and therefore the lack of binding of RAP to LA-6 may explain the difference in susceptibility of the LpR-RAP and LpR-HDLp complexes to EDTA treatment. In addition to the interactions with conserved residues and the central Trp at the docking site, other contacts between ligand and receptor were shown to play a role in the affinity and ligand specificity of the interaction between LDLR family members and their ligands[59,64,65]. Similar additional interactions between lipoprotein and LpR may also contribute to the stability of the LpR-lipoprotein complex upon EDTA-treatment.

In conclusion, our results indicate that folding of LpR and ligand-binding to LpR is Ca^{2+} dependent, as was found for other LDLR family members. However, upon complex formation, the LpR-lipoprotein complex displays a remarkable stability, which is proposed to be mediated by the stabilizing properties of the interaction interface between LpR and its lipoprotein ligand, involving LA-repeat 6 which is suggested to be more stable upon Ca^{2+} removal than the other LpR LA-repeats.

Acknowledgements

We thank Florentina Pena and Annemieke Jansens for sharing unpublished results, Sander Meijer for his help with modeling of the LA-repeats and Masja van Oort for useful discussions. We acknowledge computation time from "Red española de supercomputación" (RES, Spain) and financial support from grant BFU2007-61476/BMC (Spain).

References

1. Weers PM, Van Marrewijk WJ, Beenakkers AM & Van der Horst DJ (1993) Biosynthesis of locust lipophorin. Apolipophorins I and II originate from a common precursor. J Biol Chem 268, 4300-4303.
2. Bogerd J, Babin PJ, Kooiman FP, Andre M, Ballagny C, Van Marrewijk WJ & Van der Horst DJ (2000) Molecular characterization and gene expression in the eye of the apolipophorin II/I precursor from *Locusta migratoria*. J Comp Neurol 427, 546-558.
3. Babin PJ, Bogerd J, Kooiman FP, Van Marrewijk WJ & Van der Horst DJ (1999) Apolipophorin II/I, apolipoprotein B, vitellogenin, and microsomal triglyceride transfer protein genes are derived from a common ancestor. J Mol Evol 49, 150-160.
4. Mann CJ, Anderson TA, Read J, Chester SA, Harrison GB, Kochl S, Ritchie PJ, Bradbury P, Hussain FS, Amey J, Vanloo B, Rosseneu M, Infante R, Hancock JM, Levitt DG, Banaszak LJ, Scott J & Shoulders CC (1999) The structure of vitellogenin provides a molecular model for the assembly and secretion of atherogenic lipoproteins. J Mol Biol 285, 391-408.
5. Mahley RW & Innerarity TL (1983) Lipoprotein receptors and cholesterol homeostasis. Biochim Biophys Acta 737, 197-222.
6. Davidson NO & Shelness GS (2000) Apolipoprotein B: mRNA editing, lipoprotein assembly, and presecretory degradation. Annu Rev Nutr 20, 169-193.
7. Dantuma NP, Pijnenburg MA, Diederen JH & Van der Horst DJ (1997) Developmental down-regulation of receptor-mediated endocytosis of an insect lipoprotein. J Lipid Res 38, 254-265.
8. Dantuma NP, Potters M, De Winther MP, Tensen CP, Kooiman FP, Bogerd J & Van der Horst DJ (1999) An insect homolog of the vertebrate very low density lipoprotein receptor mediates endocytosis of lipophorins. J Lipid Res 40, 973-978.
9. Van Hoof D, Rodenburg KW & Van der Horst DJ (2003) Lipophorin receptor-mediated lipoprotein endocytosis in insect fat body cells. J Lipid Res 44, 1431-1440.
10. Rodenburg KW, Smolenaars MM, Van Hoof D & Van der Horst DJ (2006) Sequence analysis of the non-recurring C-terminal domains shows that insect lipoprotein receptors constitute a distinct group of LDL receptor family members. Insect Biochem Mol Biol 36, 250-263.
11. Van Hoof D, Rodenburg KW & Van der Horst DJ (2002) Insect lipoprotein follows a transferrin-like recycling pathway that is mediated by the insect LDL receptor homologue. J Cell Sci 115, 4001-4012.
12. Van Hoof D, Rodenburg KW & Van der Horst DJ (2005) Intracellular fate of LDL receptor family members depends on the cooperation between their ligand-binding and EGF domains. J Cell Sci 118, 1309-1320.
13. Rodenburg KW & Van der Horst DJ (2005) Lipoprotein-mediated lipid transport in insects: analogy to the mammalian lipid carrier system and novel concepts for the functioning of LDL receptor family members. Biochim Biophys Acta 1736, 10-29.
14. Van der Horst DJ & Ryan RO (2005) Lipid transport. In Comprehensive molecular insect science (Gilbert LI, Iatrou K & Gill SS, editors), 4, pp. 225-246. Elsevier. New York, NY, USA.
15. Van Hoof D, Rodenburg KW & Van der Horst DJ (2005) Receptor-mediated endocytosis and intracellular trafficking of lipoproteins and transferrin in insect cells. Insect Biochem Mol Biol 35, 117-128.

16. Roosendaal SD, Van Doorn JM, Valentijn KM, Van der Horst DJ & Rodenburg KW (2008) Lipid unloading of lipophorin affects its binding to the insect LDL receptor homologue, LpR: implications for the role of LpR-mediated endocytosis. Submitted.
17. Roosendaal SD, Kerver J, Schipper M, Rodenburg KW & Van der Horst DJ (2008) The complex of the insect LDL receptor homologue, lipophorin receptor, LpR, and its lipoprotein ligand does not dissociate under endosomal conditions. FEBS J 275, 1751-1766.
18. Maxfield FR & McGraw TE (2004) Endocytic recycling. Nat Rev Mol Cell Biol 5, 121-132.
19. Gerasimenko JV, Tepikin AV, Petersen OH & Gerasimenko OV (1998) Calcium uptake via endocytosis with rapid release from acidifying endosomes. Curr Biol 8, 1335-1338.
20. Kurniawan ND, Atkins AR, Bieri S, Brown CJ, Brereton IM, Kroon PA & Smith R (2000) NMR structure of a concatemer of the first and second ligand-binding modules of the human low-density lipoprotein receptor. Protein Sci 9, 1282-1293.
21. North CL & Blacklow SC (2000) Solution structure of the sixth LDL-A module of the LDL receptor. Biochemistry 39, 2564-2571.
22. Huang W, Dolmer K, Liao X & Gettins PGW (2000) NMR solution structure of the receptor binding domain of human alpha 2-macroglobulin. J Biol Chem 275, 1089-1094.
23. Fass D, Blacklow S, Kim PS & Berger JM (1997) Molecular basis of familial hypercholesterolaemia from structure of LDL receptor module. Nature 388, 691-693.
24. Simonovic M, Dolmer K, Huang W, Strickland DK, Volz K & Gettins PG (2001) Calcium coordination and pH dependence of the calcium affinity of ligand-binding repeat CR7 from the LRP. Comparison with related domains from the LRP and the LDL receptor. Biochemistry 40, 15127-15134.
25. Pena F, Jansens A & Braakman I (2008) Calcium is important for both early and late stages of correct LDL receptor folding. Submitted.
26. Bieri S, Atkins AR, Lee HT, Winzor DJ, Smith R & Kroon PA (1998) Folding, calcium binding, and structural characterization of a concatemer of the first and second ligand-binding modules of the low-density lipoprotein receptor. Biochemistry 37, 10994-11002.
27. Schneider WJ, Beisiegel U, Goldstein JL & Brown MS (1982) Purification of the low density lipoprotein receptor, an acidic glycoprotein of 164,000 molecular weight. J Biol Chem 257, 2664-2673.
28. Jansens A, van Duijn E & Braakman I (2002) Coordinated nonvectorial folding in a newly synthesized multidomain protein. Science 298, 2401-2403.
29. Radford SE (2003) Co-translocational misfolding in the ER of living cells. Nat Struct Biol 10, 153-154.
30. Rudenko G, Henry L, Henderson K, Ichtchenko K, Brown MS, Goldstein JL & Deisenhofer J (2002) Structure of the LDL receptor extracellular domain at endosomal pH. Science 298, 2353-2358.
31. Gent J & Braakman I (2004) Low-density lipoprotein receptor structure and folding. Cell Mol Life Sci 61, 2461-2470.
32. Jorgensen MM, Jensen ON, Holst HU, Hansen JJ, Corydon TJ, Bross P, Bolund L & Gregersen N (2000) Grp78 is involved in retention of mutant low density lipoprotein receptor protein in the endoplasmic reticulum. J Biol Chem 275, 33861-33868.

33. Bu G & Rennke S (1996) Receptor-associated protein is a folding chaperone for low density lipoprotein receptor-related protein. J Biol Chem 271, 22218-22224.
34. Sato A, Shimada Y, Herz J, Yamamoto T & Jingami H (1999) 39-kDa receptor-associated protein (RAP) facilitates secretion and ligand binding of extracellular region of very-low-density-lipoprotein receptor: implications for a distinct pathway from low-density-lipoprotein receptor. Biochem J 341, 377-383.
35. Savonen R, Obermoeller LM, Trausch-Azar JS, Schwartz AL & Bu G (1999) The carboxyl-terminal domain of receptor-associated protein facilitates proper folding and trafficking of the very low density lipoprotein receptor by interaction with the three amino-terminal ligand-binding repeats of the receptor. J Biol Chem 274, 25877-25882.
36. Culi J & Mann RS (2003) Boca, an endoplasmic reticulum protein required for wingless signaling and trafficking of LDL receptor family members in *Drosophila*. Cell 112, 343-354.
37. Hsieh JC, Lee L, Zhang L, Wefer S, Brown K, DeRossi C, Wines ME, Rosenquist T & Holdener BC (2003) Mesd encodes an LRP5/6 chaperone essential for specification of mouse embryonic polarity. Cell 112, 355-367.
38. Andersen OM, Petersen HH, Jacobsen C, Moestrup SK, Etzerodt M, Andreasen PA & Thogersen HC (2001) Analysis of a two-domain binding site for the urokinase-type plasminogen activator-plasminogen activator inhibitor-1 complex in low-density-lipoprotein-receptor-related protein. Biochem J 357, 289-296.
39. Andersen OM, Christensen LL, Christensen PA, Sorensen ES, Jacobsen C, Moestrup SK, Etzerodt M & Thogersen HC (2000) Identification of the minimal functional unit in the low density lipoprotein receptor-related protein for binding the receptor-associated protein (RAP). A conserved acidic residue in the complement-type repeats is important for recognition of RAP. J Biol Chem 275, 21017-21024.
40. Andersen OM, Schwarz FP, Eisenstein E, Jacobsen C, Moestrup SK, Etzerodt M & Thogersen HC (2001) Dominant thermodynamic role of the third independent receptor binding site in the receptor-associated protein RAP. Biochemistry 40, 15408-15417.
41. Beisiegel U, Schneider WJ, Goldstein JL, Anderson RG & Brown MS (1981) Monoclonal antibodies to the low density lipoprotein receptor as probes for study of receptor-mediated endocytosis and the genetics of familial hypercholesterolemia. J Biol Chem 256, 11923-11931.
42. Field J, Nikawa J, Broek D, MacDonald B, Rodgers L, Wilson IA, Lerner RA & Wigler M (1988) Purification of a RAS-responsive adenylyl cyclase complex from *Saccharomyces cerevisiae* by use of an epitope addition method. Mol Cell Biol 8, 2159-2165.
43. Kingsley DM & Krieger M (1984) Receptor-mediated endocytosis of low density lipoprotein: Somatic cell mutants define multiple genes required for expression of surface-receptor activity. Proc Natl Acad Sci USA 81, 5454-5458.
44. Jansens A & Braakman I (2003) Pulse-chase labeling techniques for the analysis of protein maturation and degradation. Methods Mol Biol 232, 133-145.
45. Phillips JC, Braun R, Wang W, Gumbart J, Tajkhorshid E, Villa E, Chipot C, Skeel RD, Kale L & Schulten K (2005) Scalable molecular dynamics with NAMD. J Comput Chem 26, 1781-1802.
46. Brooks BR, Bruccoleri RE, Olafson BD, Status DJ, Swaminathan S & Karplus MJ (1983) CHARMM: A program for macromolecular energy, minimization, and dynamics calculations. J Comput Chem 4, 187-217.
47. Jorgensen WL, Chandrasekhar J, Madura JD, Impey RW & Klein ML (1983) Comparison of simple potential functions for simulating liquid water. J Chem Phys 79, 926-935.

48. Ryckaert JP, Ciccotti G & Berendsen HJC (1977) Numerical integration of the Cartesian equation of motion of a system with constraints: molecular dynamics of N-alkenes. J Comput Phys 23, 327-341.
49. Essmann U, Perera L, Berkowitz ML, Darden T, Lee H & Pedersen LG (1995) A smooth particle mesh Ewald method. J Chem Phys 103, 8577-8593.
50. Martyna GJ, Tobias DJ & Klein ML (1994) Constant pressure molecular dynamics algorithms. J Chem Phys 101, 4177-4189.
51. Feller SE, Zhang Y, Pastor RW & Brooks BR (1995) Constant pressure molecular dynamics simulation: The Langevin piston method. J Chem Phys 103, 4613-4621.
52. Suhre K & Sanejouand YH (2004) El Nemo: a normal mode web server for protein movement analysis and the generation of templates for molecular replacement. Nucleic Acids Res 32, W610-614.
53. Humphrey W, Dalke A & Schulten K (1996) VMD: visual molecular dynamics. J Mol Graph 14, 33-38, 27-38.
54. Koduri V & Blacklow SC (2001) Folding determinants of LDL receptor type A modules. Biochemistry 40, 12801-12807.
55. Jackson TR, Patterson SI, Thastrup O & Hanley MR (1988) A novel tumour promoter, thapsigargin, transiently increases cytoplasmic free Ca^{2+} without generation of inositol phosphates in NG115-401L neuronal cells. Biochem J 253, 81-86.
56. Thastrup O, Cullen PJ, Drobak BK, Hanley MR & Dawson AP (1990) Thapsigargin, a tumor promoter, discharges intracellular Ca^{2+} stores by specific inhibition of the endoplasmic reticulum $Ca^{2(+)}$-ATPase. Proc Natl Acad Sci U S A 87, 2466-2470.
57. Jeon H & Blacklow SC (2005) Structure and physiologic function of the low-density lipoprotein receptor. Annu Rev Biochem 74, 535-562.
58. Fisher C, Beglova N & Blacklow SC (2006) Structure of an LDLR-RAP complex reveals a general mode for ligand recognition by lipoprotein receptors. Mol Cell 22, 277-283.
59. Blacklow SC (2007) Versatility in ligand recognition by LDL receptor family proteins: advances and frontiers. Curr Opin Struct Biol 17, 419-426.
60. Cuesta-López S, Falo F & Sancho J (2007) Computational diagnosis of protein conformational diseases: short molecular dynamics simulations reveal a fast unfolding of r-LDL mutants that cause familial hypercholesterolemia. Proteins 66, 87-95.
61. Davis CG, Goldstein JL, Sudhof TC, Anderson RG, Russell DW & Brown MS (1987) Acid-dependent ligand dissociation and recycling of LDL receptor mediated by growth factor homology region. Nature 326, 760-765.
62. Rudenko G & Deisenhofer J (2003) The low-density lipoprotein receptor: ligands, debates and lore. Curr Opin Struct Biol 13, 683-689.
63. Jensen GA, Andersen OM, Bonvin AM, Bjerrum-Bohr I, Etzerodt M, Thogersen HC, O'Shea C, Poulsen FM & Kragelund BB (2006) Binding site structure of one LRP-RAP complex: implications for a common ligand-receptor binding motif. J Mol Biol 362, 700-716.
64. Wilson C, Wardell MR, Weisgraber KH, Mahley RW & Agard DA (1991) Three-dimensional structure of the LDL receptor-binding domain of human apolipoprotein E. Science 252, 1817-1822.
65. Morrow JA, Arnold KS, Dong J, Balestra ME, Innerarity TL & Weisgraber KH (2000) Effect of arginine 172 on the binding of apolipoprotein E to the low density lipoprotein receptor. J Biol Chem 275, 2576-2580.

6

Summarizing Discussion

Summarizing Discussion

Lipid transport potentially poses a problem to multicellular organisms, as lipids are hydrophobic and aggregate in an aqueous environment. In animals, specialized lipid-binding proteins are used to circumvent this problem. A number of intriguing similarities exist with regard to lipid-binding proteins involved in lipid transport processes operative in mammals and insects. Despite these similarities, both animal groups have evolved evolutionarily to different mechanisms for mobilization of lipid substrates and make use of other carrier molecules for lipid transport, offering adaptations to their specific requirements. Perhaps the most outstanding difference in functioning relates to lipoproteins and their receptors in mammals and insects. Whereas in mammals, endocytic uptake of LDL particles, mediated by LDLR, results in their trafficking to lysosomes and subsequent degradation, insect HDLp was shown to use a selective mechanism for transfer of its hydrophobic cargo. Circulating HDLp particles may serve as a lipid donor or acceptor, dependent on the physiological situation, and function as a reusable lipid shuttle without additional synthesis or increased degradation of their apolipoprotein matrix. The recent identification of receptors of the LDLR family in insects has revealed that endocytic uptake of HDLp may constitute an additional mechanism at specific life stages, which would seem to conflict with the concept of HDLp acting as a reusable lipid shuttle. However, the lipoprotein endocytosed by the insect LDLR homologue, LpR, appeared to be recycled in a manner analogous to that of transferrin by the transferrin receptor. Such a pathway, in which the lipoprotein is ultimately resecreted, is highly comparable with the extracellular lipoprotein-mediated selective delivery of lipids, and clearly is of physiological relevance in insects although the precise function of the LpR-mediated lipoprotein recycling process awaits disclosure. The data presented in this thesis highlight both the parallels and the differences in structure of the mammalian and insect lipoprotein receptors LDLR and LpR, leading to the intriguing difference in functioning, namely ligand degradation versus ligand recycling.
The mechanism of HDLp recycling by LpR implies the LpR-HDLp complex to be stable at endosomal conditions, while the (modified) ligand must be released when it returns at the plasma membrane. Therefore, the research described in this thesis focused on structural differences that may account for the affinity and stability of the binding of HDLp to LpR. To measure the binding of HDLp to LpR, a flow cytometric assay was developed. Even though such an approach to quantify lipoprotein binding and uptake has also been used in other studies[1-8], several technical differences in our approach as compared to that used by others were apparent (**Chapter 2**). As described, an important difference between our approach and that of others is the use of stably transfected polyclonal cell lines to provide heterogeneous samples of cells that express the receptor. However, with respect to the quantification of data resulting from the use of latter cell lines, several aspects need to be

considered and are elaborated below. Polyclonal cell lines are mixtures of different cell populations that vary in the amount of receptor expression. Therefore, the flow cytometry plots obtained contain different populations of cells which differ in the amount of bound and endocytosed fluorescently-labeled ligand (Figure 1). The difference in transfection efficiency between independent transfections affects the receptor expression, thereby the distribution of the cells in the plot and thus the mean fluorescence (y-mean) of the entire plot. Since this only enables a fair comparison of samples of the same cell lines, statistical analyses were performed using a t-test for paired samples. Furthermore, the y-mean is strongly affected by the lower population, the fluorescence of the cells of which did not exceed that of untransfected cells. Therefore, based on samples of untransfected cells, these cells were excluded from the analysis by defining region 1 (R1, Figure 1), containing only cells that bound and endocytosed ligand. Quantification of the y-mean, i.e. the geometric mean of the fluorescence of the cells, resulted in a y-mean in R1 of 18.7 for sample A (Figure 1A) and of 7.5 for sample B (Figure 1B), amounting to a decrease in binding of ~ 60% when the amount of ligand binding of cells in sample B is compared to that of cells in sample A. However, a decrease in fluorescence of the cells can lead to disappearance of cells from R1 into the population of cells of which the fluorescence did not exceed that of untransfected cells. In case of a comparison of the y-mean between two different treatments, this leads to a bias in the analysis; since the y-mean in R1 of sample A is the average of 9.5 % of all the cells in the entire plot, and that of sample B is the average of 1.7 % of the cells in the plot, the y-mean of sample B is overestimated (Figure 1). To circumvent this problem, in case of a

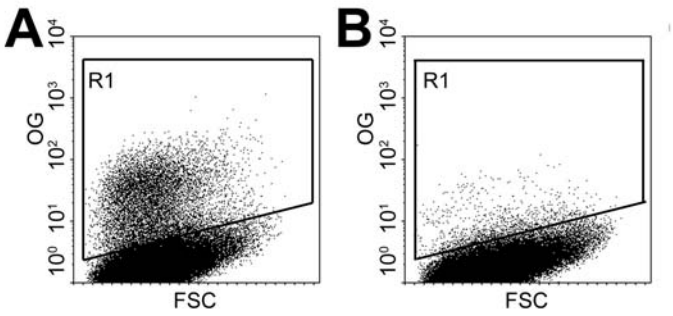

Figure 1: FACS analysis of two samples of LpR-transfected CHO cells of the same cell line. LpR-transfected CHO cells were incubated with OG-HDLp (A) or cells were pre-treated with a buffer containing 5 mM EDTA and subsequently incubated with OG-HDLp in the absence of Ca^{2+} (B). After binding and subsequent endocytosis of OG-HDLp, the cells were trypsinized and analyzed by flow cytometry. The amount of fluorescence is plotted on the y-axis (relative values), and the forward scatter (FSC, relative values) on the x-axis. Cells in region 1 (R1) are LpR-transfected CHO cells that bound and endocytosed OG-HDLp. Figure taken from Chapter 5 (Figure 5A, B).

significant difference in the amount of cells in R1 between different treatments, the y-mean was corrected using random measurements from the excluded population. In the example in Figure 1, the corrected value for the y-mean of sample B amounts to 2.6, resulting in a decrease in binding of ~ 86% compared to the binding of cells of sample A. Using the above mentioned approach, similar values for LDL release by LDLR were obtained as measured by Blacklow and colleagues for monoclonal cell lines[7,8]. Therefore, the combination of the polyclonal cell lines with this analytical approach results in a solid assay, which is less time-consuming since no monoclonal cell lines have to be produced while additionally, this assay enables the simultaneous analysis of cells that display a wide range of receptor expression levels.

Using this assay, it was demonstrated that, in contrast to the complex of LDLR and LDL, the complex of LpR and HDLp is resistant to pertinent conditions prevailing in the early endosome, such as low pH and a decrease in Ca^{2+} concentration as mimicked by treatment of the complex with EDTA, implying that for LpR and HDLp, the integrity of the complex is maintained during intracellular trafficking (Figure 2). Binding and dissociation capacities of various hybrid receptors indicated that this stability is determined by the specific interaction between HDLp and LA-repeats 2-7 of LpR. This suggests that LpR may use a different mechanism to release HDLp as compared to the mechanism of LDL release by LDLR in which the β-propeller is of vital importance[8-10]. Since our earlier studies using hybrid receptors revealed that the intracellular fate of the complex is dictated by the extracellular domain as a whole, this implies that although the stability of the complex appears to rely only on the ligand-binding domain (**Chapter 2**), for proper targeting of LpR to the ERC the combination of the ligand-binding domain and β-propeller of LpR is essential[11].

An important issue remains, however, how HDLp is released from the receptor when it is recycled back to the plasma membrane. Solely the exposure to endosomal pH followed by exposure of the complex to neutral pH, as encountered by the LpR-HDLp complex during its intracellular route, does not lead to complex dissociation (data not shown), suggesting that other factors contribute to induce ligand release. During recycling of transferrin, iron is released from transferrin due to the endosomal pH resulting in a decrease in affinity of the transferrin receptor for the resulting apotransferrin. This difference in affinity most likely accounts for the dissociation of transferrin from its receptor upon appearance at the plasma membrane[12]. Due to its expression pattern, it was hypothesized that LpR-mediated recycling of HDLp contributes to intracellular lipid delivery without degradation of its apolipoprotein matrix, in agreement with the shuttle function of HDLp in the insect blood[13]. Similar to the iron delivery by transferrin, this would imply a mechanism in which endocytosed HDLp unloads (part of) its lipid cargo intracellularly, resulting in a lower affinity of HDLp for LpR. However, contrary to our expectations, binding studies

using a partially delipidated HDLp particle with a buoyant density of 1.17 g/ml (hence designated as HDLp-1.17) revealed that LpR displayed a 2.4-fold higher affinity for HDLp-1.17 than for wt HDLp. The complex stability and endocytic fate were similar to that previously described for HDLp; the LpR-HDLp-1.17 complex is stable at endosomal conditions such as low pH and low Ca^{2+} concentration while after endocytosis, HDLp-1.17 appeared to be recycled by LpR, both in LpR-transfected CHO cells and in insect fat body tissue endogenously expressing LpR. The concept of HDLp as a reusable lipid shuttle implies that, depending on physiological or developmental needs for lipid distribution, HDLp in the hemolymph may exist in several forms with respect to relative lipid content, leading to lipid-loaded and lipid-poor particles. By experimental alternation of starvation and feeding of young adult locusts (2-4 days after imaginal ecdysis), subspecies of HDLp with a slightly higher density were identified (Van Doorn J. M., Van der Horst, D.J., Roosendaal, S.D., and Rodenburg K.W., unpublished results), suggesting that relatively lipid-poor HDLp particles may exist in the hemolymph at the physiological periods in which the receptor is expressed. Therefore, we propose that LpR specifically endocytoses circulatory lipid-poor HDLp to be reloaded during its intracellular route, resulting in a decreased affinity of the particle for LpR. The proposed mechanism allows the uptake of lipids from the strongly diminished reserves in the fat body and their release into the circulation for delivery to other tissues (**Chapter 3**).

A possible explanation for the high-affinity binding of HDLp-1.17 to LpR is the exposure of a cryptic binding site. Our studies indicate that partial delipidation leads to exposure of the amino acid sequence that contains the cleavage site of apoLp-II/I, which is rich in Lys and Arg residues that mediate the interaction between ligands and LDLR family members. However, competition binding experiments indicated that the cleavage site is not involved in the high-affinity binding of HDLp-1.17 to LpR. Additionally, the C-terminus of apoLp-I, which is exposed at the surface of both HDLp and HDLp-1.17, is not involved in either low- or high-affinity binding of lipoprotein to LpR. Based on the general binding motif of ligands for LDLR family members, potential receptor binding sites in apoLp-I and -II were identified. The motif was found several times in apoLp-I and -II, especially located in the amphipathic β-cluster as was found for the binding site of apoB-100 for LDLR (**Chapter 4**).

In general, the positively charged Lys residue in this receptor-binding motif of ligands for LDLR family members is thought to interact with the negatively charged binding pocket in the LA-repeats of the receptors, formed by coordination of a Ca^{2+} ion. Since the LpR-HDLp complex appeared to be EDTA resistant, this might suggest a difference in Ca^{2+} dependence of the LA-repeats of LpR. However, sequence comparison of the LA-repeats of LpR with those of other LDLR family members, as well as modeling studies, predicted that each LA-repeat of LpR is stabilized by a Ca^{2+}-ion[14].

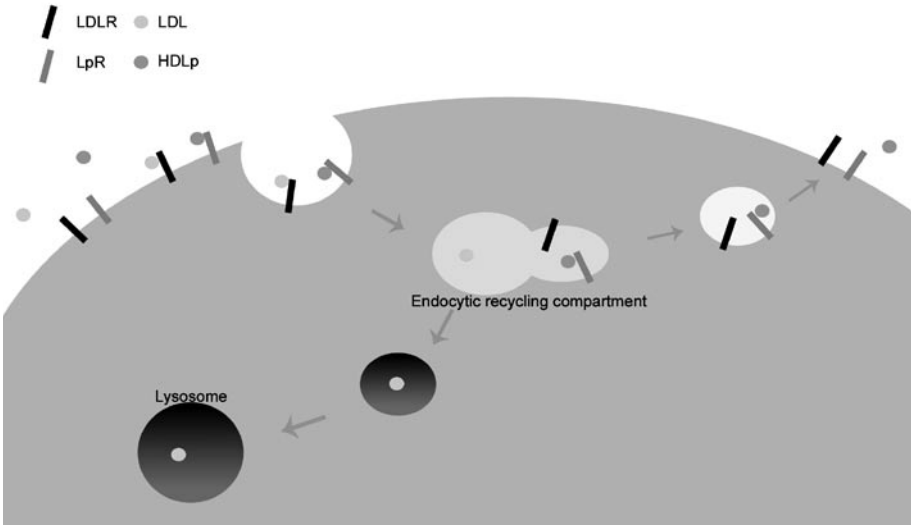

Figure 2: Human LDL and insect HDLp follow different intracellular pathways.
For a colored version of this figure see page 173.

In agreement with these studies, our results indicate that Ca^{2+} is essential for proper disulfide bond formation in LpR. In accordance with similar experiments for LDLR, also the conformation of the ligand-binding site of LpR appeared Ca^{2+}-dependent. Despite the similarities between the Ca^{2+} dependence of LpR and LDLR, EDTA treatment after binding of HDLp to its receptor is unable to dissociate the LpR-HDLp complex, in contrast to a similar treatment of the LpR-RAP or LDLR-LDL complexes, indicating that HDLp is able to stabilize the structure of the LA-repeats of LpR. This stability may be due to shielding of the Ca^{2+} ion from the chelating agent by HDLp and/or by the ability of HDLp to constrain the conformational diversity of the LA-repeats of LpR in the absence of Ca^{2+}. Models of LA-4, 5 and 6 reveal the presence of a central Trp residue and a negatively charged binding pocket required for the interaction with ligand (Figure 3), suggesting that these repeats are part of the interaction interface with HDLp. Molecular dynamics simulations suggested that although the LA-repeats 4, 5 and 6 were stable in the presence of Ca^{2+}, they significantly unfolded when Ca^{2+} was removed. However, LA-6 seemed to display a higher stability in the absence of Ca^{2+} than LA-4 and 5. Together, these results indicate that the remarkable stability of the LpR-HDLp complex must be traced back to the stabilizing properties of the interaction interface between LpR and lipoprotein, in which LA-6 may contribute to an energetically favorable interaction between HDLp and LpR in the absence of Ca^{2+} (**Chapter 5**). In addition to the susceptibility of the LpR-RAP complex to EDTA treatment, the LpR-RAP complex is also dissociated upon low pH (data not shown), which is in line with data of other studies investigating the pH

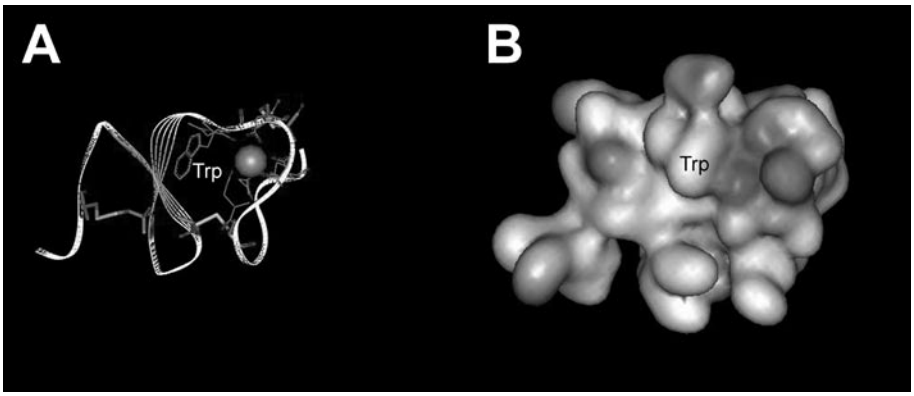

Figure 3: A Ca^{2+} cage forms an acidic binding pocket. A: Model of LA-repeat 5 of LpR. Cα backbone structure of LA-5 is indicated by the ribbon. The central Ca^{2+} ion is depicted in orange. The Ca^{2+}-coordinating residues are shown by the stick representation (negative charges are depicted in red, positive charges in blue). Disulfide bridges are shown in yellow. The repeat was modeled using Modeller 8v2, based on the structure of LA-repeats 3 and 4 of LDLR (PDB database indicator 2FCW). B: Surface potential of LA-5 of LpR based on the model depicted in A. The surface is colored according to the electrostatic potential: positive charges are depicted in blue, negative charges in red, white areas are neutral. Trp indicates the position of the central Trp residue. For a colored version of this figure see page 173.

dependence of the binding of RAP to LDLR family members[15,16]. However, RAP was shown to colocalize with LpR in the ERC[17]. Although this might be explained by the targeting of RAP to this compartment after its release by LpR, targeting of RAP to the ERC after endocytosis has only been reported in CHO cells transfected with a mutant VLDLR lacking the β-propeller, interpreted by the authors as recycling of the VLDLR-RAP complex[18]. It is not clear whether the interpretation of these data is correct. It should be noted that RAP is not a ligand for LDLR family members, but an ER resident protein acting as a chaperone for LDLR family members[19], which should release a correctly folded protein. Although RAP appears to function as chaperone for the LA-repeats of LDLR family members and not for the β-propeller, changes in the VLDLR conformation may result in a lack of dissociation of RAP at endosomal pH. Additionally, the mutant VLDLR was expressed at higher levels than wt VLDLR[18]. Therefore, as may also be the case for the targeting of RAP after endocytosis by LpR, high amounts of RAP in the early endosome may affect the targeting of RAP to lysosome or ERC.

As mentioned before, the interaction mode between LDLR family members and their ligands seems to be conserved and likely involves the electrostatic interactions between positively charged amino acid residues from the ligand and negatively charged residues of the LA-repeats. In more detail, the acidic Ca^{2+}-coordinating residues from the LA-repeats form a negatively charged binding pocket (Figure 3),

which serves as a docking site for a protruding Lys from the ligand. After docking of ligand, this initial interaction is stabilized by the central Trp present in many LA-repeats (Figure 3); for LpR the central Trp is present in LA-1-6. However, a putative splice variant of LpR lacks a central Trp in LA-3 (**Chapter 2**). Despite such a putative general binding mode, most ligands are not interchangeable between the different receptors, suggesting that ligand specificity is mediated by additional contacts between ligand and non-conserved amino acid residues of the receptor. For example, the docking sites for LDL are located in LA-4 and 5 of LDLR[10], while biochemical studies indicate that its binding site comprises LA-3-7 and EGF-A[20,21]. Since the structure of EGF-A differs from that of the LA-repeats, and LA-6 and 7 of LDLR do not contain a central Trp residue, this suggests that the contacts between LDL and these repeats differ from the electrostatic interactions between ligand and the docking sites located in LA-4 and 5. This stresses the importance of secondary contacts between ligands and non-conserved residues from adjacent loops in the LA-repeats to stabilize the interaction after docking of ligand on the LA-repeats of LDLR family members, which, with reference to our studies, probably also determine the stability of the LpR-HDLp complex at endosomal conditions. RAP has the ability to bind to almost all LDLR family members with high affinity. Its binding site comprises a pair of LA-repeats of which the specificity for RAP seems to be determined by an extra conserved amino acid residue in addition to the central Trp[22,23]. The extra acidic residue necessary for RAP binding is present in LA-1 and 2 and LA-4-6 of LpR, suggesting that LpR may be able to bind two RAP molecules. However, competition binding studies showed that RAP does not compete with the binding of an antibody raised against LA-1 of LpR, suggesting that RAP does not bind to the pair of LA-1 and 2. The lack of binding to these repeats may be explained by the lack of other residues in these repeats to stabilize the binding. However, sequence alignment of LA-repeats involved in the binding of RAP does not reveal other similarities between these repeats besides the general characteristics of LA-repeats. The lack of binding to the LA-1-2 pair suggests that RAP may either bind to the LA-4-5 pair or the LA-5-6 pair. Although mutational analysis is necessary to determine the precise binding site of LpR for RAP, binding of RAP to LA-4-5 and therefore the lack of binding of RAP to LA-6 may explain the difference in susceptibility of the LpR-RAP and LpR-HDLp complexes to EDTA treatment.

Most of the knowledge concerning the structural basis of ligand binding to LDLR family members comes from studies using RAP as a ligand. However, the structural basis for the binding of lipoproteins to LDLR family members seems to be more complex, particularly since these ligands are composed of a protein and lipid moiety that both may participate in the interaction with the receptor, directly or indirectly. For example, structural studies indicate that the basic region involved in binding of lipid-free apoE is exposed on the surface of a helix potentially in position to form contacts with the Ca^{2+}-coordinating acidic clusters of LDLR, yet apoE does not bind

to LDLR with high affinity until it is associated with lipids[23,24], which induce global rearrangements in the protein leading to the formation of supplementary contacts provided by a specific Arg[25,26]. Despite the presence of apoB-100 in LDL and VLDL, the binding of VLDL to LDLR is mediated by apoE and not by apoB-100[20]. These two examples illustrate that binding of lipoproteins to LDLR family members is affected by the lipid moiety of the lipoprotein. Our studies indicate that also changes in lipid loading of HDLp affect binding of the particle to LpR, since partial lipid depletion led to high-affinity binding to LpR, suggesting that modulation of the lipid content of HDLp may contribute to ligand release from LpR, necessary for resecretion of HDLp.

Besides the functioning of lipoproteins as a vehicle for lipids, HDLp has recently been shown to function in the specific transport and delivery of the lipid-anchored morphogens Wingless and Hedgehog during the development of the larval stages of *Drosophila*[27]. The involvement of lipoproteins in such a delivery puts forward the idea that a similar function and mechanism may also be present in the mammalian system, in which the Wingless homologue, Wnt[28], and Hedgehog[29] have equally important functions. Indeed, recently it was hypothesized that LDL might transport Hedgehog through the mammalian bloodstream[30]. Morphogens like Hedgehog and Wnt use their lipid anchors to bind to lipoprotein particles, resulting in a morphogen-lipoprotein complex that is able to interact with two independent receptors on the cell surface: one specific to the morphogen and the other to the apolipoprotein. Such a cooperative binding may increase the affinity of the morphogen-lipoprotein complex to cells, which contributes to a restricted diffusion of morphogens and determines the intercellular distribution of these lipid-anchored proteins[31]. However, a recent paper showed that Patched, the receptor for Hedgehog, is also a lipoprotein receptor that in addition to its role in the Hedgehog pathway appeared to be involved in lipid homeostasis[32], indicating that the machinery for delivery of morphogens or lipids are not mutually exclusive. With respect to ligand recycling by LpR it is of particular interest that in the *Drosophila* wing disc the massive endocytosis of lipophorin induced by either Patched or a *Drosophila* homologue of LpR, LpR2, results in a decrease instead of a rise in the amount of lipid-containing vesicles, suggestive of a similar recycling mechanism as was found in locust fat body tissue[32]. In line with these findings, LpR mutant flies do not show any major alterations in fat body TAG content. However, they display alterations in lipid metabolism (J. Culi, personal communication), suggestive of a role for LpR in LpR-mediated endocytosis of specific hydrophobic compounds such as signaling metabolites or carotenoids.

As compared to mammals, the different functioning of similar lipid-binding proteins and their receptors in the insect system renders the latter system a useful and important alternative model for studying the molecular mechanisms underlying processes of lipid transport and utilization, also related to human disorders and

disease. Moreover, in other aspects of lipid metabolism, particularly in the mechanism of fat storage and mobilization, mammals and insects recently appeared to be very similar, underscoring the value of a non-mammalian model organism in elucidating the molecular aspects of the regulation of energy homeostasis and dysfunction of this balance resulting in obesity. For example, packaging fat in intracellular lipid droplets and the mechanisms guiding mobilization of stored fat are conserved between mammals and insects. These lipid droplets are progressively recognized to represent ubiquitous metabolic organelles that are surrounded by a phospholipid monolayer layer coated with specific proteins that participate in the regulation of TAG storage and lipolysis[33-35]. Like mammalian adipocytes, insect fat body cells accumulate TAG in intracellular lipid droplets that provide the major long-term energy reserve of the animal organism, for which *Drosophila* recently emerged as a powerful system[36-38]. Generation of loss-of-function mutants evidenced that simultaneous loss of the receptor for AKH -and thus the signaling pathway for lipid mobilization related to β-adrenergic signaling in mammals- and the lipid droplet-associated TAG lipase brummer (bmm), a homologue of human adipose TAG lipase (ATGL), caused extreme obesity and blocks acute storage fat mobilization in flies[38]. To further demonstrate the functional similarity between mammalian and *Drosophila* TAG lipases, bmm was shown to localize at the lipid droplet surface and to antagonize a perilipin-related lipid droplet surface protein (LSD-2)[37] that functions as an evolutionary conserved modulator of lipolysis[36].

Clearly, therefore, insect model organisms like *Drosophila* offer an exciting strategy for obesity research in view of the existence of powerful tools for genetic mapping and high-throughput methods for creation of mutants and phenocopies allowing for identification of genes representing potential targets for effective prevention or treatment of obesity[39]. Recently it has been argued that *Drosophila* also provides an ideal model for conducting research on nutrigenomics, which refers to the complex effects of the diet on the genome, epigenome and proteome of an organism[40]. Long-term effects of diet range from obesity and associated diseases such as diabetes and cardiovascular disease to increased or decreased longevity, and although models like yeast and *Caenorhabditis elegans* have sequenced genomes like *Drosophila*, the latter has an adipose-like fat body and a lipid transport system, making it a closer model to humans[40].

References

1. Iwasaki T, Takahashi S, Ishihara M, Takahashi M, Ikeda U, Shimada K, Fujino T, Yamamoto TT, Hattori H & Emi M (2004) The important role for betaVLDLs binding at the fourth cysteine of first ligand-binding domain in the low-density lipoprotein receptor. J Hum Genet 49, 622-628.
2. Maczek C, Recheis H, Bock G, Stulnig T, Jurgens G & Wick G (1996) Comparison of low density lipoprotein uptake by different human lymphocyte subsets: a new method using double-fluorescence staining. J Lipid Res 37, 1363-1371.
3. Nagele H, Gebhardt A, Niendorf A, Kroschinski J & Zeller W (1997) LDL receptor activity in human leukocyte subtypes: regulation by insulin. Clin Biochem 30, 531-538.
4. Mazurov AV, Preobrazhensky SN, Leytin VL, Repin VS & Smirnov VN (1982) Study of low density lipoprotein interaction with platelets by flow cytofluorimetry. FEBS Lett 137, 319-322.
5. Raungaard B, Heath F, Brorholt-Petersen JU, Jensen HK & Faergeman O (1998) Flow cytometry with a monoclonal antibody to the low density lipoprotein receptor compared with gene mutation detection in diagnosis of heterozygous familial hypercholesterolemia. Clin Chem 44, 966-972.
6. Hattori H, Hirayama T, Nobe Y, Nagano M, Kujiraoka T, Egashira T, Ishii J, Tsuji M & Emi M (2002) Eight novel mutations and functional impairments of the LDL receptor in familial hypercholesterolemia in the north of Japan. J Hum Genet 47, 80-87.
7. Boswell EJ, Jeon H, Blacklow SC & Downing AK (2004) Global defects in the expression and function of the low density lipoprotein receptor (LDLR) associated with two familial hypercholesterolemia mutations resulting in misfolding of the LDLR epidermal growth factor-AB pair. J Biol Chem 279, 30611-30621.
8. Beglova N, Jeon H, Fisher C & Blacklow SC (2004) Cooperation between fixed and low pH-inducible interfaces controls lipoprotein release by the LDL receptor. Mol Cell 16, 281-292.
9. Davis CG, Goldstein JL, Sudhof TC, Anderson RG, Russell DW & Brown MS (1987) Acid-dependent ligand dissociation and recycling of LDL receptor mediated by growth factor homology region. Nature 326, 760-765.
10. Rudenko G, Henry L, Henderson K, Ichtchenko K, Brown MS, Goldstein JL & Deisenhofer J (2002) Structure of the LDL receptor extracellular domain at endosomal pH. Science 298, 2353-2358.
11. Van Hoof D, Rodenburg KW & Van der Horst DJ (2005) Intracellular fate of LDL receptor family members depends on the cooperation between their ligand-binding and EGF domains. J Cell Sci 118, 1309-1320.
12. Dautry-Varsat A, Ciechanover A & Lodish HF (1983) pH and the recycling of transferrin during receptor-mediated endocytosis. Proc Natl Acad Sci USA 80, 2258-2262.
13. Van Hoof D, Rodenburg KW & Van der Horst DJ (2003) Lipophorin receptor-mediated lipoprotein endocytosis in insect fat body cells. J Lipid Res 44, 1431-1440.
14. Roosendaal SD, Kerver J, Schipper M, Rodenburg KW & Van der Horst DJ (2008) The complex of the insect LDL receptor homologue, lipophorin receptor, LpR, and its lipoprotein ligand does not dissociate at endosomal conditions. FEBS J 275, 1751-1766.

15. Lee D, Walsh JD, Mikhailenko I, Yu P, Migliorini M, Wu Y, Krueger S, Curtis JE, Harris B, Lockett S, Blacklow SC, Strickland DK & Wang YX (2006) RAP uses a histidine switch to regulate its interaction with LRP in the ER and Golgi. Mol Cell 22, 423-430.
16. Estrada K, Fisher C & Blacklow SC (2008) Unfolding of the RAP-D3 helical bundle facilitates dissociation of RAP-Receptor complexes. Biochemistry 47, 1532-1539.
17. Van Hoof D, Rodenburg KW & Van der Horst DJ (2002) Insect lipoprotein follows a transferrin-like recycling pathway that is mediated by the insect LDL receptor homologue. J Cell Sci 115, 4001-4012.
18. Mikhailenko I, Considine W, Argraves KM, Loukinov D, Hyman BT & Strickland DK (1999) Functional domains of the very low density lipoprotein receptor: molecular analysis of ligand binding and acid-dependent ligand dissociation mechanisms. J Cell Sci 112, 3269-3281.
19. Bu G & Rennke S (1996) Receptor-associated protein is a folding chaperone for low density lipoprotein receptor-related protein. J Biol Chem 271, 22218-22224.
20. Esser V, Limbird LE, Brown MS, Goldstein JL & Russell DW (1988) Mutational analysis of the ligand binding domain of the low density lipoprotein receptor. J Biol Chem 263, 13282-13290.
21. Jeon H & Blacklow SC (2005) Structure and physiologic function of the low-density lipoprotein receptor. Annu Rev Biochem 74, 535-562.
22. Andersen OM, Christensen LL, Christensen PA, Sorensen ES, Jacobsen C, Moestrup SK, Etzerodt M & Thogersen HC (2000) Identification of the minimal functional unit in the low density lipoprotein receptor-related protein for binding the receptor-associated protein (RAP). A conserved acidic residue in the complement-type repeats is important for recognition of RAP. J Biol Chem 275, 21017-21024.
23. Fisher C, Beglova N & Blacklow SC (2006) Structure of an LDLR-RAP complex reveals a general mode for ligand recognition by lipoprotein receptors. Mol Cell 22, 277-283.
24. Blacklow SC (2007) Versatility in ligand recognition by LDL receptor family proteins: advances and frontiers. Curr Opin Struct Biol 17, 419-426.
25. Fisher C, Abdul-Aziz D & Blacklow SC (2004) A two-module region of the low-density lipoprotein receptor sufficient for formation of complexes with apolipoprotein E ligands. Biochemistry 43, 1037-1044.
26. Morrow JA, Arnold KS, Dong J, Balestra ME, Innerarity TL & Weisgraber KH (2000) Effect of arginine 172 on the binding of apolipoprotein E to the low density lipoprotein receptor. J Biol Chem 275, 2576-2580.
27. Panakova D, Sprong H, Marois E, Thiele C & Eaton S (2005) Lipoprotein particles are required for Hedgehog and Wingless signalling. Nature 435, 58-65.
28. Seto ES & Bellen HJ (2004) The ins and outs of Wingless signaling. Trends Cell Biol 14, 45-53.
29. Cohen MM, Jr. (2003) The hedgehog signaling network. Am J Med Genet A 123, 5-28.
30. Bijlsma MF, Peppelenbosch MP & Spek CA (2006) Hedgehog morphogen in cardiovascular disease. Circulation 114, 1985-1991.
31. Neumann S, Harterink M & Sprong H (2007) Hitch-hiking between cells on lipoprotein particles. Traffic 8, 331-338.

32. Callejo A, Culi J & Guerrero I (2008) Patched, the receptor of Hedgehog, is a lipoprotein receptor. Proc Natl Acad Sci USA 105, 912-917.
33. Londos C, Brasaemle DL, Schultz CJ, Segrest JP & Kimmel AR (1999) Perilipins, ADRP, and other proteins that associate with intracellular neutral lipid droplets in animal cells. Semin Cell Dev Biol 10, 51-58.
34. Gross DN, Miyoshi H, Hosaka T, Zhang HH, Pino EC, Souza S, Obin M, Greenberg AS & Pilch PF (2006) Dynamics of lipid droplet-associated proteins during hormonally stimulated lipolysis in engineered adipocytes: stabilization and lipid droplet binding of adipocyte differentiation-related protein/adipophilin. Mol Endocrinol 20, 459-466.
35. Martin S & Parton RG (2006) Lipid droplets: a unified view of a dynamic organelle. Nat Rev Mol Cell Biol 7, 373-378.
36. Grönke S, Beller M, Fellert S, Ramakrishnan H, Jäckle H & Kühnlein RP (2003) Control of fat storage by a *Drosophila* PAT domain protein. Curr Biol 13, 603-606.
37. Grönke S, Mildner A, Fellert S, Tennagels N, Petry S, Muller G, Jäckle H & Kühnlein RP (2005) Brummer lipase is an evolutionary conserved fat storage regulator in *Drosophila*. Cell Metab 1, 323-330.
38. Grönke S, Muller G, Hirsch J, Fellert S, Andreou A, Haase T, Jäckle H & Kühnlein RP (2007) Dual lipolytic control of body fat storage and mobilization in *Drosophila*. PLoS Biol 5, e137.
39. Kulkarni MM & Perrimon N (2005) Super-size flies. Cell Metab 1, 288-290.
40. Ruden DM, De Luca M, Garfinkel MD, Bynum KL & Lu X (2005) *Drosophila* nutrigenomics can provide clues to human gene-nutrient interactions. Annu Rev Nutr 25, 499-522.

Nederlandse Samenvatting

Nederlandse Samenvatting

Ons lichaam bestaat uit ontelbare cellen. In de cel bevindt zich een celkern, waarin het erfelijk materiaal is opgeslagen in de vorm van desoxyribonucleïne zuur, oftewel DNA. Het DNA vormt een code, een soort kookboek, voor het maken van eiwitten (proteïnen). Eiwitten zijn de werkpaarden in ons lichaam en hebben allerlei functies. Eiwitten zijn onder andere betrokken bij het transport van stoffen, bijvoorbeeld vetten, in en uit de cel. Het transporteren van vetten is lastig aangezien ze niet oplosbaar zijn in water. Vandaar dat dieren speciale lipoproteïnen hebben. Lipoproteïnen, de naam zegt het al, bestaan uit lipid (Gr. λιπος) en eiwit (proteïne). Lipoproteïnen zorgen ervoor dat de hydrofobe vetten wel in een waterige omgeving, zoals je bloedbaan, vervoerd kunnen worden. Een lipoproteïne is een deeltje wat ongeveer 7.5-22 nanometer (= een miljoenste millimeter) groot is. Je kunt je zo een deeltje het best voorstellen als een bonbon met vulling. De buitenkant van het lipoproteine bevat wateroplosbare componenten, zoals eiwitten, de vulling is wateronoplosbaar, namelijk vetten. De grootte van het lipoproteïne hangt af van de hoeveelheid vet in het deeltje. De hoeveelheid lipid bepaalt ook de dichtheid van het deeltje. Aan de hand van de dichtheid worden de lipoproteïnen ingedeeld in verschillende klassen. Mensen hebben veel verschillende lipoproteïnen met verschillende dichtheden en verschillende eiwitten. Insecten hebben ook lipoproteïnen; om het verschil met de lipoproteïnen van de mens aan te geven zijn deze lipoforinen genaamd (Gr. φορος, dragen). Het "high-density lipophorin", oftewel HDLp, is het meest voorkomende lipoforine in insecten. Het HDLp bevat twee eiwitten, apolipoforine I en II. Deze twee eiwitten zijn ontstaan door het door midden knippen (klieving) van een groter eiwit genaamd apolipoforine II/I. Apolipoforine II/I is evolutionair verwant aan het menselijke eiwit apolipoproteïne B. Apolipoproteïne B is het eiwit van het menselijke "low-density lipoprotein", oftewel LDL, beter bekend als "slecht cholesterol". Behalve cholesterol bevat LDL ook andere vetten. In de weefsels en organen, vooral de lever, wordt het LDL opgenomen door de cellen om afgebroken te worden. De opname van LDL gebeurt door een eiwit, de LDL receptor. De LDL receptor bevindt zich in de celmembraan, waardoor een deel van het eiwit uitsteekt aan de buitenkant van de cel. Hierdoor kan het een LDL deeltje van buiten de cel binden. Als het deeltje gebonden is, worden de receptor en het LDL deeltje naar binnen gehaald door de cel, zodat de vetten gebruikt of opgeslagen kunnen worden. Direct na opname komt het complex van LDL en de LDL receptor in een compartiment in de cel, een zogenaamd "early endosome". Hier is de zuurgraad (pH) lager dan buiten de cel, waardoor het LDL loslaat van de LDL receptor. Vervolgens kan het LDL worden afgebroken in de cel, terwijl de receptor weer terug gaat naar de celmembraan en opnieuw LDL kan binden (Zie Figuur 2 van hoofdstuk 6, p173).
Een belangrijk verschil met het zoogdierensysteem is dat in insecten HDLp niet in de cel wordt opgenomen (geëndocyteerd) en afgebroken, zoals LDL. In plaats

daarvan worden de vetten als het ware uitgeladen en door andere eiwitten de cel in getransporteerd. Ondanks dit verschil is er wel een soortgelijk eiwit als de LDL receptor gevonden, oftewel een LDL receptor homoloog, de lipoforine receptor, LpR. Het onderzoek beschreven in dit proefschrift richt zich op de karakterisatie van LpR, waarvoor de Afrikaanse treksprinkhaan, *Locusta migratoria*, als diermodel is gebruikt. Eerder onderzoek heeft aangetoond dat LpR ook HDLp bindt en endocyteert in insectenweefsel, maar ook in zoogdiercellen als die LpR kunnen maken. Echter, nadat het HDLp naar binnen is gehaald wordt het niet afgebroken maar weer naar buiten getransporteerd, waarna het opnieuw gebruikt kan worden om vetten te transporteren in de circulatie van het insect (Zie Figuur 2 van hoofdstuk 6, p173). Tijdens mijn onderzoek heb ik het mechanisme en de functie van dit recyclingmechanisme verder onderzocht vanuit een structuurbiologische invalshoek. Eiwitten bestaan uit een ketting van aminozuren die op een bepaalde manier is opgevouwen, waardoor eiwitten een bepaalde structuur krijgen. Aan de hand van de eigenschappen van de aminozuren en bekende structuren van eiwitten (homologen) kan de structuur (conformatie) van een eiwit voorspeld worden. LpR is een homoloog van de LDL receptor, en de twee receptoren bestaan uit dezelfde domeinen (Zie Figuur 7, hoofdstuk 1, p20). Een belangrijk onderdeel van deze receptoren is het ligandbindend domein. Dit domein bestaat uit "LDLR type A repeats", die elk bestaan uit een sequentie van ongeveer 40 aminozuren met bepaalde eigenschappen. Er is veel onderzoek gedaan naar de LA-repeats van de LDL receptor. Hieruit blijkt dat de aminozuurketen van een LA-repeat veel negatief geladen aminozuren bevat. Aangezien deze aminozuren elkaar afstoten wordt de structuur gestabiliseerd door een positief geladen calcium ion (Zie Figuur 3, hoofdstuk 6, p173). Het calcium ion neutraliseert slechts een deel van de lading, via de overgebleven negatief geladen aminozuren kunnen positief geladen aminozuren van het LDL binden aan de receptor.

In dit onderzoek hebben we met behulp van fluorescerend gelabelde lipoproteïnen de binding van het insecten lipoforine (HDLp) aan LpR onderzocht in vergelijking met de binding van menselijk LDL aan de LDL receptor. Zoals eerder beschreven laat het LDL los van de LDL receptor als het in een zuurdere omgeving (lagere pH) komt zoals het early endosome. LDL en de LDL receptor gaan dan allebei naar een andere plek in de cel. Aangezien HDLp en LpR vanuit het early endosome allebei worden gerecycled, hebben we bestudeerd of HDLp en LpR aan elkaar kunnen blijven zitten bij lage pH. Uit deze proeven bleek dat HDLp aan LpR gebonden blijft bij lage pH, wat het aannemelijk maakt dat het complex van HDLp en LpR in zijn geheel gerecycled wordt. Behalve een lage zuurgraad is ook de hoeveelheid calcium lager in early endosomes. Aangezien calcium essentieel is voor de structuur van het ligand-bindende domein van de LDL receptor, en de aminozuurvolgorde van LpR lijkt op die van LDL receptor, hebben we ook getest of het weghalen van calcium de binding van HDLp aan LpR verstoort. Uit deze proeven bleek dat het weghalen van calcium niet leidt tot het verbreken van de binding van HDLp aan LpR. Dit betekent

dat in de cel HDLp en LpR aan elkaar blijven zitten en als complex gerecycled worden (**Hoofdstuk 2**, zie ook Figuur 2 hoofdstuk 6, p173).
Dit mechanisme roept tenminste twee vragen op. Ten eerste, hoe laat het HDLp dan los als het weer buiten de cel op de membraan komt? Ten tweede, wat is het nut van recycling van HDLp voor het insect? Uit eerder onderzoek naar de aanwezigheid van LpR tijdens de levenscyclus van de sprinkhaan bleek dat LpR alleen gemaakt wordt vlak na een vervelling (het mechanisme waardoor jonge sprinkhanen kunnen groeien), of in sprinkhanen die een tijd lang geen eten hebben gehad. Dit suggereert dat de opname van HDLp nodig is tijdens en vlak na energiekostende processen zoals vervelling, bijvoorbeeld om meer vet op te kunnen nemen in de cel in tijden waarin de reserves zijn verbruikt. Aangezien het HDLp wordt gerecycled, suggereert dit dat na opname van het HDLp de vetten uit het deeltje worden afgegeven in de cel, waarna het deeltje, dat nu minder lipid bevat, wordt uitgescheiden. Dit impliceert dat een deeltje met minder lipid, en dus een hogere dichtheid, slechter aan de receptor moet binden. Om dit te testen hebben we een deeltje gemaakt met minder lipid, HDLp-1.17. Vervolgens hebben we de binding van HDLp-1.17 aan LpR bestudeerd. Uit deze experimenten blijkt dat het HDLp-1.17 beter aan LpR bindt dan gewoon HDLp. Uit verdere experimenten blijkt dat ook HDLp-1.17 wordt gerecycled. Deze resultaten suggereren dus eerder een omgekeerd mechanisme, namelijk dat er vet uit de cel wordt opgenomen door HDLp tijdens recycling (**Hoofdstuk 3**).
Als er lipid uit het lipoproteïne wordt gehaald, dan kan dat ervoor zorgen dat de vouwing van de aminozuurketen, de conformatie, verandert, zoals de kleur van een ballon verandert als er meer lucht in zit. Uit onze studies in hoofdstuk 3 blijkt dat de conformaties van apolipoforine I en II in HDLp-1.17 enigzins veranderd zijn ten opzichte van de conformaties van deze eiwitten in HDLp. Apolipoforine I en II, de eiwitten van het HDLp, zijn ontstaan door klieving van apolipoforine II/I. In tegenstelling tot in HDLp wordt in HDLp-1.17 de klievingssite geëxposeerd aan de oppervlakte van het lipoforine, en zou daarom theoretisch in staat zijn om aan LpR te binden. Aangezien HDLp-1.17 sterker bindt aan LpR, hebben we onderzocht of de klievingssite belangrijk is voor de sterkere binding van HDLp-1.17 aan LpR. Uit studies met behulp van antilichamen die binden aan de uiteinden van apolipoforine I en II blijkt echter dat de ontstane uiteinden na de klieving niet betrokken zijn bij binding van HDLp-1.17 aan LpR (**Hoofdstuk 4**).
In hoofdstuk 2 hebben we laten zien dat het weghalen van calcium er niet voor zorgt dat HDLp en LpR loslaten van elkaar. Dit is verbazingwekkend aangezien de structuur van de LA-repeats van de LDL receptor gestabiliseerd wordt door calcium (Zie ook Figuur 3, Hoofdstuk 6, p173). Vandaar dat we hebben onderzocht of calcium nodig is voor de vouwing en de conformatie van LpR. Hieruit bleek dat calcium essentieel is voor de juiste vouwing van LpR. We laten ook zien dat het verwijderen van calcium uit LpR voordat HDLp gebonden is aan LpR ervoor zorgt dat HDLp niet meer aan LpR kan binden. Dit suggereert dat de structuur van de LA-repeats ontwricht wordt

na verwijdering van calcium. Echter, als HDLp eenmaal gebonden is aan LpR lijkt de verwijdering van calcium de structuur niet te verstoren en blijft het complex intact. Dit suggereert dat als HDLp gebonden is aan LpR het in staat is om het calcium af te schermen of vast te houden, waardoor het complex niet kapot gaat. Moleculaire dynamica studies laten zien dat de structuur van één van de LA-repeats (LA-6) minder lijkt te worden verstoord door verwijdering van calcium dan die van de andere repeats (Zie Figuur 8, hoofdstuk 5, p169). Deze eigenschap van LA-6 zou een rol kunnen spelen bij de stabiliteit van het LpR-HDLp complex.
Uit de resultaten van dit onderzoek blijkt dat binding van HDLp aan LpR leidt tot de formatie van een bijzonder stabiel complex, dat bestand is tegen een lage pH en de verwijdering van calcium. Verder blijkt dat de hoeveelheid lipid de binding van het lipoforine aan LpR beinvloedt, waarschijnlijk door verschillen in de conformaties van apolipoforine I en II. Aangezien LpR en HDLp homologen zijn van respectievelijk de LDL receptor en LDL, geven deze studies inzicht in de binding van liganden aan soortgelijke receptoren in dieren en mensen. De verschillen tussen lipoproteïnen en hun receptoren in mensen en insecten maken die laatste tot een interessant en belangrijk alternatief model voor de bestudering van lipidtransport en -metabolisme.

Dankwoord

Dankwoord

"Een pittig onderwerp, dat is het geheim,
de rest geknutsel als met schaar en lijm"
Drs. P.

Ruim vier jaar knutselen in het lab en dan nu een boekje. Toch was het niet altijd zo simpel als het hierboven staat. Gelukkig hebben velen mij met raad en daad ter zijde gestaan. Veel dank hiervoor!

Als eerste mijn promotor: **Dick**, bedankt voor je kritische blik en je grandioze inzet en geduld tijdens het schrijven. Ik heb een hoop geleerd van onze discussies en moet wel glimlachen als ik weer eens een figuur ergens anders wil plaatsen.

Mijn copromotor, **Kees**, bedankt voor al je enthousiasme voor dit project, en de vele interessante discussies hierover. Ze waren niet altijd kort, maar daarvoor moet ik ook hand in eigen boezem steken.

De leden van de begeleidingscommissie, beste **Ineke** en **Ger**, onze laatste besprekingen zijn alweer een tijd geleden, maar ze waren de basis voor het neerzetten van de FACS assay. Bedankt voor jullie interesse in mijn werk en de kritische noot.

Het ontwikkelen van deze FACS assay was toch wel het grootste geknutsel. **Ger**, ontzettend bedankt voor het meedenken en al je hulp met apparatuur en labels. **Steve**, thank you for sharing all the inside information considering your assay, the LDL receptor and the stimulating comments you made, I really enjoyed meeting you and discussing our work. **Maria** en **Wim**, er zijn een aantal computers op vastgelopen, maar gelukkig hadden jullie een goede oplossing voor de kwantificering dat de analyse een stuk eenvoudiger maakte.

Ik kijk met veel plezier terug op alle samenwerkingen met anderen die aan LDL receptoren werken. **Jürgen**, bedankt voor je tomeloze inzet, de altijd inspirerende discussies en het doen van alle vouwingsproeven, waarvan soms de resultaten iets later kwamen; ik citeer: "Ik ben er nog niet aan toegekomen want ik ben sinds kort vader van…." Veel plezier met de wonderen van de LDL receptor en met je gezin!
Javier, thank you very much for your enthusiasm, your quick replies and a great stay in Zaragoza (where I learned how to pour out cider). I hope you will enjoy

your stay in Utrecht. **Santiago**, I will try not to bother you again with many nervous e-mails. Thank you for your tremendous work with the MD studies and the pictures that were every time just in time.
Sander, bedankt voor de gezelligheid, de discussies over LA-repeats en natuurlijk voor je hulp bij het modeleren. We maken nog wat moois van die publicaties!

Natuurlijk wil ik ook mijn directe collega's bedanken: allereerst mijn kamergenootje **Masja**, vanaf de eerste dag waren we Jut en Jul. Bedankt voor een luisterend oor, kritische blik op de "wolken" en liters thee. **Yvonne**, door jou werden we een driemanschap in onze meidenkamer. Bedankt voor de altijd gezellig lunches, ik blijf het raar vinden dat je nu opeens wel thee drinkt! **Jan**, de opperknutselaar, je wist overal een oplossing voor, van sprinkhanen tot de kapotte CV-ketel. Bedankt voor al het werk en al je hulp. Geniet van je rust en van Noa! **Jana**, altijd had je DNA constructen weer op tijd klaar en de lastigste hybriden zo gemaakt, het maakte mijn werk een stuk makkelijker. **Dennis**, bedankt dat je me de fijne kneepjes van het werken met LpR hebt bijgebracht. **Koert**, bedankt voor je analytische kijk op mijn experimenten en op tenniswedstrijden. **Marcel**, altijd in voor een goed gesprek en altijd behulpzaam met alles. **Karine**, merci bien voor je hulp met de EM. **Wil**, bedankt voor je interesse, gezelligheid, en goede adviezen. **Marcelle**, bedankt voor het delen van je jarenlange evaring met eiwitwerk. Behalve de stofwisselingskant wil ik ook graag de "endo's" hartelijk bedanken voor de gezelligheid. **Hugo**, bedankt voor het organiseren van menig film/discussie avond. **Jan**, bedankt voor je steun als mijn mentor, later overgenomen door **Jenny** en **Shirinka**. Jullie allen bedankt voor de goede gesprekken.

Henk, **Ko** en **Cor**, de dierverzorgers, bedankt voor jullie hulp. Het was altijd een verrassing welke muziek jullie draaiden! **Frits**, microscoopexpert, je zorgde altijd weer voor de mooiste plaatjes. Vergeet niet om af en toe gitaar te spelen.

Het IB en de vele leuke "medebewoners" in het Kruytgebouw zorgden voor welkome afwisselingen in de vorm van labuitjes, aio-avonden en retraites. **Marnix** en **Thijs**, altijd in voor een extra biertje. Op de 5e verdieping, **Jarno**, **Erik**, **Bart**, **Miriam**, **Elsa**, **Jan Andries**, **Paul**, bedankt voor de gezelligheid tijdens labuitjes, de vele antilichamen en interessante discussies (over puntige schoenen en sprookjes).
De aio's van de zesde verdieping, met name **Jacob** (we komen elkaar vast weer eens tegen), **Robin** (alles goed in het hoge noorden?), **Cathelijne** en **Erica**. Bedankt voor de altijd gezellig aio avonden en retraites, en de introductie met Goldschläger (lekker in thee en vla!). En natuurlijk ook bedankt voor het "lenen" van het eerste potje cyclodextrine, toch de basis van een heel hoofdstuk.

Jorien, altijd een steun en toeverlaat. Ik ben blij dat je mijn paranimf bent, wanneer gaan we weer dansen?
Manon, we zijn nog niet in Stockholm, maar jij gaat in ieder geval de goede kant op. Bedankt voor de FACS discussies en adviezen (nooit geweten dat tegeltjes als FACS plotjes kunnen fungeren) tijdens etentjes en wandelingen, en de gezellige theateravonden.

Mijn familie, bedankt voor jullie interesse en steun. **Papa**, met je wiskundelessen heb je een belangrijke basis gelegd, bedankt voor de levendige discussies en je goede adviezen. **Kirsten**, bedankt voor je ontwerp, het laat me mijn onderzoek eens van een totaal andere kant zien.

Lieve **Bas**, de lijst is eindeloos; van een kopje thee tot je hulp bij mijn data. Bedankt voor je rust, je aanmoediging en bovenal je liefde.

Sigrid Dagmar Roosendaal was born on June 29th 1980 in Dissen am Teutoburger Wald (Germany). In 1998 she finished secondary school and started with the study Biology at Utrecht University. During her study, she participated in the research on carbohydrate-antibody interactions at the department of Bio-Organic Chemistry, Utrecht University, in cooperation with The Eijkman-Winkler Center for medical microbiology, infectious diseases and inflammation at the Utrecht Medical Center, under supervision of Prof. Dr. J. P. Kamerling and Dr. D. J. Lefeber. During a second research internship she participated in the research on O-mannosyltransferases which was performed at the Biochemistry and Biophysics Department of Texas A&M University, College Station, USA, under supervision of Dr. V. M. Panin and Dr. A. A. M. Thomas. After obtaining her Masters degree in 2003, she enrolled as a PhD student at the Division of Endocrinology and Metabolism of the Department Biology of Utrecht University. The results of that research are described in this thesis. Additionally, she contributed to the education of undergraduate students in Biology and Biomedical Sciences and she participated in the Institute of Biomembranes. She is currently working as scientist assay development at AMT (Amsterdam Molecular Therapeutics).

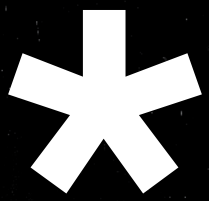

Curriculum Vitae

Sigrid Dagmar Roosendaal werd op 29 juni 1980 geboren te Dissen am Teutoburger Wald (Duitsland). In 1998 behaalde zij het gymnasium diploma aan het Gemeentelijk Gymnasium in Hilversum, waarna zij begon met de studie Biologie aan de Universiteit Utrecht. Tijdens haar studie verrichte zij onderzoek naar koolhydraat-antilichaam interacties bij de vakgroep Bio-Organische Chemie aan de Faculteit Scheikunde van de Universiteit Utrecht i.s.m. het Eijkman Winkler Instituut voor microbiologisch onderzoek van het Utrecht Universitair Medisch Centrum, onder supervisie van Prof. Dr. J. P. Kamerling en Dr. D. J. Lefeber. Gedurende een tweede wetenschappelijke stage deed zij onderzoek naar O-mannosyltransferases aan Texas A&M University, College Station, Verenigde Staten. Deze stage was onder supervisie van Dr. V. M. Panin en Dr. A. A. M. Thomas. In 2003 behaalde zij haar doctoraal examen en begon zij als promovendus bij de leerstoelgroep Endocrinologie en Metabolisme van het Departement Biologie van de Universiteit Utrecht. De resultaten van het daar verrichte onderzoek onder leiding van Prof. Dr. D. J. van der Horst en Dr. K. W. Rodenburg vormen de basis van dit proefschrift. Tevens leverde zij een bijdrage aan het onderwijs aan studenten Biologie en Biomedische wetenschappen binnen de Universiteit Utrecht en participeerde zij in het Instituut voor Biomembranen. Momenteel werkt zij als wetenschapper bij AMT (Amsterdam Molecular Therapeutics).

List of Publications
List of Abbreviations

List of Publications

Lyalin D, Koles K, Roosendaal SD, Repnikova E, Van Wechel L, Panin VM.
The *twisted* gene encodes *Drosophila* protein O-mannosyltransferase 2 and genetically interacts with the *rotated abdomen* gene encoding *Drosophila* protein O-mannosyltransferase 1.
Genetics. 2006 Jan;172(1):343-53.

Roosendaal SD, Kerver J, Schipper M, Rodenburg KW, Van der Horst DJ.
The complex of the insect LDL receptor homolog, lipophorin receptor, LpR, and its lipoprotein ligand does not dissociate under endosomal conditions.
FEBS J. 2008 Apr;275(8):1751-66.

Van der Horst DJ, Roosendaal SD, Rodenburg KW.
Circulatory lipid transport: lipoprotein assembly and function in an evolutionary perspective.
Mol Cell Biochem. 2008, in press.

List of Abbreviations

AKH : adipokinetic hormone
apoB-100 : apolipoprotein B-100
apoE : apolipoprotein E
apoLp-I : apolipophorin I
apoLp-II : apolipophorin II
calcium : Ca^{2+}
CHO : chinese hamster ovary
DAG : diacylglycerol
EGF : epidermal growth factor
ERC : endocytic recycling compartment
FACS : fluorescence-activated cell sorter
FFA : free fatty acids
FITC : fluorescein isothiocyanate
FSC : forward scatter
HDLp : high-density lipophorin
LA : LDLR type A
LDL : low-density lipoprotein
LDLR : LDL receptor
LLTP : large lipid transfer protein
LpR : lipophorin receptor
LRP : LDLR-related protein
MD : molecular dynamics
OG : oregon green
PL : phospholipids
RAP : receptor-associated protein
s.e.m. : standard error of the mean
TAG : triacylglycerol
Tf : transferrin
TMR : tetra-methyl rhodamine
VLDL : very-low-density lipoprotein
Vtg : vitellogenin
VtgR : vitellogenin receptor

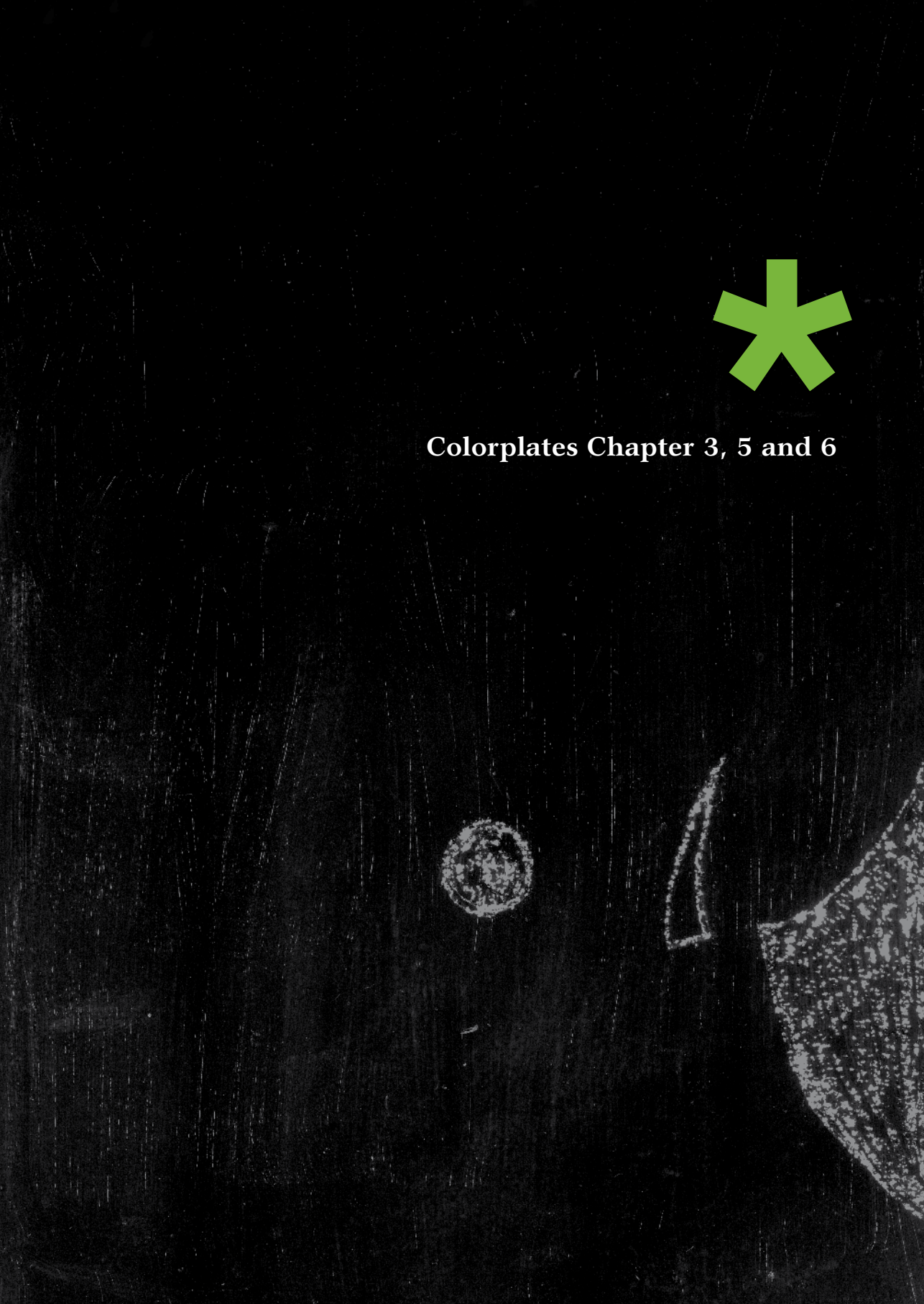

Colorplates Chapter 3, 5 and 6

Colorplates Chapter 3

Colorplates Chapter 3

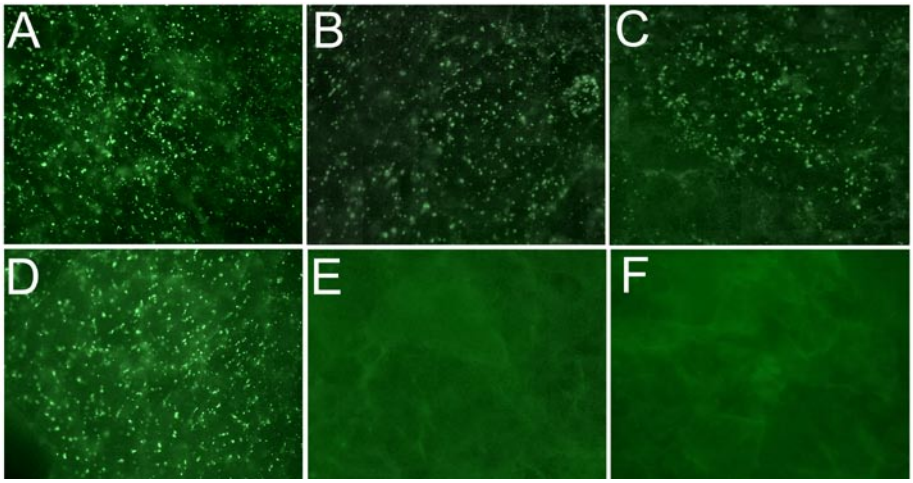

Figure 5. Endocytosis of HDLp-1.17 by LpR endogenously expressed by locust fat body tissue. Fluorescence microscopy images of fat body tissue incubated with OG-HDLp-1.17 (A-C) or OG-HDLp (D-F). Tissue from young adult animals (two days after ecdysis) was incubated with OG-HDLp-1.17 (A), OG-HDLp-1.17 in the presence of an equimolar amount of HDLp (B), or in the presence of a 10-fold excess of HDLp (C). Panels D-F show the reciprocal experiment, in which tissue was incubated with OG-HDLp (D), OG-HDLp in the presence of an equimolar amount of HDLp-1.17 (E) or OG-HDLp in the presence of a 10-fold excess of HDLp-1.17 (F).

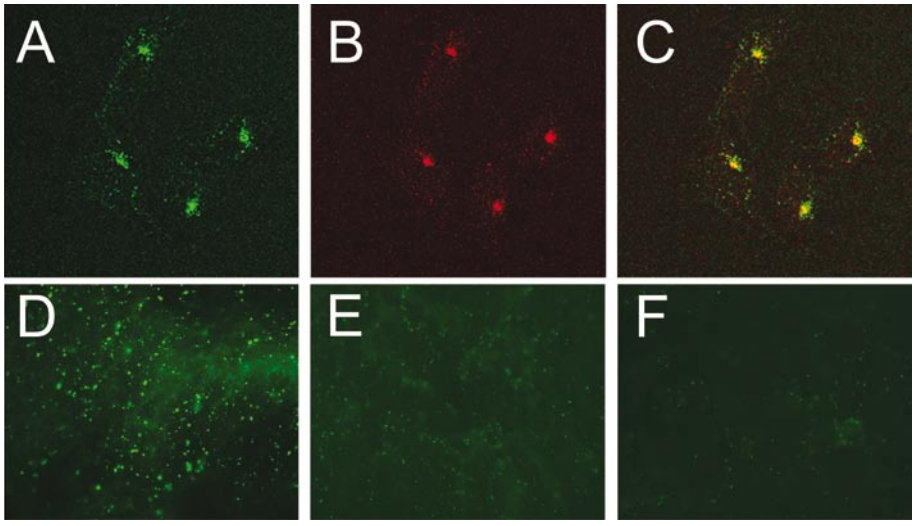

Figure 7. LpR-mediated recycling of HDLp-1.17 in CHO(LpR) cells and locust fat body tissue. Fluorescence microscopy images of CHO(LpR) cells used in a pulse-chase experiment with OG-HDLp-1.17 (A) and TMR-Tf (B). Endocytosis (the pulse) was followed by a 10-min chase in serum-free medium. Colocalization was visualized by merging the two images (C). Insect fat body of young adult animals (2 days after ecdysis) endogenously expressing LpR was either only pulsed with OG-HDLp-1.17 (D), or subsequently chased in insect growth medium for 1 h (E) or 2 h (F).

Colorplates Chapter 5

Colorplates Chapter 5

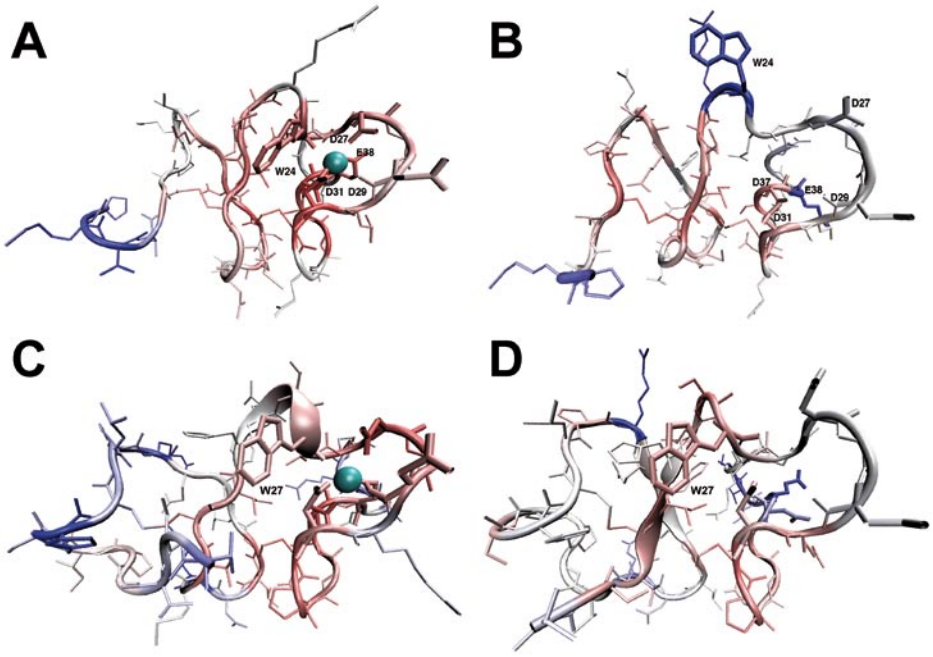

Figure 8: Three-dimensional models of LA-5 and LA-6 of LpR in the presence (A, C) and absence (B, D) of Ca^{2+}. Images show the last snapshot after 10 ns for LA-5 (A, B) and LA-6 (C, D). The models are colored according to the RMSD of the Cα of the amino acid residues, ranging from red (0 Å), via white (3 Å), to blue (6 Å). Important residues mentioned in the text are indicated by one-letter code, numbers are based on individual repeats. The Ca^{2+} ion is depicted as a green sphere.

Colorplates Chapter 6

Colorplates Chapter 6

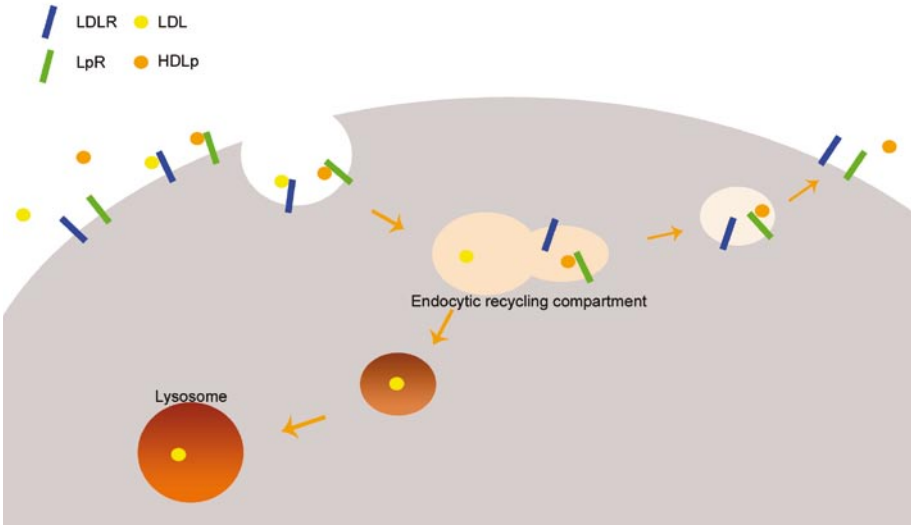

Figure 2: Human LDL and insect HDLp follow different intracellular pathways.

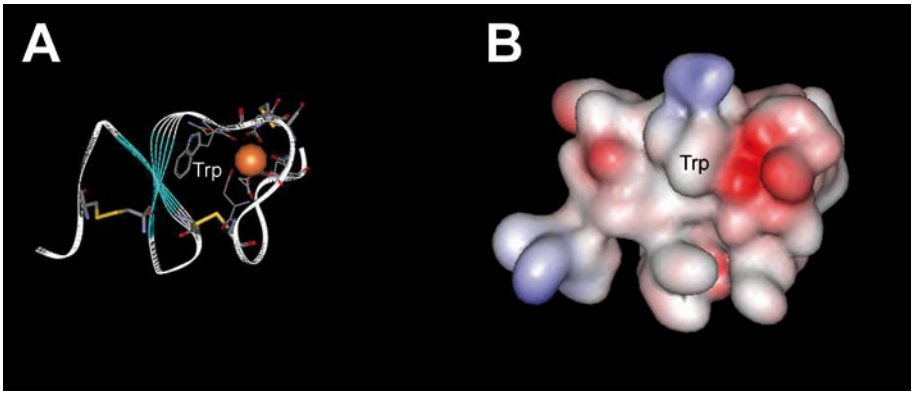

Figure 3: A Ca^{2+} cage forms an acidic binding pocket. A: Model of LA-repeat 5 of LpR. Cα backbone structure of LA-5 is indicated by the ribbon. The central Ca^{2+} ion is depicted in orange. The Ca^{2+}-coordinating residues are shown by the stick representation (negative charges are depicted in red, positive charges in blue). Disulfide bridges are shown in yellow. The repeat was modeled using Modeller 8v2, based on the structure of LA-repeats 3 and 4 of LDLR (PDB database indicator 2FCW). B: Surface potential of LA-5 of LpR based on the model depicted in A. The surface is colored according to the electrostatic potential: positive charges are depicted in blue, negative charges in red, white areas are neutral. Trp indicates the position of the central Trp residue.